FHWA-NJ-2012-009

DESIGN FOR DEFLECTION CONTROL VS. USE OF SPECIFIED SPAN TO DEPTH RATIO LIMITATIONS

FINAL REPORT
10/19/2012

Submitted by

M. Ala Saadeghvaziri, Shabnam Darjani, Sunil Saigal, and Ali Khan

Department of Civil and Environmental Engineering
New Jersey Institute of Technology
University Heights, Newark, NJ 07102-1982

NJDOT Research Project Manager
Nazhat Aboobaker, Ph.D.

In cooperation with

New Jersey
Department of Transportation
Bureau of Research
and
U.S. Department of Transportation
Federal Highway Administration

DISCLAIMER STATEMENT

"The content of this report reflects the views of the author(s) who is(are) responsible for the facts and accuracy of data presented herein. The contents do not necessarily reflect the official views or policies of the New Jersey Department of Transportation or the Federal Highway Administration. This report does not constitute a standard, specification, or regulation."

TECHNICAL REPORT
STANDARD TITLE PAGE

1. Report No.	2. Government Accession No.	3. Recipient's Catalog No.
FHWA-NJ-2012-009		

4. Title and Subtitle

DESIGN FOR DEFLECTION CONTROL VS. USE OF SPECIFIED SPAN TO DEPTH RATIO LIMITATIONS

5. Report Date

10/19/2012

6. **Performing Organization Code**

7. Author(s)

M. Ala Saadeghvaziri, Shabnam Darjani, Sunil Saigal, and Ali Khan

8. Performing Organization Report No.

9. Performing Organization Name and Address

Department of Civil and Environmental Engineering
New Jersey Institute of Technology
University Heights
Newark, NJ 07102-1982

10. Work Unit No.

11. Contract or Grant No.

NJDOT 2012-009

12. Sponsoring Agency Name and Address

N.J. Department of Transportation
1035 Parkway Avenue
P.O. Box 600
Trenton, NJ 08625-0600

Federal Highway Administration
U.S. Department of Transportation
Washington, D.C.

13. Type of Report and Period Covered

Final Report

Jan 2009 – Oct 2012

14. Sponsoring Agency Code

15. Supplementary Notes

16. Abstract

High performance steel (HPS) are more durable and stronger, thus, it will result in designs that are more flexible / economical. However, the serviceability requirements on deflection can control the design of such sections due to their flexibility. This is a flaw in existing serviceability criterion that negates applications of HPS. The criterion is almost a century old and does not appear to be based on rational and/or scientific principles. This project through a comprehensive parameter study using finite element method, proposes changes to existing NJDOT Design Manual; and more importantly provides a more rational serviceability criterion that ensures human safety and structural performance while allowing for application of HPS.

17. Key Words	18. Distribution Statement
Highway Bridges, Deflection, Serviceability, HPS	No Restrictions.

19. Security Classification (of this report)	20. Security Classification (of this page)	21. No of Pages	22. Price
Unclassified	Unclassified	119	

Form DOT F 1700.7 (8-69)

ACKNOWLEDGEMENTS

This research and development study was supported by the New Jersey Department of Transportation and the Federal Highway Administration. The results and conclusions are those of the authors and do not necessarily reflect the views of the sponsors.

TABLE OF CONTENTS

Page

LIST OF TABLES

Page

LIST OF FIGURES

Page

EXECUTIVE SUMMARY

Over the past couple decades there have been significant developments in availability of new materials and technologies suitable for civil infrastructure such as highway bridges. High performance steel (HPS) is one such a material that offers higher yield strength, enhanced weldability, and improved toughness. As a result of higher strength it can result in lighter and much more economical designs. Furthermore, due to shallower girder depth, HPS can alleviate clearance requirement that is often critical, especially in urban areas. However, live-load deflection and span-to-depth (L/D) limitations of bridge design specifications negate the economical implementation of HPS.

AASHTO Standard Specifications limit live load service deflection to L/800 for general bridges and to L/1000 for bridges that are used by pedestrians. These limits are applied to steel, reinforced concrete, and other bridge types. The AASHTO LRFD Bridge Specifications has made these limitations optional; thus, transferring the responsibility for deflection control and serviceability requirements to the engineer and owner. These limits were originally employed presumably to avoid “undesirable structural or psychological effects due to their deformations.” However, results of prior studies, including a comprehensive study sponsored by NCHRP, indicate that deflection and L/D limits do not necessarily address these objectives. Other bridge response parameters such as acceleration and vibrational characteristics are more important factors affecting psychological discomfort.

Initially literature review was conducted, which highlighted the need for development of the “next generation” serviceability requirements. Thus, the next phase of the research included development of a reliable and effective finite element model to be used in an extensive parameter study. The finite element parameter study included both 2-D and 3-D models. Among the parameters studied are: truck speed, span length, bridge frequency, speed and k parameters (related to previous three factors and the most critical to bridge vibration), damping ratio, number of axles, truck to axle length ratio, number of spans, spatial effect (3-D effect), bracing, and the boundary conditions. Although not specifically among the initial tasks a limited field measurements was also conducted. These were two bridges on I-80E over I-287N and the Smith Road. The former is a steel bridge while the other is a reinforced concrete bridge. Both bridges have similar structural stiffness and satisfy AASHTO deflection requirements. However, their dynamic responses are significantly different highlighting the importance of other parameters to bridge dynamic response. Numerical simulation of bridge acceleration is quite sensitive to modeling assumptions and it is something that has not been investigated in prior work as they are mostly were concerned with only the bridge displacement. Therefore, great effort was devoted to enduring accurate modeling of bridge acceleration under various loading conditions. The study also included several case studies.

As a result of this study recommendations are made to improve existing NJDOT Design Manual. Furthermore, a new and more rational serviceability criterion is proposed that ensures human safety and bridge performance while allowing for application of high

performance materials. The proposed approach will have national implications and is in line with other independent findings. Future research needs to facilitate implementation are also outlined.

BACKGROUND

Through the development and usage of high-strength materials, the design of more flexible bridges is unavoidable. AASHTO Standard Specifications limit live load deflection to L/800 for general bridges and L/1000 for bridges that are used by pedestrians. The exact origin of the existing limits is not known; however, apparently it is used to avoid undesirable structural and psychological effects due to bridge vibration. That is, the intention is to limit vibration and human discomfort through deflection limits.

The use of existing deflection limits negates application of high strength materials, such as High Performance Steel (HPS). For these materials result in designs that are much lighter and shallower (more flexible), thus, have higher global deflection. Research shows when the optional deflection limits are neglected in large span bridges, significant weight and cost savings, up to 20 percent (Clingenpeel 2001, Nagy 2008), may be realized.

Results of prior studies indicate that deflection and L/D limits do not necessarily reduce vibration. Structural performance can be assured by more detailed design criteria that include other important bridge dynamic characteristics rather than simple global deflection check. Human susceptibility is also more influenced by the derivatives of deflection rather than the deflection itself. Although these limits have been made optional, they are still being used by transportation agencies and designers mainly due to the lack of an appropriate and rational guideline that can address bridge vibration and human comfort.

Therefore, there is a need for a more rational bridge vibration control guideline that enhances structural performance and human comfort while allowing the application of high strength materials.

High Performance Steel vs. Conventional Steel

High performance steel (HPS) offers high yield strength (Figure 1), high fracture toughness, good weldability, and the ease of fabrication with the choice of weathering performance (Homma et al. 2008). As a result of higher strength it can result in lighter and much more economical designs. Furthermore, due to shallower girder depth, HPS can alleviate clearance requirement that is often critical, especially in urban areas. However, live-load deflection limits of bridge design specifications negate the economical implementation of HPS.

The fracture toughness of high performance steel is much higher than the conventional bridge steel. Figure 2 shows the Charpy V-Notch (CNV) transition curves for HPS 70W (HPS 485W) and conventional 50W steel. The Charpy V-Notch test is a standardized high strain-rate test which determines the amount of energy absorbed by a material during fracture. This absorbed energy for HPS 70W is much higher than 50W steel at the same temperature.

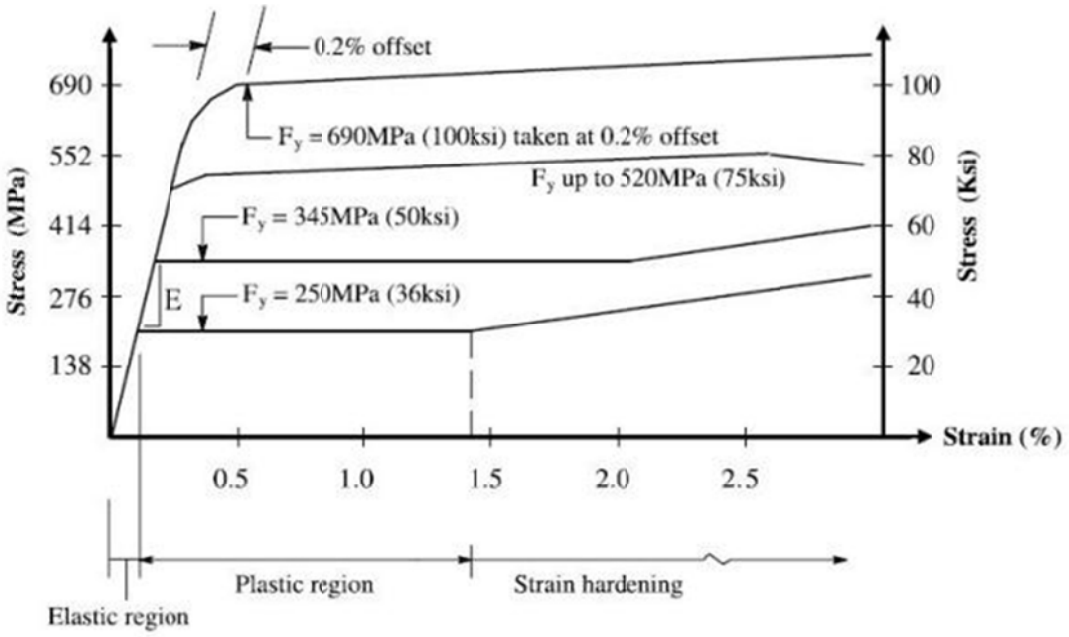

Figure 1. Stress-strain curves for different types of steel (Gergess and Sen 2009).

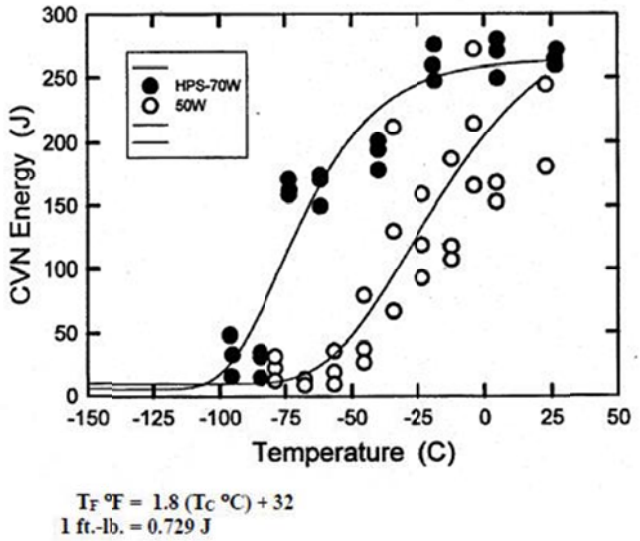

Figure 2. CVN transition curve for HPS-70W (70 ksi) compared to 50W steel (Fisher and Wright 2007)

As it can be seen, the ductile-brittle transition temperature for HPS-70W is lower than 50W steel and HPS provides a toughness level that far exceeds the toughness for convectional steel. Although the cost of these newly invented materials is higher than ordinary grade 50W steel, the advantages due to higher strength are more than the difference in material costs (Dexter et al. 2004).

AASHTO Deflection and L/D Criteria

AASHTO LRFD (2007) Specifications limits live load service I deflection to L/800 for general bridges and to L/1000 for bridges that are used by pedestrians (Article 2.5.2.6.2). The criterion has been made optional since 1998 in AASHTO LRFD while it had been mandatory in earlier editions of AASHTO (AASHTO LFD 1996). As it is mentioned in article C3.6.1.3.2 (C2.5.2.6.1), live load deflection is a service issue (service I) and should be taken as the larger of “that resulting from the design truck alone” or “that resulting from 25 percent of the design truck taken together with the design lane load” (Article 3.6.1.3.2). Deflection should not be controlled for permit truck or heavier trucks which are used for strength limit states. The live load shall be taken from Article 3.6.1.3.2 (article 2.5.2.6.2). The design truck used in deflection control is identical to HS20 truck of past Standard Specifications. HS20 truck is shown in Figure 3 (section 3.6.1.2.2 AASHTO 2007)

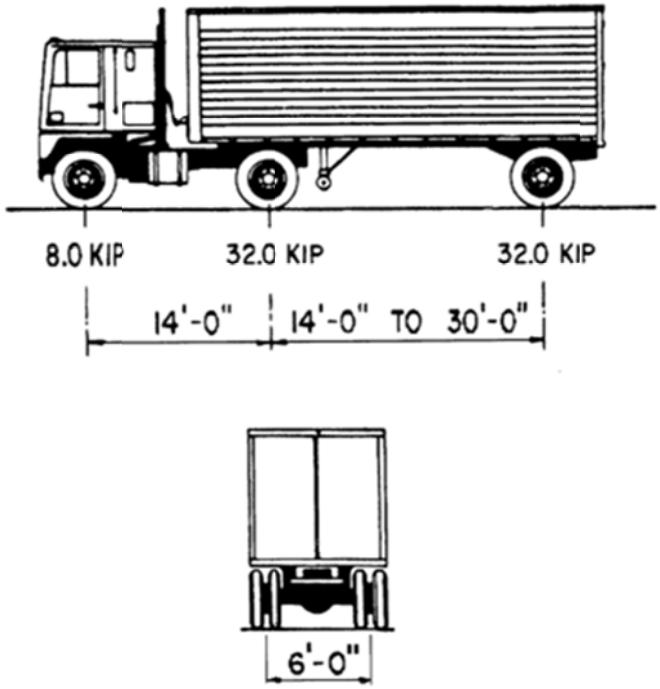

Figure 3. Characteristics of the Design Truck.

The design lane load is equal to 0.64 kips/ft and it is uniformly distributed in longitudinal direction (section 3.6.1.2.4 AASHTO LRFD). Transversely, the design lane load shall be assumed to be uniformly distributed over a 10.0-ft. width. The force effects from the design lane load shall not be subjected to dynamic load allowance (section 3.6.1.2.4 and 3.6.2.1 AASHTO LRFD). Dynamic load allowance, impact Factor, only applies to the design truck and shall be taken as 33 percent of the static load. This value is provided in Table 1 in section 3.6.2.1.1 AASHTO LRFD 2007. According to AASHTO LRFD, field tests indicate that in the majority of highway bridges, the dynamic component of the response does not exceed 25 percent of the static response to vehicles. However, the specified live load combination of the design truck and lane load,

represents a group of exclusion vehicles that are at least 4/3 of those caused by the design truck alone on short and medium span bridges. The specified value of 33 percent in Table 1 is the product of 4/3 and the basic 25 percent (C3.6.2.1 AASHTO LRFD 2007). The factor to be applied to the static load shall be taken as: (1+IM/100).

Table 1 - Dynamic Load Allowance, impact factor (IM).

Component	*IM*
Deck Joints—All Limit States	75%
All Other Components	
• Fatigue and Fracture Limit State	15%
• All Other Limit States	33%

The live load portion of Load Combination Service I of Table 3.4.1-1 (section 2.5.2.6.2, AAHTO 2007) should be used; therefore, live load factor is equal to 1. Exact computation of live load deflection can be complicated for non-prismatic beams (when the cross section is not constant throughout the beam). For non-prismatic beams, deflections are computed using the moment of inertia of the beam at the point of maximum positive moment (Tonias and Zhao 2007).

“The criteria shall be considered optional” except for “orthotropic decks”, “precast reinforced concrete three-sided structures”, and “Metal grid decks and other lightweight metal and concrete bridge decks”. “In the absence of other criteria, the following deflection limits may be considered for steel, aluminum, and/or concrete construction” (Article 2.5.2.6.2).

- One stringer of the bridge with the proportional deck width should be considered for deflection estimation.
- Static deflection for truck can be found by locating the HL-93 truck (HS 20) over the span as shown in Figure 4.
- The deflection due to lane load should be calculated. Lane load is equal to 0.64 kips/ft and is transversely distributed in 10 ft.
- Impact factor which is equal to 1.33 should only apply to the deflection resulted from truck, and not the lane load.
- The deflection should be taken as the larger of “that resulting from the design truck alone” or “that resulting from 25 percent of the design truck taken together with the design lane load”.
- Multiple presence factor and distribution factor should be applied to the deflection obtained from previous step.

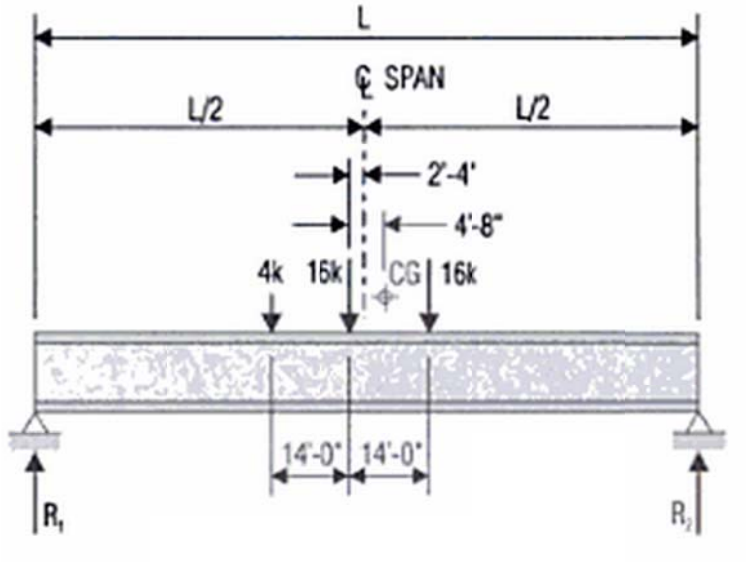

Figure 4. Deflection calculation for AASHTO Design Truck (Tonias and Zhao 2007)

Distribution factor is used to apply the appropriate amount of live load to a single stringer from the standard HL93 loading. AASHTO assumes all stringers deflect equally when calculating live load deflection (section 2.5.2.6.2). “For a multibeam bridge, this is equivalent to saying that the distribution factor for deflection is equal to the number of lanes divided by the number of beams.”

$$\text{Distribution Factor} = \frac{Number\ of\ Lanes}{Number\ of\ Stringers} \qquad \text{Equation 1}$$

The multiple presence factor (Table 2) is applied to reduce the total deflection when there are more than two lanes, assuming not all the lanes are fully loaded (Article 3.6.1.1.2-1)

Table 2 - Multiple Presence Factors, m.

Number of Loaded Lanes	Multiple Presence Factors *m*
1	1.20
2	1.00
3	0.85
>3	0.65

Table 3 shows the values for span-to-depth ratio in AASHTO LRFD (2007).

Table 3 - Minimum Depth for steel bridges

Minimum Depth for Steel Bridges with Concrete Deck	Simple Spans	Continuous Spans
Overall Depth of Composite I-Beam (D)	0.040*L (L/D<25)*	0.032*L (L/D<31)*
Depth of I-Beam Portion of Composite I-Beam (d)	0.033*L (L/d<30)*	0.027*L (L/d<37)*
Trusses (Including deck)	0.100*L (L/D<10)*	0.100*L (L/D<10)*

Deflection Criteria vs. Economical Use of HPS

Deflection control is not usually effective on design for those types of steel with the yield stress less than 50 ksi. However, when the bridge is designed for higher strength steel materials, sometimes, deflection control is the factor which appears to be critical. This is even more critical when higher strength materials such as 100W steel is used for design or for the higher ration of L/D (Azizinamini et al. 2004, Nagy 2008, Roeder 2004). Figure 5 shows the results obtained by Roeder et al. (2004). In this study a typical simply supported bridge with the span length equal to 105 ft and slab width equal to 42.5 ft, with five equally spaced stringers was considered. Slab thickness is equal to 8.5 in, and the distance between stringers is equal to nine ft. Optimal designs were completed for three material configurations including all 50W, all HPS 70W, and a hybrid girder with HPS 70W flanges and 50W webs. Noting that d is the total beam depth, and L is the span length. It can be seen in Figure 5 that with the optimal design and an L/d = 25, the 70W girder fails to meet L/800 deflection criterion and for L/d = 30 all designs fail to meet the L/800 deflection criterion.

Research shows that the use of HPS in bridges is not beneficial if deflection limits being controlled by designers. Homma and Sauce (1995) performed a study on existing highway bridges and redesigned them for HPS of various strength levels. The results indicated that for efficient use of higher strength materials, a certain modification is required for the existing code criteria. Clingenpeel (2001) investigated the economic use of HPS 70W in steel bridge design using various span lengths, girders spacing and yield strength. The parameter study considering weight, performance, deflection, and cost indicate that the most economical use of HPS 70W is a hybrid girder with 70W flanges where a lower number of girders is used. Another study by Nagy (2008) investigates the effect of L/D and the use of HPS on deflection criteria and weight savings. It was shown in this study that span to depth ratio has a significant effect on live load deflection. All of the designs that failed L/800 deflection criteria were hybrid 70W girders with high L/D ratio. A study by Horton (2000) reported a 12 percent cost benefits by using HPS for steel bridges. Figures 6 and 7 show the comparison for different material configurations in this study.

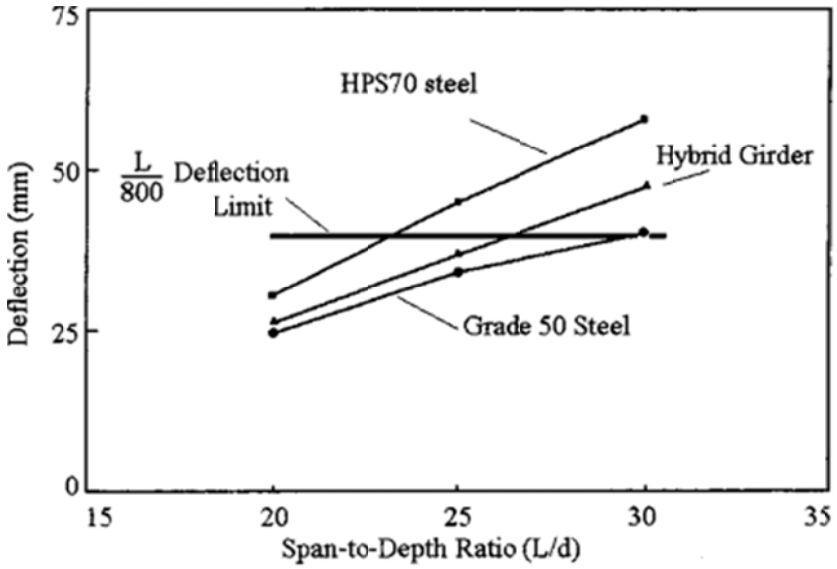

Figure 5. Deflection versus span to depth ratio for Example Bridge (Roeder 2004)

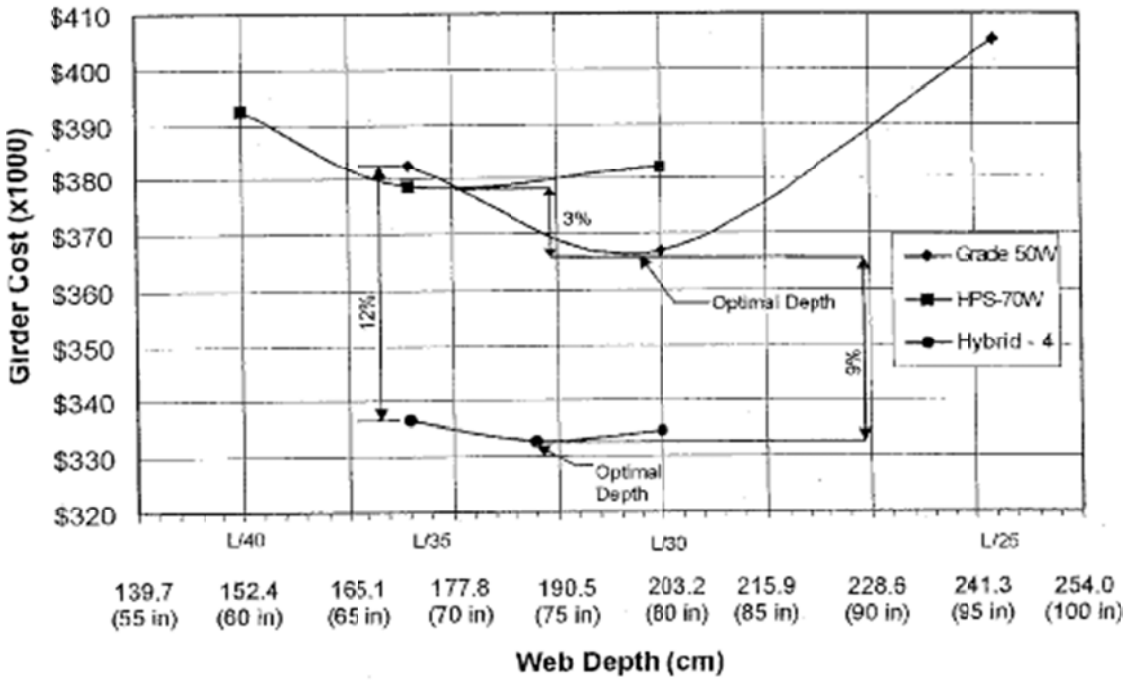

Figure 6. Spans of 200 ft with nine ft girder spacing for three different material configurations

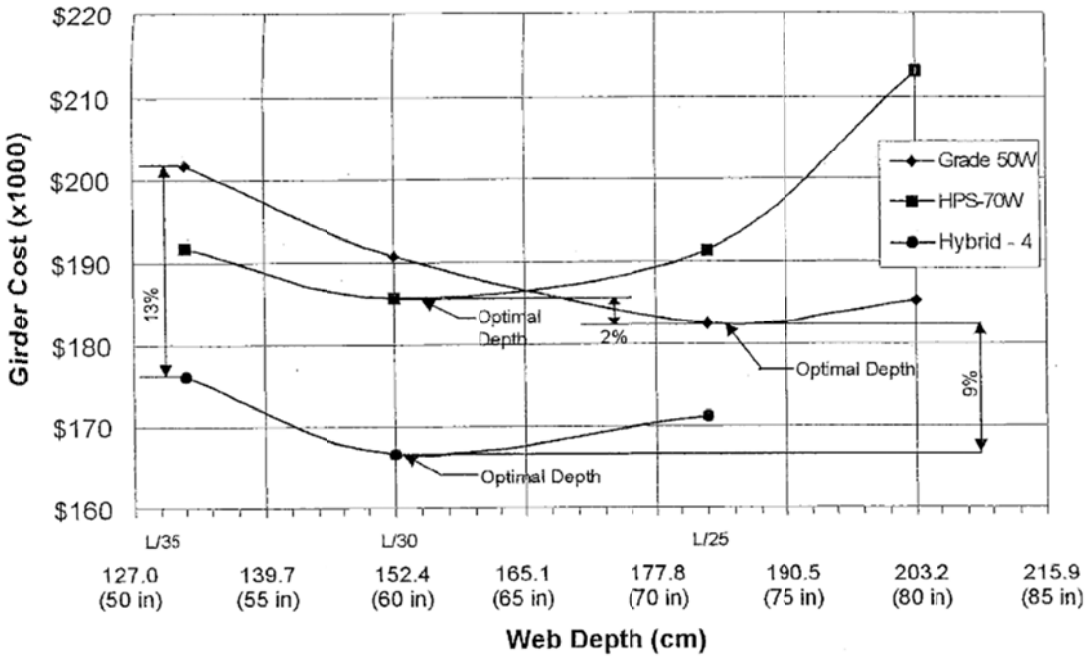

Figure 7. Spans of 150 ft and 12 ft girder spacing for three material configurations

Vibration vs. Deflection Criteria

Initially AASHTO specifications did not have explicit live load limits. In 1930's, Bureau of Public Roads conducted a study on impact of vibration on human. As a result of this study, live load deflection limit, L/800, was added to AASHTO Specifications in 1936 after it was found that steel highway bridges with high vibrations had static deflection greater than L/800 (ASCE 1958, Fountain & Thunman 1987). Detail information on these studies are not available, however, bridges included wood plank decks and the superstructure samples were either pony trusses, simple beams, or pin-connected through-trusses (Roeder 2002).

In 1958, a committee of American Society of Civil Engineering (ASCE 1958) reviewed the history of bridge deflection limits along with a survey of data on bridge vibration, field measurements, and human perception of vibration. Their survey showed no evidence of serious structural damage attributable to excessive live-load deflection. The report states:

> *"The few examples of damaged stringer connections or cracked concrete floors could probably be corrected more effectively by changes in design than by more restrictive limitations on deflection. Both the historical study and the results from the survey indicated clearly that unfavorable psychological reaction to bridge deflection was probably the most frequent and important source of concern regarding the flexibility of bridges. However, those characteristics of bridge vibration which are considered objectionable by pedestrians or passengers in vehicle cannot yet be defined."*

The committee recommended that no changes be made at the time, because those characteristics of bridge vibration which were considered objectionable by pedestrians or passengers in vehicle could not have been defined. They recommended using a more restrictive deflection limit for bridges in which composite action was taken into account in design. It was also recommended that further attempts be made to determine what constitutes objectionable vibration of highway bridges and to develop design criteria which will limit them. Two years later, in 1960, a more conservative limit of L/1000 was added for bridges used by pedestrians. Since then many studies were conducted to address these goals. However, none has been adopted by AASHTO Specifications because of the lack of consensus.

OBJECTIVES

In light of the background information provided and consistent with the project's RFP, the objectives of this research and development project are:

- To evaluate deflection control limits and provide recommendations considering the desire to economically use high performance steel such as HPS 70,
- To verify applicability of the listed span-to-depth ratios and establish ratio limitations that addresses the use for structural steel grades 50 and 70.
- To provide a simple and practical method to calculate bridge vibrational parameters.
- To propose a new and more rational serviceability requirement that will not penalize the use of high performance material while ensuring human comfort and safety.

In support of the above objectives this study will provide the following tasks:

1. Literature search of the current state of the practice.
2. Finite Element Modeling and bridge simulation
3. Parameter study on bridge dynamic response and deflection
4. Evaluation of deflection limits vs. bridge durability and damage.
5. Evaluation of applicability of L/D ratio
6. Case studies on two New Jersey bridges designed with HPS.
7. Field Measurements (this task was not within initial research scope and was added later)
8. Developing new and more rational methods for vibration control and bridge durability.

LITERATURE REVIEW

Deflection limitations, as stated in AASHTO LRFD Bridge Design Specifications, can be traced back to 1871 with a set of specifications established by the Phoenix Bridge Company. These specifications limited the passage of a train and locomotive traveling at 30 mi/h to 1/1200 the span length. In 1905, Railway Engineering Association (AREA) provided that ‘‘pony trusses’’ and plate girders should preferably have a depth no less than 1/10 of the span, and rolled beams and channels used as girders should preferably have a depth no less than 1/12 of the span (Table 4).

> *“If depths less than these are used, the sections shall be increased so that the maximum deflection does not exceed these limits.” (ASCE 1958)*

Table 4 - Depth-to-Span ratios per AREA and AASHTO (ASCE 1958)

Year (s)	Trusses	Plate Girders	Rolled Beams
A.R.E.A.			
1905	1 / 10	1 / 10	1 / 12
1907, 1911, 1915	1 / 10	1 / 12	1 / 12
1919, 1921, 1950, 1953	1 / 10	1 / 12	1 / 15
A.A.S.H.O.			
1913, 1924	1 / 10	1 / 12	1 / 20
1931	1 / 10	1 / 15	1 / 20
1935, 1941, 1949, 1953	1 / 10	1 / 25	1 / 25

In the 1930's the Bureau of Public Roads conducted a study that attempted to link the objectionable vibrations felt on a sample of bridges with bridge properties. As a result of this study, Live load deflection limit, L/800, was added in the 1936 specifications after it was found that steel highway bridges with high vibrations had static deflection greater than 1/800th of the span length. However, the bridges built in that era had wood plank decks, and the superstructures were pony trusses, simple beams, or pin-connected through-trusses (Roeder et al., 2002). These bridges were non-composite, and rarely contained continuous spans. ASTM A7 steel with 33000 psi yield strength was the accepted steel for bridge design and construction (Barker et al., 2008). The L/1000 deflection limit was established in 1960, reportedly, after a baby in a carriage was “awakened while being pushed across a bridge on a bridge”. This more sever deflection limit was established for the bridges open to pedestrian traffic after the mother wrote a complaint letter to the Governor and attributed her baby’s response to the bridge shaking (Fountain and Thunman, 1987). In 1958, a survey conducted by ASCE committee (ASCE 1958) showed no evidence of serious structural damage that could be attributed to excessive deflection.

> *“The few examples of damaged stringer connections or cracked concrete floors could probably be corrected more effectively by changes in design than by more restrictive limitations on deflection. Both the historical study and the results from the survey indicated clearly that unfavorable psychological*

reaction to bridge deflection was probably the most frequent and important source of concern regarding the flexibility of bridges. However, those characteristics of bridge vibration which are considered objectionable by pedestrians or passengers in vehicle cannot yet be defined."

Tilly et al. (1984) found that human were disturbed by vibration long before the bridge damaged structurally. Brown (1977) stated that all bridges except very light bridges were little affected structurally by vibrations though humans may be bothered totally. Nowak and Grouni (1988) have shown that deflection and vibration criteria should be derived by considering human reaction to vibration rather than structural performance. Wright and Walker (1971) reported such limits were based on the reactions of people to the bridge vertical acceleration. Therefore it had been concluded that the deflection limitation was an issue to avoid unfavorable psychological reaction due to bridge vibration than to provide more structural durability for bridge structures. It is now generally agreed that the primary factor affecting human sensitivity is acceleration, rather than deflection, velocity, or the rate of change of acceleration for bridge structures (AASHTO 2003; Billing and Green, 1984; Postlethwaite, 1944; Blanchard et al., 1977). On the other hand, calculating deflection was much easier than calculating acceleration of the bridge. Therefore, it has been more practical to limit the deflection. Table 5 shows the development of deflection criteria from 1871 to 1960.

Table 5 - Evaluation of deformation requirements in bridge design.

Year	Agency	Deflection Limits
1871	PBC	1/1,200 of span length (at train speed: 30 mph)
1936	Bureau of Public Roads	1/800 of span length (for vibration controls)
1938	AASHO	1/800 of span length
1960	AASHTO	1/1000 of span length (for pedestrian bridges)

Vibration and Human Comfort

In 2002, NCHRP conducted a study on live load deflection. The study was conducted by Roeder et al. and provided a comprehensive review on literatures the results of which were reported in this study. According to literatures (ASCE, 1958; Nowak and Grouni, 1988; Write and Walker, 1971; Nevels and Hixon, 1973; Goodpasture and Goodwin, 1971, PCA 1970; Roeder et al., 2002), there is no evidence of serious damage on bridge structures due to flexibility while the damage is invariably a consequence of local deformations such as connection rotations and twisting of cross beams relative to support members; therefore, deflection criteria should be derived by considering human reaction to vibration rather than structural performance. It has been noted in literatures

that human discomfort can be classified as either physiological or psychological. Psychological discomfort is caused by unexpected motion while physiological discomfort results from a low frequency, high amplitude vibration such as seasickness (Roeder et al., 2002; Wright and Green, 1959). There is a general agreement that human response to vibration is subjective and it is not directly measurable. However, it can be reported as perceptible, unpleasant, and tolerable.

In general, several factors influence the level of perception and the degrees of sensitivity of people to vibration. Among them, one can note position of the human body, excitation source characteristics, exposure time, floor and deck system characteristics, level of expectancy and type of activity engaged in (Moghimi 2008; Wiss 1974; Smith 1988).

A survey of highway bridges' users in the USA (Smith, 1988) indicated that, in the majority of cases, reports of disturbing vibration come from pedestrians. It appeared that the reason for this is that the drivers and passengers inside the vehicles seldom notice the oscillations of bridges, perhaps because their vehicle's normal vibration obscures these. Oehler (1970) confirmed this and stated that only pedestrians or occupants of stationary vehicles objected to bridge vibration. Furthermore, it has been shown (Smith, 1988; Moghimi, 2008) that pedestrians are less susceptible to the vertical component of vibration when walking than when standing. Human beings can tolerate less vibration vertically than in any other directions (Postlethwaite 1944). Besides, because of the frequent occurrences in bridge due to moving loads, this structure is generally rigid in the horizontal plane (except the wind-induced horizontal oscillation occurring in very long suspension bridges). Therefore, human response to bridge vibration is directly related to the characteristics of vertical motion of the bridge (Irwin, 1978; Machado, 2006). People do not respond to vibration which persists for fewer than five cycles (Wright and Walker, 1971). Therefore, only the dynamic component of the bridge motion, which does persist for a number of cycles after the loading leaves the bridge, is of the concern for human response. That is why people are less susceptible to vibration damped out rapidly (Wright and Walker, 1971). Bridge damping ratio is relatively small and it is from 1 percent to 6 percent . British code recommends considering damping ratio of 0.03 for steel bridges, 0.04 for composite bridges, and 0.05 for concrete bridges (Brown, 1977).

Scales of Vibration Intensity

Among the existing criteria for perceptible vibration, the displacement amplitude of the bridge under truck load was the main concern in several studies (Reiher and Meister 1931; Goldman 1948). It was because of that calculating deflection was much easier and more practical than calculating other characteristics of vibration. Most of these research projects were upon floor and footbridge vibrations. Reiher and Meister (1931) suggested a base curve for acceptable human response to the vibration (Figure 8). In this curve, displacement amplitude is limited for various frequencies, and human response was ranged from imperceptible to very disturbing.

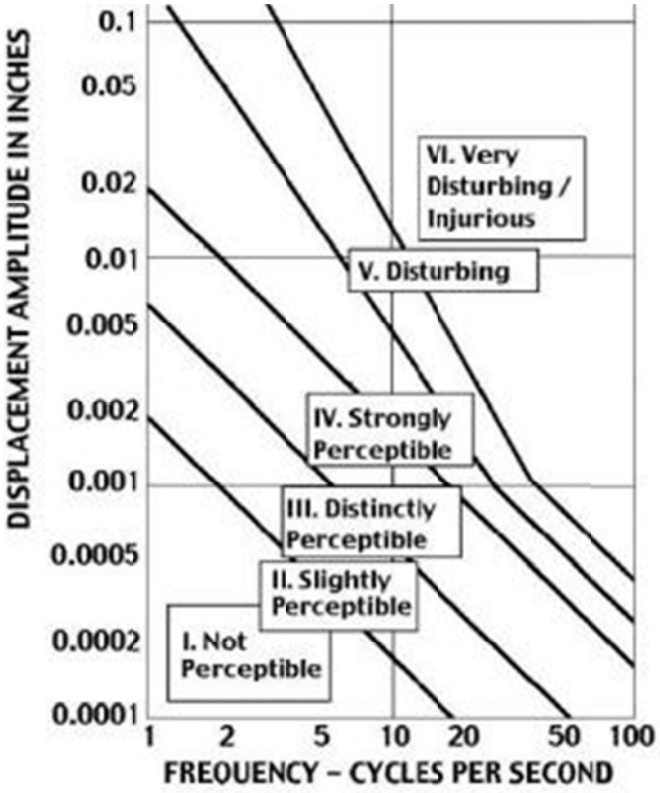

Figure 8. Human perceptible vibration according (Reiher and Meister 1931)

In 1948, Goldman tried to construct perception curves by combining experimental results of different authors including Reiher and Meister (1931) and presented a set of revised averaged curves (Figure 9) corresponding to three tolerance levels:

- The threshold of perception,
- The threshold of discomfort, and
- The threshold of tolerance (Machado, 2006).

Higher values of vertical motion are acceptable in bridges, when compared to residential or office buildings, because users are out in the open and are more aware of the presence of wind or traffic. Furthermore, people crossing a bridge are exposed to vibration for a relatively short period of time (Moghimi 2008). One of the first efforts which investigated human response to Bridge Vibration was made by Janeway (1950). He limited the product of vibration amplitude and cubic frequency, $\mathbf{af^3}$, to 2, for frequencies from 1 Hz to 6 Hz, and the product of vibration amplitude and squared frequency, $\mathbf{af^2}$, to 1/3 for frequencies from 6 Hz to 20 Hz (Machado, 2006). However, during a field test done by Oehler (1957) 34 spans were investigated to examine Janeway's suggestion, and the results were not in agreement with Janeway's suggestion. The product of amplitude and frequency, **af**, is investigated in another study (Wiss and Parmelee, 1944) and the range was found from 0.018 to 0.062 cps-in for distinctly perceptible and 0.18 cps-in for strongly perceptible. Figure 10 shows two

strongly perceptible and unacceptable limits according to Janeway and Wiss and Parmelee. As it can be seen, these two limits overlap for frequencies greater than 2.5 Hz.

Wright and Green (1964) compared the levels of vibration from 52 bridges to levels based on Reiher and Meister's scale and Goldman's work. They showed that 25 percent of the bridges reached the intolerable level indicated by Reiher and Meister's and Goldman's work. They concluded that there was no known scale of vibration intensity which may be directly related to the kind of vibrations experienced in highway bridges. Human reaction to motion was very complex and cannot be consistently described in terms of any single parameter or function. No simple correlation between measures of human reaction to vibration and the principle theoretical and design parameters describing bridge motion was apparent from existing data. Simple geometrical or static considerations such as L/D ratio or deflections due to static live loads did not provide adequate means of controlling undue vibration (Wu 2003).

There were other scales limitation rather than deflection limitation that were suspicious to influence on bridge vibration perceptible by human beings. In a study by Manning, (1981), it is concluded that if the time to travel the span be equal to the fundamental period of the bridge, the maximum dynamic response of the bridge occurs.

Two other studies (Bartos, 1979; Tilly et al., 1984) argue that the natural frequency of the bridge should be out of the range of vehicle natural frequency (1.5-5 Hz); otherwise, unacceptable dynamic effect is unavoidable. Bartos (1979) stated that AASHTO deflection limitation leads most medium span steel bridges to have the natural frequency of 2.5 Hz which coincides with the typical truck frequency. Blanchard, Davies and Smith (1977) recommended using dampers or other means to reduce the response for the bridges with natural frequencies between 4-5 hertz. It is valuable to mention that the maximum deflection in the Ontario Code was reduced to L/450 to reduce the natural frequency of the medium span bridges to 1.5 Hz which is out of the natural frequency of the truck. Also Ontario Code specified raising the impact value if natural frequency of the bridge was in the range of 1.0 to 6.0 Hz (Bartos, 1979).

In Gaunt and Sutton's (1981) study of bridge vibration, it is indicated that human body was sensitive to the derivatives of displacement rather than the displacement. For the frequency range of 1 to 6 Hz, people were most susceptible to jerk value (the first derivation of the acceleration), for frequencies ranged from 6 to 20 Hz, acceleration, and for frequency ranged from 20 to 60 Hz, the value of velocity was affected on human response. Also according to ISO (1989), the frequency for maximum sensitivity to acceleration is in the range of 4 to 8 Hz for vibration in the vertical direction and 0 to 2 Hz for horizontal direction. Furthermore, there are some evidences showing that structures with unpleasant vibration had considerable acceleration and that excessive vibration could not be attributed to low value of displacement observed in those structures. Mallock (Zeivanovic, 2005) investigated some London houses with unpleasant vibrations at 10-15 Hz, and found acceleration level up to 2.3 percent g while the corresponding displacement amplitude was around 0.001 in.

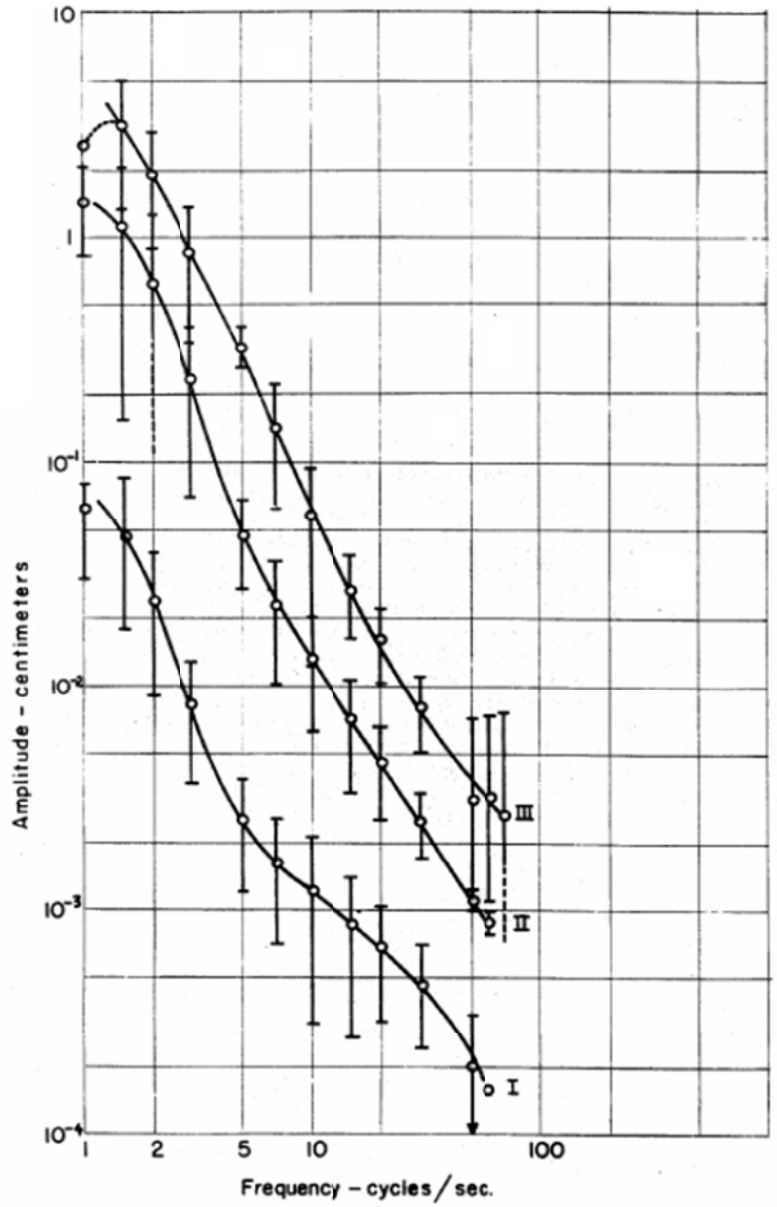

Figure 9. Average amplitude of vibration (Goldman 1948)

Most of the literatures agree with the notion that human response to vibration is more attributed to bridge acceleration rather than other characteristics of the vibration. According to Goldman (1948) the minimum acceleration for human discomfort due to bridge vibration is about 4.6 percent g (18 in/sec2) while the perceptible value is only 0.25 percent g (1 in/sec2). This minimum value occurred around a frequency of 5 Hz which is the main resonant frequency of the human body (Machado 2006). Figure 11 shows a set of revised averaged curves corresponding to three tolerance levels: I, The threshold of perception, II, The threshold of discomfort, and III, The threshold of tolerance (Machado, 2006).

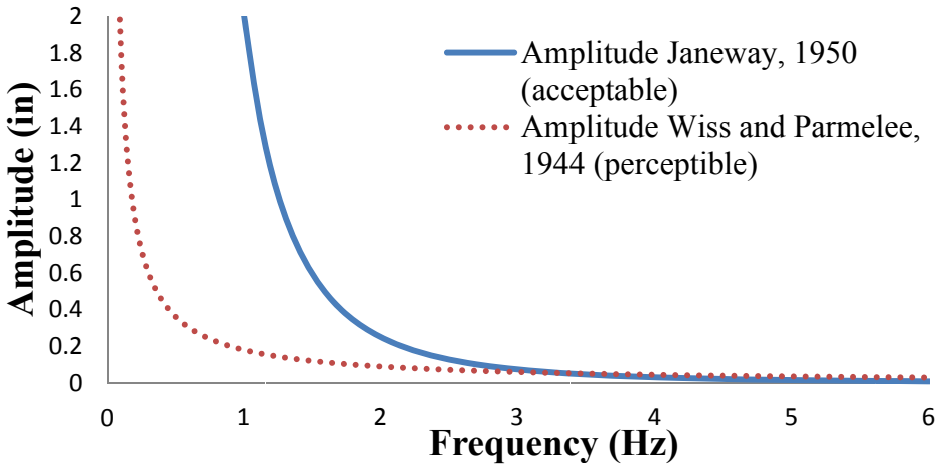

Figure 10. Human perceptible vibration according (Janeway 1950; Wiss and Parmelee 1944)

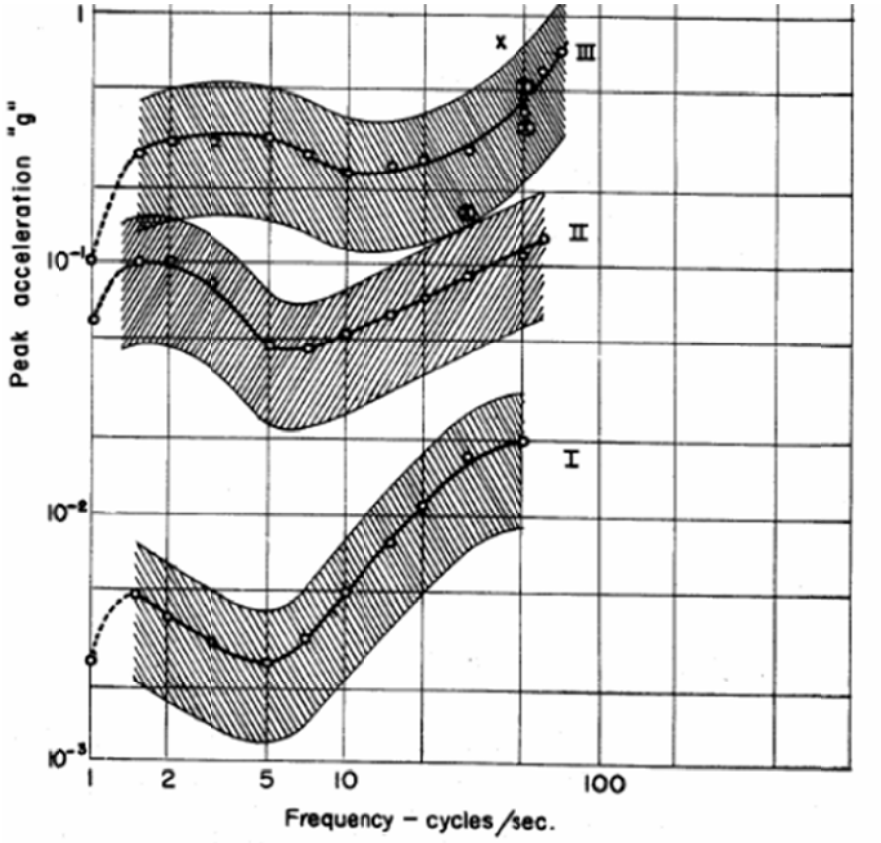

Figure 11. Average peak accelerations (Goldman 1948)

Another study (Postlethwaite, 1941) limited the acceleration to 0.03 percent g for those structures with the natural frequency less than 1 Hz. In the frequency range of 1 to 6 hertz, the value of acceleration for strongly noticeable from 1.5 percent g to 1.8 percent g and for uncomfortable vibrations is from 6 percent g to 16 percent g. During a field study done in 1980 (Billing and Green, 1984), human response was also measured.

The range of accelerations for response was 1.5 percent g to 2.5 percent g for slightly perceptible, 5.2 percent g for distinctly perceptible and 7.6 percent g for strongly perceptible.

A study by Tilly, Cullington, and Eyre (1984) includes a review of British Specification for footbridge written by the British Standard Institution. The acceleration is limited to one-half the square root of the first bending frequency for frequencies up to 4 Hertz (this limit of 0.5 f ½ was developed primarily for pedestrian bridges). For frequency between 4 to 5 hertz, a reduction factor is applied to the bridge response and for frequency higher than 5 hertz, a bridge is too difficult to excite therefore vibration can be ignored. These limits are also suggested by Blanchard, Davies and Smith (1977).

Figure 12 shows the comparison between three different codes in terms of acceleration limits to control undesirable bridge vibration, British Specification, Ontario code and ISO. According to ISO, at vibration magnitude below the relevant curve, complaints regarding vibration are rare, and therefore these magnitudes can be regarded as acceptable limits (Moghimi and Ronagh, 2008). Table 6 shows the summary of literature results on acceleration limiting.

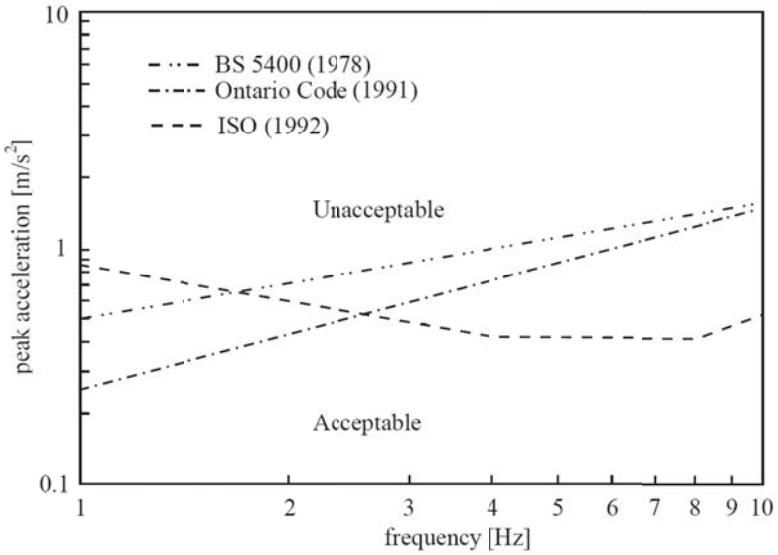

Figure 12. Acceptability of vertical vibrations for outdoor footbridges (Zivanovic et al., 2005)

Among all parameters affecting bridge acceleration, surface roughness and vehicle velocity have the most significant effect on bridge acceleration for both simple and continuous span bridges (Amaraks, 1975; Dewolf, 1997). Vehicle speed was found to have the greatest effect on the maximum girder acceleration and also can influence on the maximum deflection up to 40 percent (Dewolf, 1997). The acceleration due to surface roughness can be as much as five times of smooth surface (Amaraks, 1975). Dewolf (1997) reported that deflection changed 5-12 percent when surface roughness changed from smooth to one inch surface roughness amplitude, while acceleration increased by 50 to 75 percent .

Span length is another parameter which contributes to bridge acceleration. Span length also is a parameter to evaluate bridge longitudinal flexibility. The longer span results in the more flexibility in bridge superstructure and acceleration increases by flexibility. However, flexibility was found to have a minor influence on overall dynamic bridge behavior compared to surface roughness and vehicle speed (Amaraks, 1975; Dewolf, 1997). Initial oscillation of the vehicle suspension was also investigated in these two studies. It was found that initial oscillation caused 30 to 50 percent increase in maximum acceleration (Amaraks, 1975) and increased the maximum deflection by 2.5 times (Dewolf, 1997).

Table 6 - Summary of literature results on acceleration limitation.

Study by	Postlethwaite (1941)		Billing and Green (1984)	Goldman (1948)	British* (1978)	Ontario (1991)	ISO (1989)
frequency	< 1 Hz	1-6	___	5	5	5	5
Slightly Perceptible	___	1.5-1.8 % g	1.5-2.5% g	0.4%g	___	___	___
Distinctly Perceptible			2.5-5.2% g		___	___	___
Strongly Perceptible			5.2-7.6% g		___	___	___
acceptable	0.03% g	1.8-6 % g	___	8%g	11% *	8% g	5% g
uncomfortable	___	6-16% g	___	___	___	___	___
Tolerance	___	___	___	50% g	___	___	___

*For frequency between 4 to 5 hertz, a reduction factor is applied to the bridge response. This value is without considering reduction factor.

Number of axles moving on the bridge was another aspect which was considered in Amaraks study. The results indicated that maximum accelerations were approximately the same for two and three axle vehicle model, but were about two third of the magnitudes produced by the single axle vehicle model.

Contrary to acceleration that most of the researchers tried to limit it as a concern associated with human comfort, in a few research, limiting velocity was suggested to control bridge vibration. Manning (1981) recommended that the velocity amplitude be no greater than 0.2 in/sec, and New Zealand (1994) Bridge Manual limited maximum vertical velocity to 2.2 inch/sec to control vibration (Walpole, 2001; Wu 2003).

Vibration and Structural Performance

Although research show there is no evidence of damage that can be directly attributed to the bridge excessive deflection, there is a presumption that limiting deflection controls the excessive vibration which can contribute to fatigue failures and concrete deck problems. Vibrations have become an increasingly important factor in the design of bridges due to the development of high strength materials which result in lighter structures and slender members. Results of previous studies show bridge damages could not be reduced by limiting vibration through deflection limitation and that there should be better ways to limit vibration than to limit deflection.

Damage in bridge superstructure can be classified as damages in steel girders, connections and concrete deck. Field tests and investigations of damaged structure indicate that cracking is more common in steel girder webs close to connections, and concrete bridge decks in negative moment region over interior supports.

Cracking of plate girder webs is one of the most common damage in bridges and occurs in the gap between the web stiffeners and the girder flanges (Figure 13). Among thirteen damaged bridges investigated in a study done by Roeder et al. (2002), six were included to suffer from this kind of damage and all except one of them passed the AASHTO deflection check.

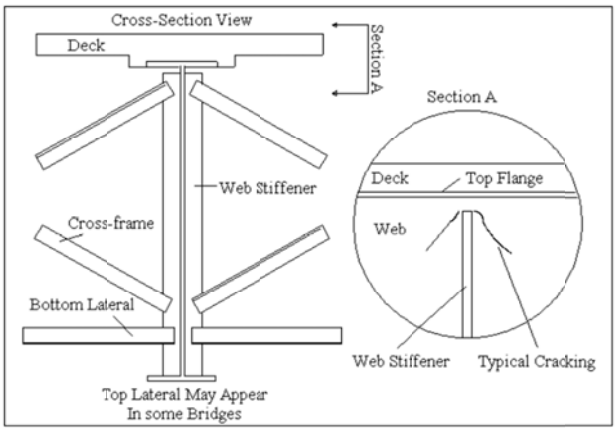

Figure 13. Typical Web Cracking at Diaphragm Connections (Roeder et al., 2002)

This damage is caused by differential girder deflections due to unequally loaded lanes. When one lane is loaded while the others are unloaded, the differential deflection between girders under the load and adjacent girders induces local stresses at the diaphragm to girder connection. Figure 14 shows the relative deflection between girders. To decrease this kind of damage, more flexibility in girder web to out of plane bending and less stiffness in diaphragm connection can be beneficial (Roeder et al., 2002). This cracking is also called as out of plane distortional fatigue in most studies (Fisher 1990, Nishikawa et al., 1998).

Another type of web cracking can be seen in stringer cross beams. This is due to the relative stiffness of the stringers, cross beams, the primary superstructure and their connections. All three bridges with this type of damage in Roeder's (2002) study did satisfy the standard deflection check and even more restrictive criteria enforced by the states. Global deflection limits cannot prevent this type of damage and there is also no clear method for controlling differential stiffness between stringers and cross beams. Figure 14a shows the cross beam deformation due to relative deflection of two adjacent girders. As it can be seen girders are too stiff to deform in lateral direction while cross beam is flexible enough to deform easily. If the cross beam is unrestrained against twisting, cracking may occur at the cross beam-superstructure connection and this damage is caused by the differential twist rotation of the cross beam relative to the small rotation and deformation expected in the bridge superstructure (Roeder et al., 2002).

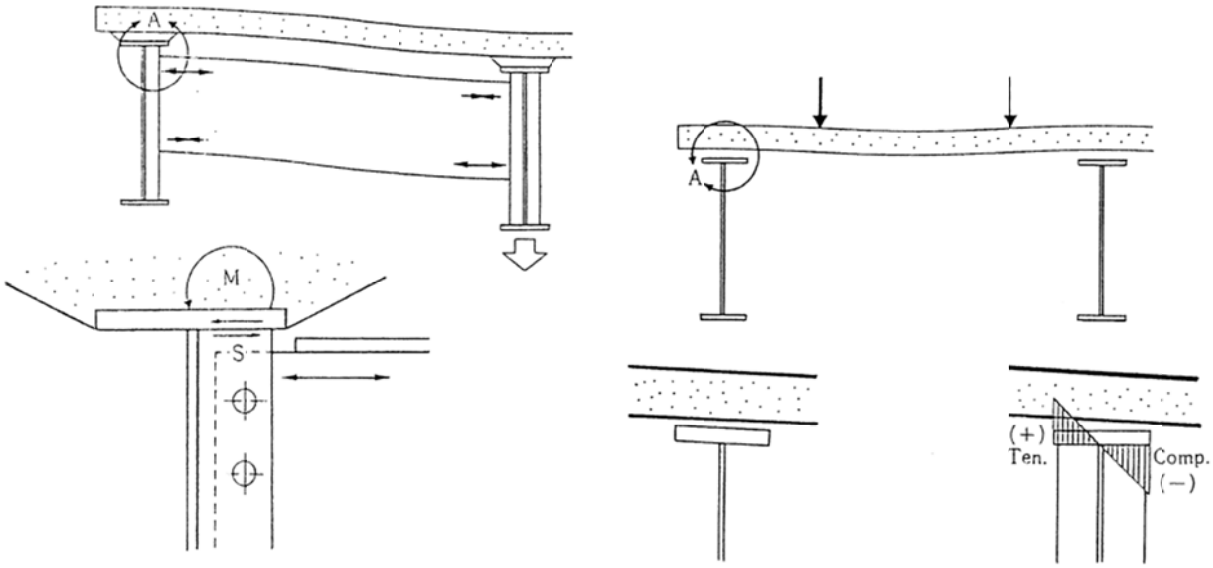

Figure 14. **(a)** Typical Relative deflection of main girders. **(b)** Deflection of reinforced concrete (Nishikawa et al., 1998).

In 1998, Nishikawa et al. investigated fatigue of steel highway bridges in Japan. They indicated that the deck lateral deflection and differential girders deflection significantly influence fatigue-induced girder cracking (Figure 14 and 15). It was concluded that structural details should be designed to prevent fatigue problem due to distortion-induced stress and live load deflection limits might be one of the countermeasures against the distortion-induced fatigue problem. It has to be noted that the problems pointed to in this study (Figure 15) are all related to local rotations and lateral deformations. Therefore, the global deflection limits cannot reduce any of those damages as long as they are caused by transverse flexibility.

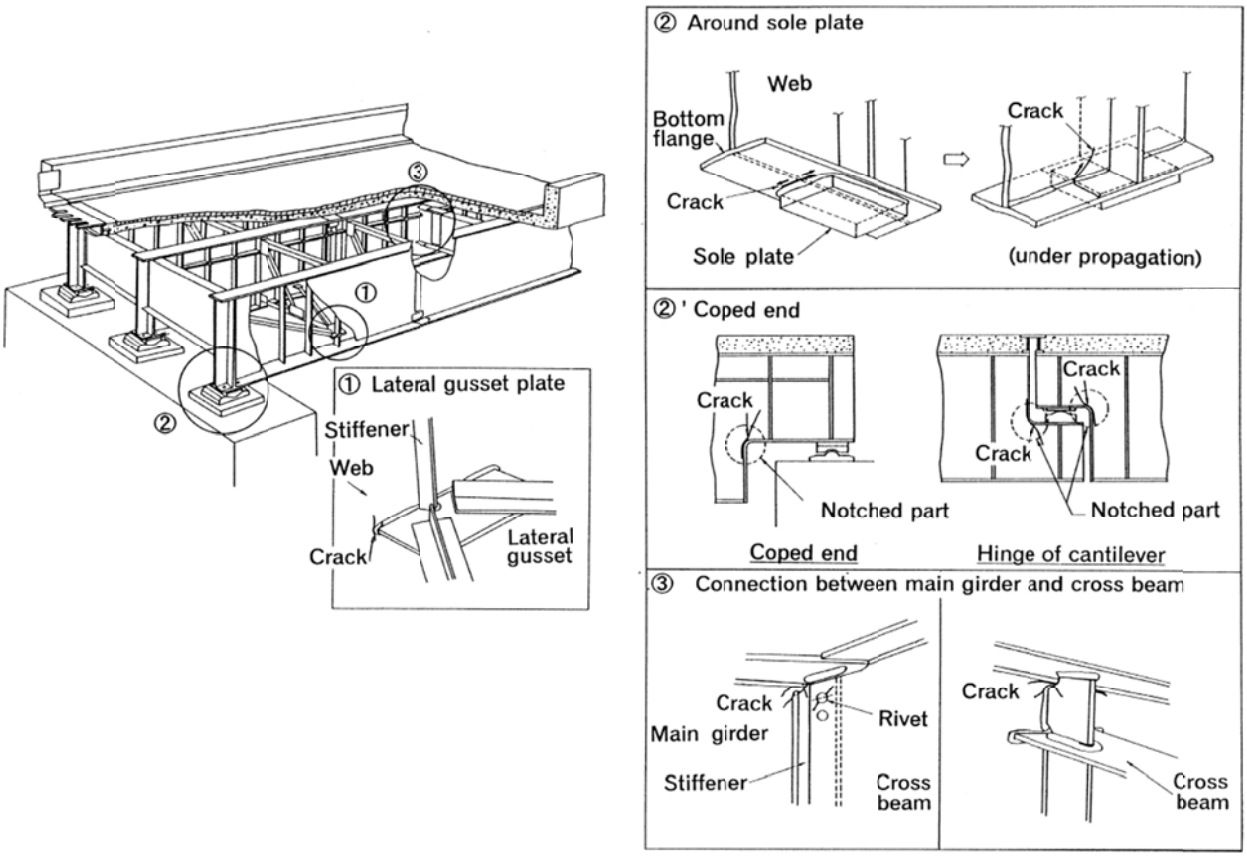

Figure 15. Typical fatigue cracks in plate girders (Nishikawa et al., 1998).

Deck Deterioration

Literature shows that among all bridge damages, only concrete deck deterioration can be attributed to excessive bridge deflection directly and all other damages in bridge structures are caused by local deformation such as connection rotations and twisting or deformation of members relative to each other. According to Roeder et al. (2002), there are four main types of deck deterioration: spalling, surface scaling, longitudinal cracking, and transverse cracking. Spalling is normally caused by corrosion of reinforcement and freeze/thaw cycles of the concrete. Scaling is caused by improper finishing and curing of the concrete and the simultaneous effects of freeze-thaw cycles and de-icing salts.

Longitudinal cracks occur as a result of poor mix design, change in temperature, live load effects and a reflection of shrinkage cracking (Roeder et al., 2002). The slab thickness and distance between girders significantly affects on deck transverse flexibility and directly causes longitudinal cracks in concrete slab. These cracks are distributed throughout the entire length of a bridge deck and do not concentrate on a specific part of the bridge deck (Fountain and Thunman, 1987; Kansas State Highway Commission, 1965; and Krauss and Rogalla, 1996; Roeder et al., 2002).

Zhou et al. (2004) applied a Finite element analysis to investigate the effect of transverse flexibility on deck cracking. In their study the effect of slenderness ratio, connection between girders due to diaphragm and composite interaction between steel girders and concrete deck are investigated. It is concluded in this study that transverse flexibility significantly influences on longitudinal deck cracking. The slenderness ratio is defined as:

$$\lambda = S_g / t_s$$

Where, S_g is the distance between girders and t_s is the slab thickness. The value of stresses shown in Figure 16 indicates how lateral flexibility affects longitudinal cracking.

When composite interaction is taken to account the stresses in concrete deck are half of the stresses in the case without considering composite interaction. Furthermore, connections between girders through diaphragms significantly reduce stresses in concrete deck. Therefore, what influences longitudinal cracking is related to deck transverse flexibility and limiting flexibility in longitudinal direction does not help to reduce this kind of cracking.

Transverse deck cracking is the most possible categories where the existing deflection limit may be beneficial to prevent damages. This kind of deck cracking is observed to be located in negative moment region over interior supports in continuous spans. Since limiting the overall deflection would limit the negative bending moments, it may provide a beneficial effect to reduce this type of cracking. In Roeder's (2002) study, among thirteen bridges, only two of them were observed to have this kind of damage. Moreover, this cracking is also attributable to plastic shrinkage of the concrete, drying shrinkage of the hardened concrete combined with deck restraint, settlement of the finished plastic concrete around top mat of reinforcement, long term flexure of continuous spans under service loads, traffic induced repeated vibration, and environmental phenomenon (Roeder et al., 2002).

Krauss and Rogalla (1996) surveyed 52 transportation agencies throughout the US and Canada and conducted analytical, field and laboratory research as noted by Roeder et al. (2002). The survey was sent to develop an understanding of the magnitude and mechanistic basis of transverse cracking in recently constructed bridge decks. The stresses were examined in more than 18000 bridges by analytical parametric study. The longitudinal tensile stresses in the concrete deck, which result in transverse cracking, were largely caused by concrete shrinkage and changing bridge temperature and, to lesser extent, traffic. It was concluded that cracking is more common among multi span continuous steel girder structures due to restraint provided by joints and bearings, and the less likely to have deck cracking for concrete girder bridges where deck and the girders shrink together. It was felt that reducing deck flexibility may potentially reduce early cracking (Wu, 2003; Roeder et al., 2002). This ia also among the recommendations and conclusions of a comprehensive study conducted by Saadeghvaziri and Hadidi (2002, Hadidi & Saadeghvaziri 2005).

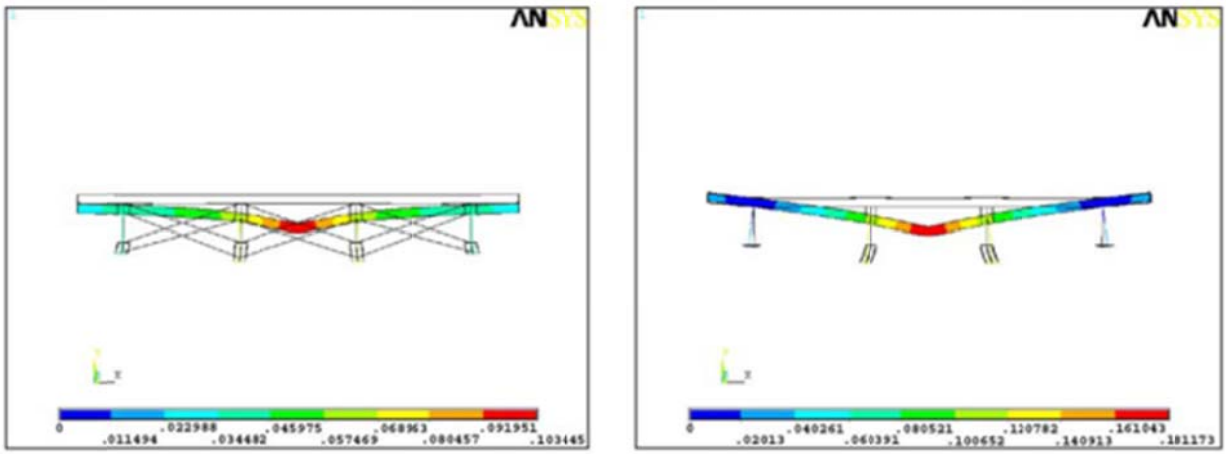

(a) Non-composite deck–with and without diaphragm

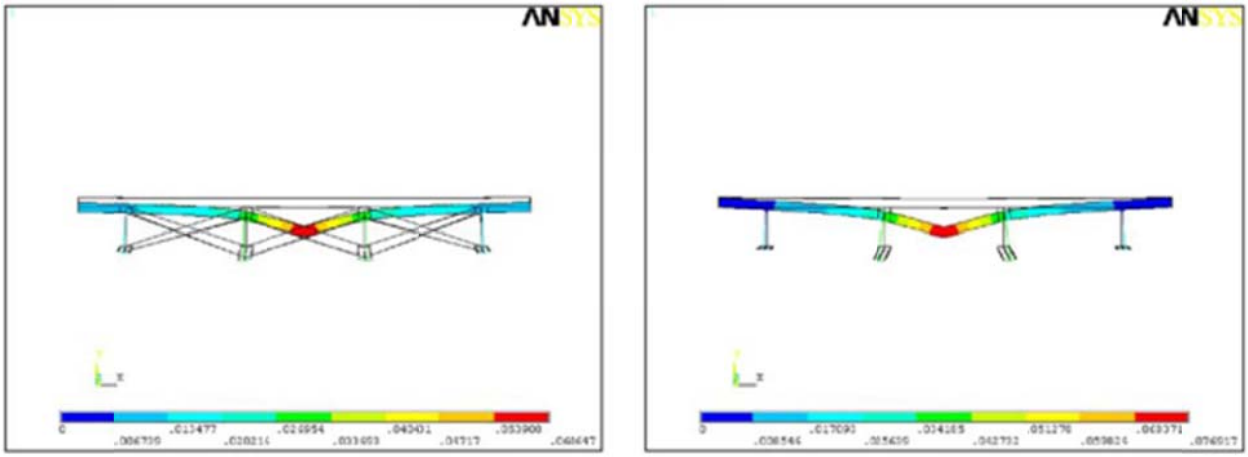

(b) composite deck–with and without diaphragm

Figure 16. Deformed configuration under 3000 lb load at the center (Zhou et al., 2004)

Bridge flexibility in longitudinal direction is different from transverse direction. Span length, type of supports, and composite interaction influence on longitudinal flexibility; while transverse stiffness is attributed to slenderness, composite interaction and connection between girders through diaphragms. Although some statistical studies reported deck cracking due to excessive span length and flexibility, more accurate studies show no evidence of deck deterioration due to the longitudinal flexibility (Goodpasture and Goodwin 1971; Novels and Dixon 1973; and Wright and Walker 1971).

Goodpasture and Goodwin (1971) investigated 27 bridges to determine which type of bridges exhibited the most cracking. These bridges including plate girders, rolled beams, concrete girders, pre-stressed girders, and trusses. The effect of stiffness on transverse cracking was evaluated for 10 of the continuous steel bridges. No correlation between girder flexibility and transverse cracking intensity could be established.

Nevels and Hixon (1973) completed field measurements on 25 I-girder bridges to determine the causes of bridge deck deterioration. The total sample of 195 bridges consisted of simple and continuous plate girder and I-girder as well as prestressed concrete beams with span lengths ranging from 40 to 115 ft. The work showed no relationship between flexibility and deck deterioration.

In 1970 a study by Portland Cement Association in corporation with Federal Highway Administration, FHWA, (PCA 1970; and Fountain and Thunman 1987) provided substantial evidence of no correlation between bridge type and either the amount or degree of deck deterioration. In 1995 another study funded by PCA (Dunker and Rabbat 1990 and 1995; Roeder, 2002) claimed that steel bridges have greater damage levels than concrete bridges due to greater flexibility and deflection. Roeder et al. (2002) argue that since no bridges were inspected and the condition assessment and the statistical evaluation were based entirely upon the National Bridge Inventory data, there are several reasons for questioning this inference. First, the damage scale in the inventory data is very approximate, and the scale is not necessarily related to structural performance. Second, the age and bridge construction methods are not considered in the statistical evaluation. It is likely that the average age of the steel bridges is significantly older than the prestressed concrete bridges used for comparison. Therefore, any increased damage noted with steel bridges may be caused by greater wear and age and factors such as corrosion and deterioration. Finally, there are numerous other factors that affect the bridge inventory condition assessment. As a consequence, the results of this study must be viewed with caution.

Another survey conducted by New York Department of Transportation (Alampalli, 2001) to investigate the correlation between bridge vibration and bridge deck cracking. The study was limited to New York State steel girder superstructures built between 1990 and 1997. Of the 384 bridge spans (233 Bridges) inspected, 242 exhibited some form of cracking. 227 decks cracked transversely, 44 cracked longitudinally, and 29 bridge decks exhibited both forms of cracking. The effects of span length, traffic volume, type of bearing, and vibration severity were investigated. Since it was not easily possible or practical to quantitatively evaluate/ measure bridge vibration through visual inspection or with simple instrumentation by field personnel, vibration ratings in that study were more subjective and made the results of the study qualitative. The conclusion of this statistical study is as follows:

1. Vibration severity is the most significant parameter influencing bridge deck cracking. Higher severity equates to higher deck cracking. Decks with noticeable vibration cracked most severely.

2. Long spans exhibit more deck cracking than shorter spans.

3. Traffic volume is the least significant factor, of the three considered, in influencing the bridge deck cracking. But, high traffic volume generated more cracking than low traffic volume.

4. Bridge bearing do not influence the deck cracking severity.

5. Bridge with noticeable vibration combined with longer span length exhibited significant bridge deck cracking.

It has to be noted that the deck cracking is not located at the location of maximum deflection, strain or curvature in the bridge girder but located in region of negative bending moment over interior supports and at the ends of outside spans. Negative transverse deck moments lead to tension at the top of the deck and possible deck cracking. Since increasing span length results in less negative moment, negative moments are decreased with increasing flexibility. This cracking may at least be partially caused by restraint provided by joints and bearings (Roeder et al., 2002; Write and Walker 1971).

Wright and Walker indicated no evidence of spalling, scaling or longitudinal cracking to associate with girder flexibility. The results of Wright and Walker's study are shown in Figure 17 where ***H***, is the stiffness parameter and is defined as the ratio of stiffness of the beam, $E_b I_b$, and slab stiffness for the span length, ***L***. In the following equation, ***E, h***, and ***v*** are the modulus of elasticity, thickness, and Poisson's ratio for the deck slab, respectively, and ***h*** and ***L*** are in like units.

$$H = \frac{E_b I_b}{\frac{E L h^3}{12 (1-v)^2}}$$

It can be seen that for the same span length of a bridge, more flexibility (less H) results in less negative moment.

In another study (Fountain and Thunman 1987) it is stated that stiffer deck can produce more cracking because the effects of volume change on the tensile stresses due to deck/beam interaction increase as the beam stiffness increases.

Through the discussion on literature review, it can be concluded that:

- Differential deflection between adjacent girders causes load transfer from girder to girder by the bracing diaphragms and the bridge deck, and this transfer induces local deformation and stresses in the girder web, connections and cross beams which causes cracking.

- Transverse flexibility (slenderness) can cause damage in deck and also can increase differential deflection of adjacent girders and cause damage in girders.

- Negative moment is higher in stiffer supports and less restraint in supports leads to less negative moment over superstructure, therefore deck cracking is increased over the internal supports in continuous spans.

Alternatives Limitations

Since many studies indicated that deflection limitation do not influence on vibration severity, alternative methods were formed to provide better ways to limit vibration.

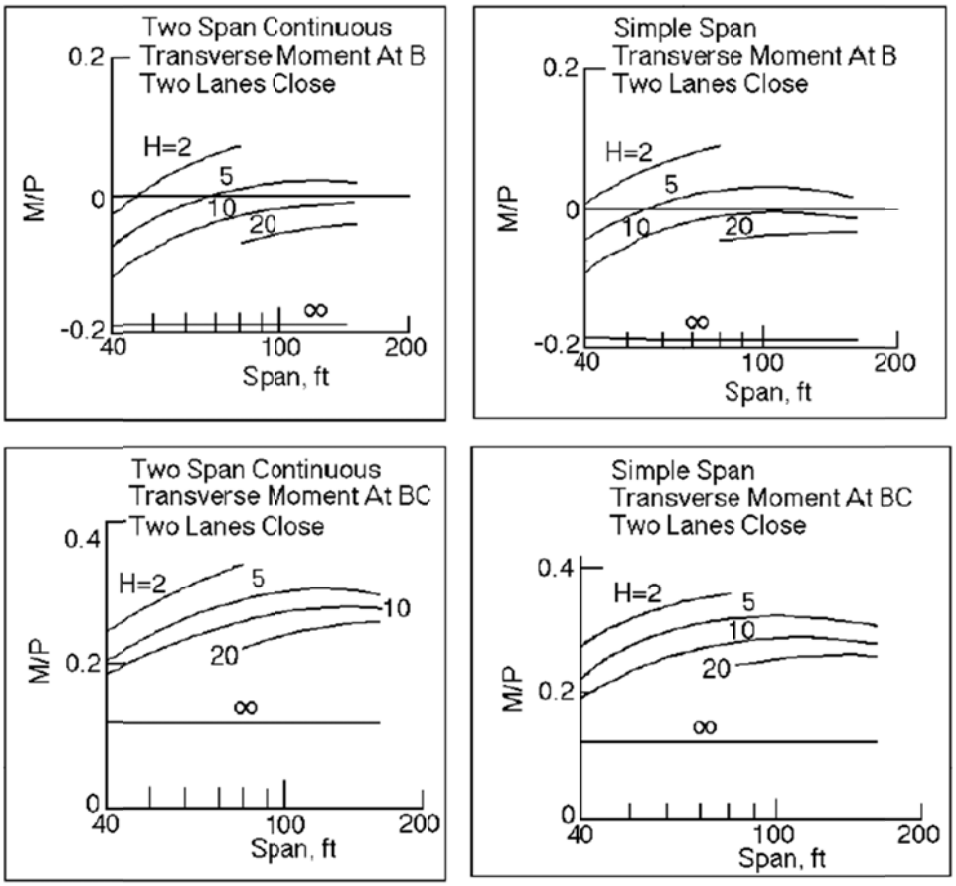

Figure 17. Effect of flexibility on transverse moment in deck (Wright and Walker, 1971)

Canadian Standards and Ontario Highway Bridge Code

In 1976, Ontario's Ministry of Transportation and Communications decided to write its own bridge design code, breaking away from the AASHTO code, because it considered the AASHTO code too conservative (Bartos, 1979).

Static Deflection limitation is based on natural frequency of the bridge in both Canadian Standard and Ontario Highway Bridge code. This relationship was developed from extensive field data collection and analytical studies conducted by Wright and Green in 1964 (Wu 2003; Roeder et al., 2002). It was drawn as a graph (Figure 18) for different types of bridges, without sidewalk, with little pedestrian and with significant pedestrian using sidewalk. The natural frequency can be calculated using equation 2.

$$f_{obs} = 0.95 f_{calc} + 0.072$$ Equation 2

f_{obs} is the natural frequency of the bridge that would be observed in the field, and f_{calc}. is the natural frequency calculated analytically using equation 2.

$$2\ \text{Hz} < f_{calc} = \frac{\pi}{2L^2}\sqrt{\frac{E_b I_b g}{w}} < 7\ \text{Hz}$$ Equation 3

L, E_b, I_b, and w are stringer length, modulus of elasticity, moment of inertia of the steel beam, and weight per unit length of the beam including the concrete slab, respectively.

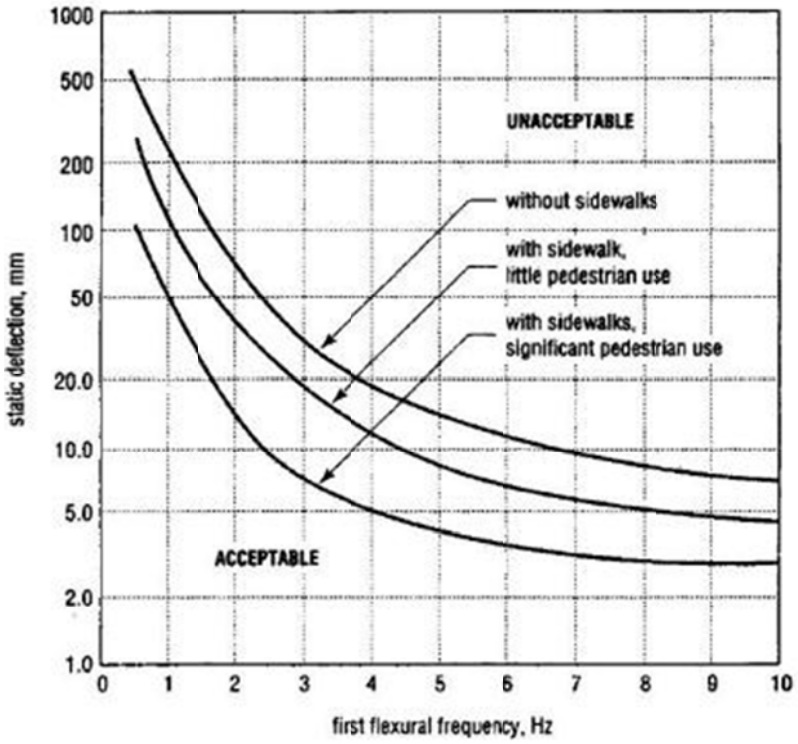

Figure 18. Deflection limits per Ontario Code (Ministry of Transportation, 1991 and CSA International, 2000)

To compute live load deflection in both Canadian Standard and Ontario code, one truck (without considering lane load) is placed at the center of a single lane. Live load factor and dynamic load allowance (Figure 19) must be applied to truck load and gross moment of inertia of the cross sectional area is used in calculation (Roeder et al., 2002, Wu, 2003). To control bridge vibration, Ontario code also limits acceleration through the graph shown in Figure 12.

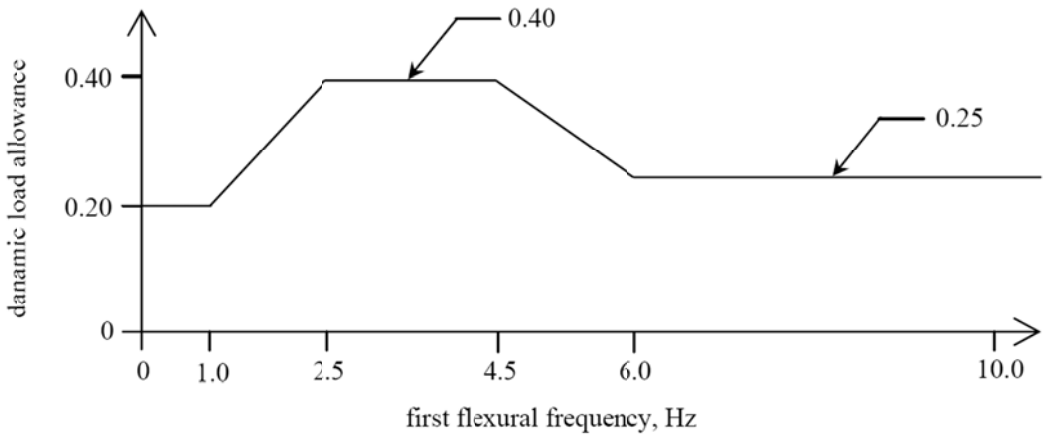

Figure 19. Dynamic load allowance (Ministry of Transportation, 1991 and CSA International, 2000)

European Codes

Most European Common Market countries base their design specifications upon the Eurocodes (Dorka, 2001), which are only a framework for national standards. Each country must issue a "national application document (NAD)" which specifies the details of their procedures. A Eurocode becomes a design standard only in connection with the respective NAD. Thus, there is considerable variation in the design specifics from country to country in Europe. If an NAD exists for a specific Eurocode, then this design standard is enforced when it is applied to a building or a bridge. There is no deflection or additional checks applied for controlling bridge vibration in Europe. However, a “vibration factor” is used to account for full live load in calculating extra stresses due to vibrations in European Bridge Codes. For long span or slender pedestrian bridges, a frequency and modal analysis is also usually performed (Wu, 2003).

British Specification

British Standard Institution (BD 37/01, 2002) limits the bridge acceleration to one-half the square root of the first bending frequency for frequencies up to 4 Hertz for assessing vibration serviceability of bridges. This limit of 0.5 $f^{0.5}$ was developed primarily for pedestrian bridges.

$$a_{\text{limit}} = 0.5\sqrt{f} \quad (\text{m/s}^2)$$

Equation 4

For frequencies between 4 to 5 hertz, a reduction factor is applied to the bridge response and for frequencies higher than 5 hertz, a bridge is too difficult to excite therefore vibration can be ignored. The British code recommends that in design

calculations, a damping value of 0.03 should be used for steel bridges, a value of 0.04 for composite bridges and a value of 0.05 for concrete bridges (Brown, 1977).

Australian Specifications

Australian Specification requires using a curve, shown in Figure 20, to limit the static deflection as a function of the first flexural frequency of road bridges with sidewalk. For many years, earlier versions of Australian code have adopted L/800 deflection criterion to control the deflections of highway bridge girders. This serviceability criterion is assumed to place more emi/hasis on the elastic response of structures to service loads, namely prevented rapid structure deterioration by controlling crack widths under short term loads and controlling vibration as appropriate to the situation (Machaco, 2006).

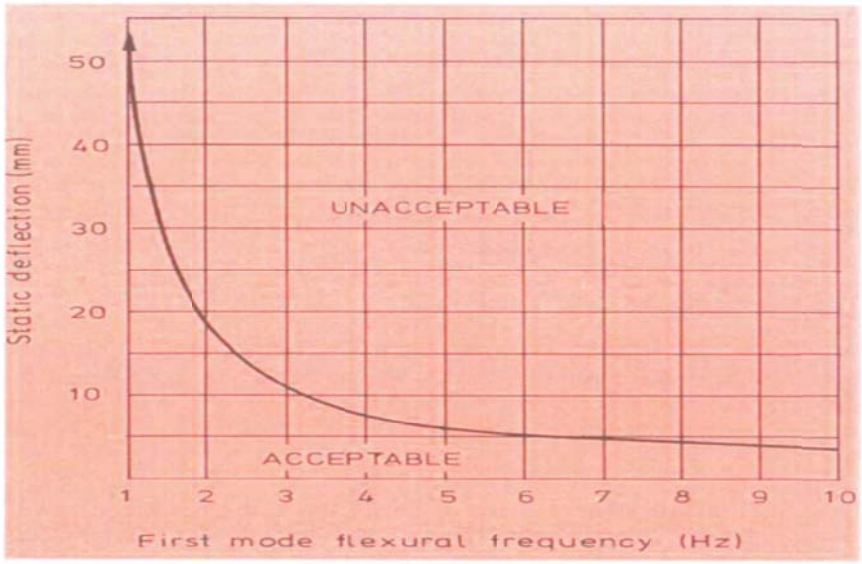

Figure 20. Deflection limits per Australian Code (Wu, 2003)

New Zealand Code

Older version of Bridge manual in New Zealand employed limits on L/D and deflection, but in 1994 version, velocity is limited to 2.2 in/sec under two 27 kips axle loads of one HN unit. This limit is only used for bridges with pedestrian traffic or stationary vehicle traffic (Walpole 2001; Roeder 2002).

International Organization for Standards (ISO)

The International Standards Organization (ISO) recommends vibration limits in terms of peak acceleration via the root-mean-square (RMS) and frequency (Ebrahimpour, 2005). Root-mean-square of the acceleration during time record is defined as:

$$\mathrm{RMS} = \sqrt{\frac{\int_{t_1}^{t_2} \ddot{x}(t)^2 \mathrm{d}t}{t_2 - t_1}}$$

Equation 5

Where $\ddot{x}(t)$ is the acceleration time history, and t_1 and t_2 define the beginning and end of the time interval considered. As shown in Figure 21, a baseline curve is used by ISO and different multipliers are used for different occupancies.

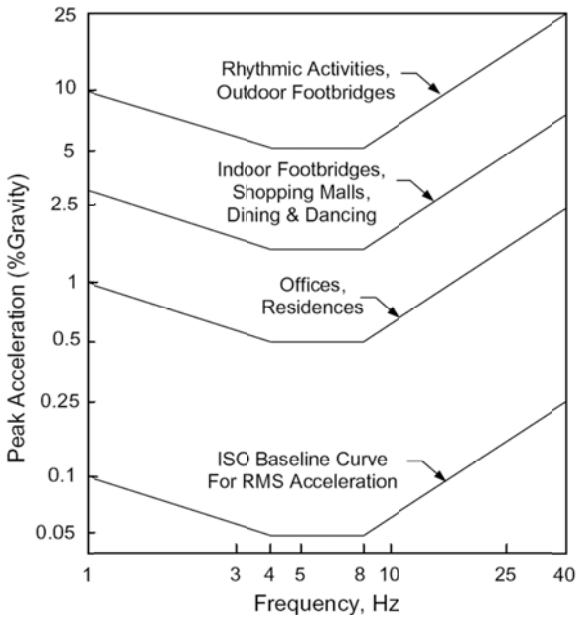

Figure 21. Peak acceleration for human comfort for vibrations due to human activity (ISO 1989).

Wright and Walker:

In 1971, The American Iron and Steel Institute (AISA) formed a study with the objective of reviewing the current AASHTO deflection limits for multi-stringer steel highway bridges. This study conducted by Wright and Walker. They suggested acceleration limitation rather than using deflection limits and proposed a simple formula for calculating bridge acceleration.

$$a = DI\ \delta_s\ (2\ \pi\ f_b)^2$$

Equation 6

δ_s is the static deflection as a result of live-load, with a wheel load distribution factor of **0.7**, on one stringer, or beam, acting with its share of the deck.

f_b, Natural frequency, for both simple span and continuous span is the same and is calculated using eq. 7.

$$f_b = \frac{\pi}{2L^2}\sqrt{\frac{E_b I_b g}{w}}$$ Equation 7

L, E_b, I_b, and ***w*** are stringer length, modulus of elasticity, moment of inertia of the steel beam, and weight per unit length of the beam including the concrete slab, respectively.

DI is impact factor and is calculated as speed parameter plus **0.15**. The determination of speed parameter is half of the vehicle speed divided by the multiplication of span length and natural frequency.

$$DI = \alpha + 0.15$$ Equation 8

$$\alpha = \frac{v}{2 f_b L}$$ Equation 9

If the acceleration exceeds the limit **100 in/s^2** a redesign is necessary. The acceleration limit was taken to be the threshold of unpleasant to few for human response from what was proposed by Wright and Green (1959). Table 7 shows the peak acceleration thresholds for the human response to vertical vibrations.

In 1981, Gaunt and Sutton compared Wright and Walker suggestion for simplify the bridge acceleration to the field test they did and found the results in agreement (DeWolf et al., 1985).

Wright and Walker suggested considering additional parameters such as the relative flexural stiffness and torsional stiffness of the cross section in design procedure. They stated that because reliable evidence on human reaction to bridge motions is so severely limited, the recommended acceleration criterion should receive empirical confirmation prior to any adoption (Machado 2006).

Table 7 - Peak acceleration limit for human response to vertical vibrations (Wright and Walker 1971)

Human Response	Amplitude of Acceleration (in./sec²)	
	Transient	Sustained
Imperceptible	5	0.5
Perceptible to few	10	1
Perceptible to some	20	2
Perceptible	50	5
Unpleasant to few	100	10
Unpleasant to some	200	20
Unpleasant	500	50
Intolerable to few	1000	100
Intolerable to some	2000	200
Intolerable		

The Serviceability Criterion for FRP Bridges by Demitz at al. (2003)

Since composite materials possess a higher modulus of elasticity and lower weight than traditional materials, applying deflection limitations established for traditional bridges should be investigated for advanced composite materials. In order to establish a new deflection limitation for bridges constructed with advanced composite materials, Demitz et al (2003) conducted a parametric analytical study included three traditional bridges and three FRP bridges. They concluded that the L/400 limit is ideal for truck speed 60 mi/h if damping was not considered. When damping ratio is considered, this limit is acceptable even for higher truck speeds.

FINITE ELEMENT MODELING

As it was mentioned, existing finite element (FE) software provides an ideal platform for parameter study of bridges subjected to moving loads. However, one has to be careful in selecting the modeling parameters as the acceleration and velocity time histories are quite sensitive to such assumptions.

Exact Solution

For a simply-supported beam subjected to a constant traveling load P at a constant value, the exact solution can be derived (Chopra 2007). The exact solution and simple models in this study were used to verify the finite element results and accuracy of the FE models. The exact solution equations are quite involved and only the response parameters for the case of zero damping are provided here. The solution for damped case is similar, albeit significantly longer. The exact solutions for both cases were programmed with MATLAB and used in this study for purposes of comparison. The results in this study were all investigated at mid span, as at different vehicle velocities it is demonstrated that the maximum dynamic deflection occurs at the vicinity of the bridge mid-span (±3%) (Esmailzadeh and Jalili 2002). The general displacement solution is equal to:

$$u_{(x,t)} = \sum_{n=1}^{\infty} q_{n(t)}.\phi_{n(x)}$$

Equation 10

Where $\boldsymbol{\varphi_n}$ is the mode shape for mode $\boldsymbol{n}$ and $\boldsymbol{q_n}$ is the corresponding modal equation. With the consideration of damping ratio (ζ), that is equal to (Fushun et al. 2007):

$$q_{n(t)} = \frac{2P_0}{mL\omega_n\sqrt{1-\zeta^2}} \int_0^t \sin(\frac{n\pi v\tau}{L}).e^{-\zeta\omega_n(t-\tau)}.\sin(\omega_n\sqrt{1-\zeta^2}(t-\tau)).d\tau$$

Equation 11

$$q_{n(t)} = \begin{cases} \dfrac{2P_0}{mL}\dfrac{1}{\omega_n{}^2-(n\pi v/L)^2}(\sin\dfrac{n\pi vt}{L}-\dfrac{n\pi v}{\omega_n L}\sin\omega_n t) & t \le L/v \\ \dfrac{2P_0}{mL}\dfrac{1}{\omega_n{}^2-(n\pi v/L)^2}\dfrac{n\pi v}{\omega_n L}\left[(-1)^n\sin\left(\omega_n(t-L/v)\right)-\sin\omega_n t\right] & t \ge L/v \end{cases}$$

Equation 12

Where $\boldsymbol{L}$ is span length, $\boldsymbol{v}$ is the velocity of load $\boldsymbol{P_0}$, and $\boldsymbol{\omega_n}$ is natural circular frequency ($2\ \boldsymbol{\pi}\ \boldsymbol{f}$). The solution of this equation for zero damping is provided in this study:

Solution for damped case is similar although significantly longer. Natural frequency (f) for simply supported beam can be calculated using equation suggested by Wright and Walker (1979) for simply supported beams. By differentiating the displacement equation once and twice, velocity and acceleration equations can be derived. These equations have been solved and programmed in MATLAB (2007) and were compared to FE results.

Moving Load Model

The validation of FE results can be confirmed by comparing the results of FE models with exact solution which was discussed earlier. The moving load (truck) is modeled by applying the concentrated load at various nodes with the duration equal to element length divided by the moving load velocity (Figure 22). Time function is defined as a triangular function as shown in Figure 22. Due to the sudden application of rectangular time function (Figure 22) to each node, the results of velocity and acceleration can be very inaccurate. However, the results for displacement and moment are satisfactory using either time functions.

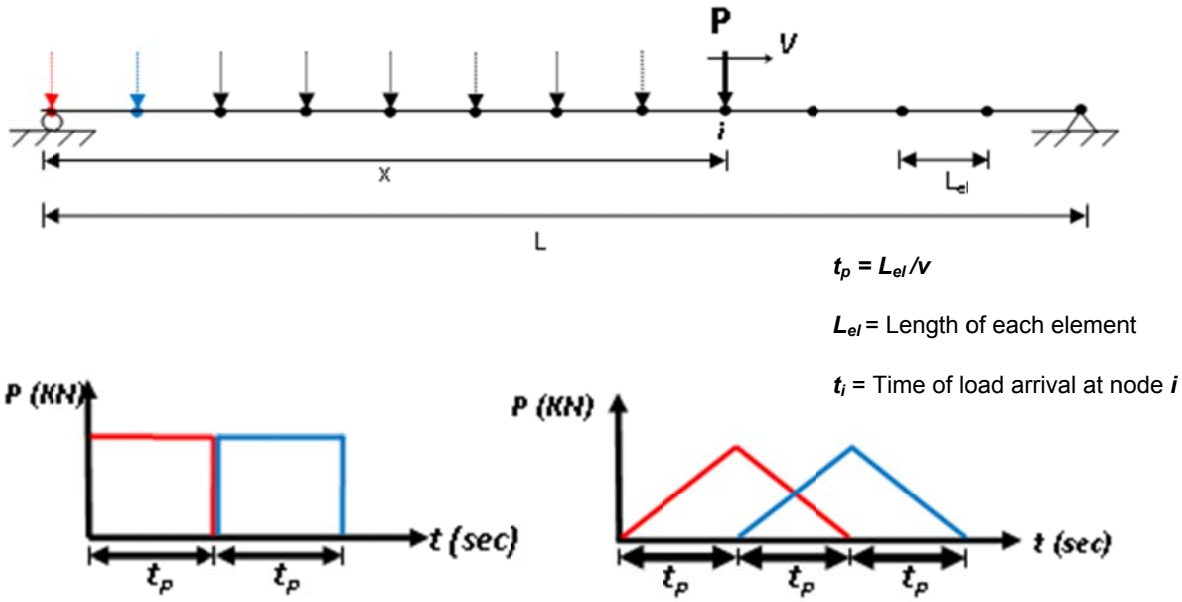

Figure 22. Moving load modeling and types of Time Function

Figure 23 shows displacement, velocity and acceleration time histories for both time functions using the direct integration analysis method with damping ratio (ζ) 0 percent , time step (dt) of 0.01 second, and load discretization (t_p) 0.01 sec are plotted.

bridge vibration while the load is over the bridge is called “steady state” part of the vibration. When the load exits the bridge, the bridge continues vibrating until it is damped out entirely and returns to the static equilibrium. This is the “transient” part of the bridge response. As it can be seen the displacement results are very accurate in both steady state and transient parts of the vibration regardless of the type of time function used to model the moving load. Noting that in this example, at time equal to 1.4 seconds, the load exits the span and deflection is equal to zero at 1.4 sec.

However, acceleration has significant error when the rectangular time function is used. Velocity results inaccuracy is not as bad as the acceleration although unlike displacement they are affected by the type of time function. Note that the time function

duration must be an integer factor of the time step used in integrating the differential equations.

Time step is also important to accurate modeling of the problem and affect all three dynamic responses (displacement, velocity and acceleration). In order to investigate the influence of time step on response results, two time steps of 0.01 sec and 0.04 sec were used. As it can be seen in Figure 24 the error is more significant in acceleration response although displacement and velocity contain small errors.

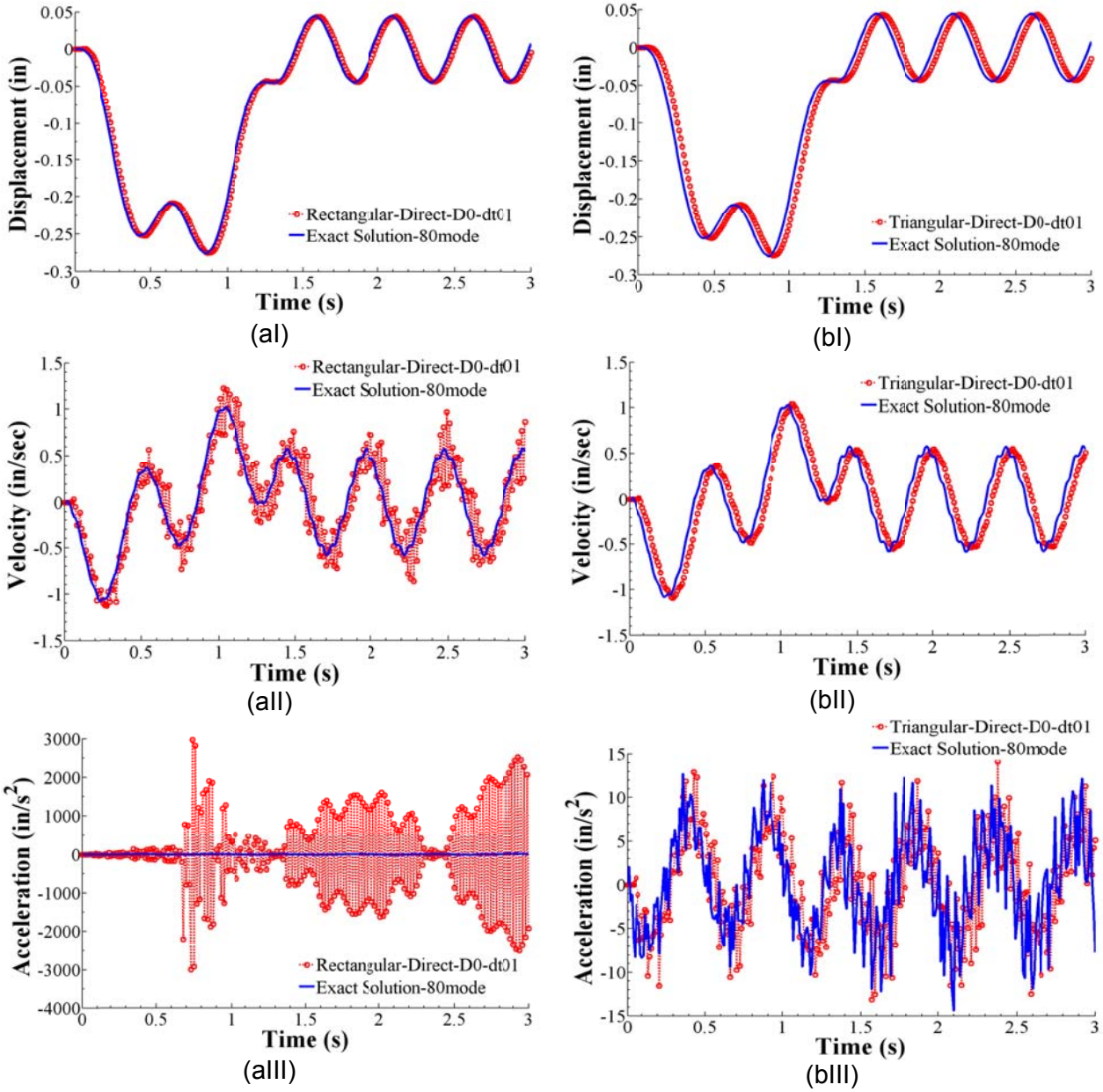

Figure 23. Effect of rectangular (a) and triangular (b) Time Function on bridge displacement (I), Velocity (II) and acceleration (III).

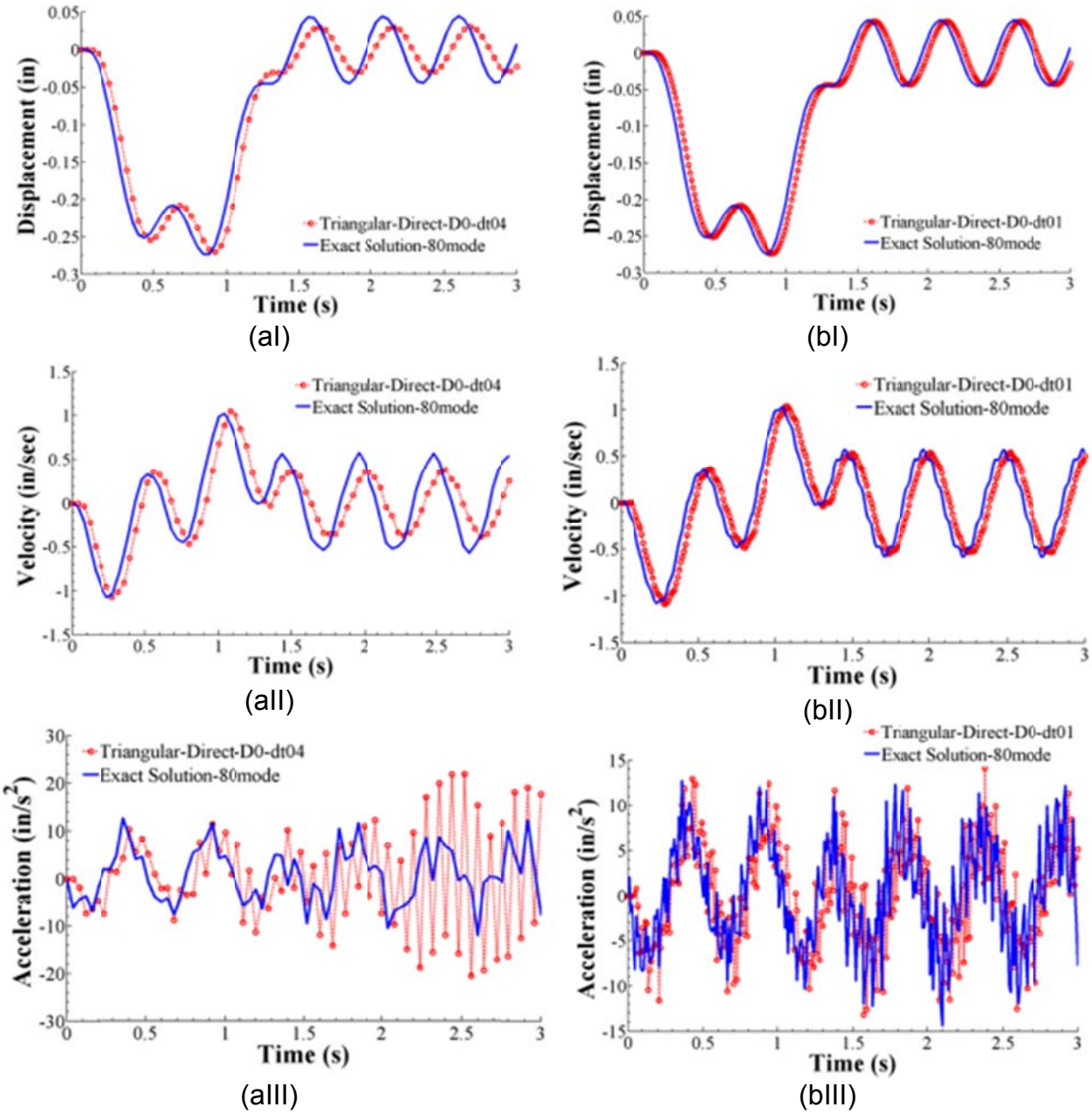

Figure 24. Effect of 0.04sec (a) and 0.01sec (b) Time Step on bridge displacement (I), velocity (II), and acceleration (III).

The results presented here highlight the importance of correctly selecting the finite element model parameters. This determination was made through a significant number of analyses and once the confidence was established in the accuracy of the model, it was used for parameter study, the results of which are discussed in the following sections.

Dynamic response determination is sensitive to modeling parameters with acceleration being the most sensitive. This has not received much attention in the literature. Parameters that have to be considered in modeling in order to obtain acceptable results for acceleration and velocity are as follows:

- Time step should be taken as the element length divided by load speed.
- Time function should be triangular starting from zero and increasing gradually to reach its maximum value during one time step and decreasing from its maximum value to zero in another time step.
- Loads should be applied exactly on nodes; otherwise, the results for acceleration are significantly different.

If the concrete deck is not entirely supported at approaches, when the load enters and exits the bridge from some locations other than over girders, it causes local numerical problems in computation.

PARAMETER STUDY

The parameters considered are vehicle velocity, span length, bridge natural frequency, speed parameter, damping ratio, number of spans, and load sequence. Vehicle velocity (V), span length (L), and bridge frequency (f) have the most influence on bridge dynamic response. These three parameters have been investigated in a combined parameter called speed parameter (α) by several researchers (Majka and Hartnett 2007, Fryba 1972, Wright & Walker 1972) prior to this study. Speed parameter is defined as α=V/2Lf. However, in this study it is shown that k-parameter, which is equal to Lf/V, better explains the structure response characteristic due to a moving load. After introducing k-parameter in this chapter, it will be used for the rest of the study for comparison. Noting that k-parameter is equal to half of the inverse speed parameter.

Speed Parameter and k-parameter

Using the exact solution equations, the bridge responses have been graphed for different speed parameters in Figure 25. Many cases were analyzed by varying V, L, and f while holding α constant. It was determined the bridge dynamic responses are not affected by these variations and are the same for the same ***α*** (Figure 25). The results are presented in dimensionless units and displacement graph is compared with the results of another study by Saadeghvaziri (1993). Dimensionless displacement or dynamic load amplification (IM + 1) is calculated by dividing dynamic displacement to static displacement ($\boldsymbol{\delta_{st}}$). Dimensionless velocity and acceleration is defined by dividing the maximum velocity and acceleration to the product of static deflection and natural frequency ($\boldsymbol{\omega.\delta_{st}}$) or the squared natural frequency ($\boldsymbol{\omega^2.\delta_{st}}$), respectively.

The peaks in displacement and acceleration graphs can be explained in light of the time it takes for moving load to travel over a bridge. In harmonic motion displacement is extremum at ***0.25T*** and ***0.75 T*** (Figure 26). Therefore, if the maximum/minimum vibration displacement occurs at the same time that the maximum bridge displacement under moving load occurs, the total bridge displacement would be at the highest/lowest values.

The time taken for the load to traverse the span is $\boldsymbol{t_d}$ (duration) and it is equal to ***L/V***. Thus, at ***L/2V*** the load is at the middle span causing the maximum displacement at that point. If at that moment bridge vibration is in the ***(n±0.25) T***, the minimum and the maximum displacement occurs. The value of ***α*** obtained by equation 13 is the critical ***α*** in its vicinity. Noting that, ***n*** is a positive integer number.

$$\frac{L/2}{V} = (n \pm 0.25).T_b \Rightarrow \alpha = \frac{V}{2Lf_b} = \frac{1}{4(n \pm 0.25)} \qquad \text{Equation 13}$$

Table 8 shows the values of speed parameter in which the maximum and the minimum displacement of the bridge occurs. The response pattern (namely peaks and valleys) can be further explained in light of the number of cycles that the bridge vibrates while the vehicle is on the bridge. Figure 27 shows the same graphs as those shown in Figure

25 but responses are plotted versus the ratio of t_d (the time to transverse the span- load duration) to the bridge natural period (T_b), which is equal to:

$$k = \frac{t_d}{T_b} = \frac{L \cdot f}{V} = \frac{1}{2.\alpha}$$ Equation 14

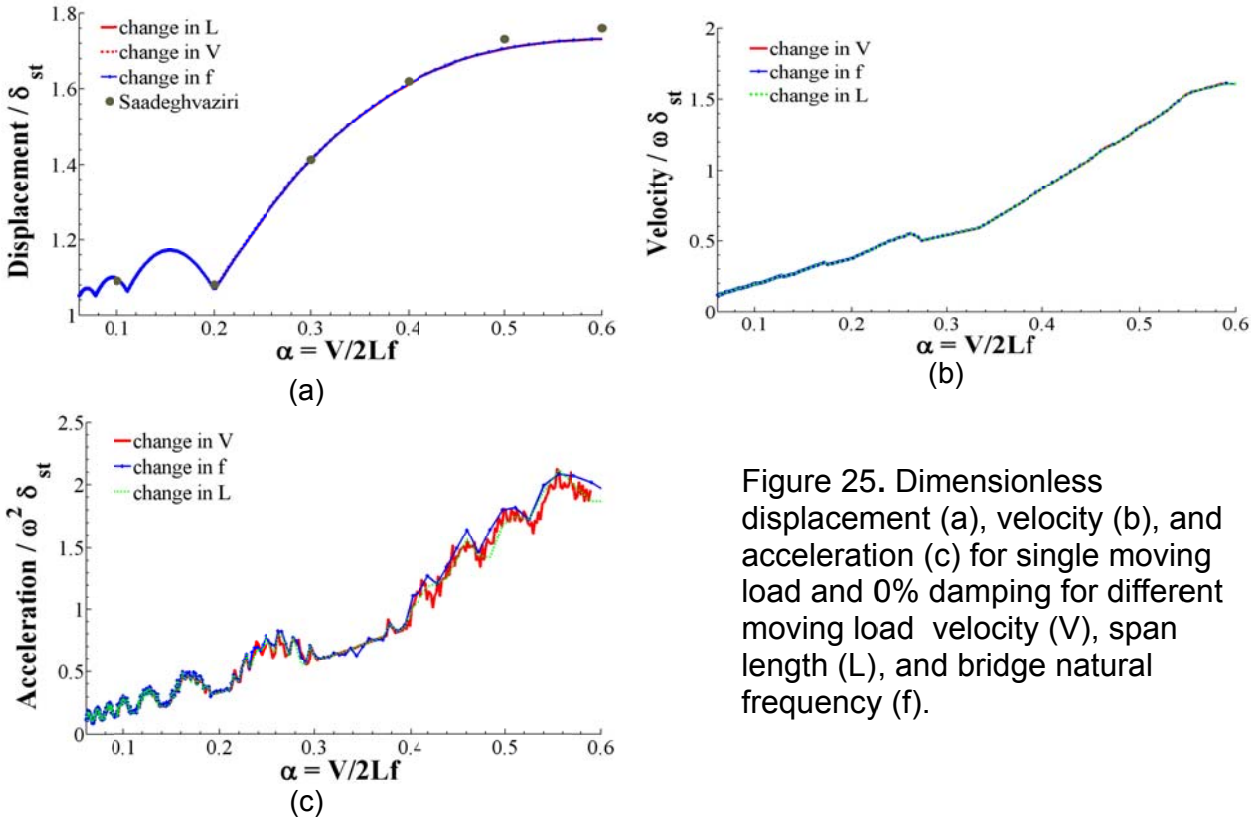

Figure 25. Dimensionless displacement (a), velocity (b), and acceleration (c) for single moving load and 0% damping for different moving load velocity (V), span length (L), and bridge natural frequency (f).

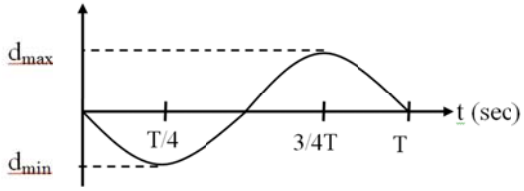

Figure 26. Simple harmonic motion (vibration)

Table 8 - Maximum and minimum of displacements

Displacement	max	min	max	min	max	min	max
n ± 0.25	0.75	1.25	1.75	2.25	2.75	3.25	3.75
α	0.333	0.2	0.143	0.111	0.091	0.077	0.067

The values of "***k***" on the graphs explain the number of cycles that bridge vibrates (with its natural frequency) while the vehicle is on the bridge.

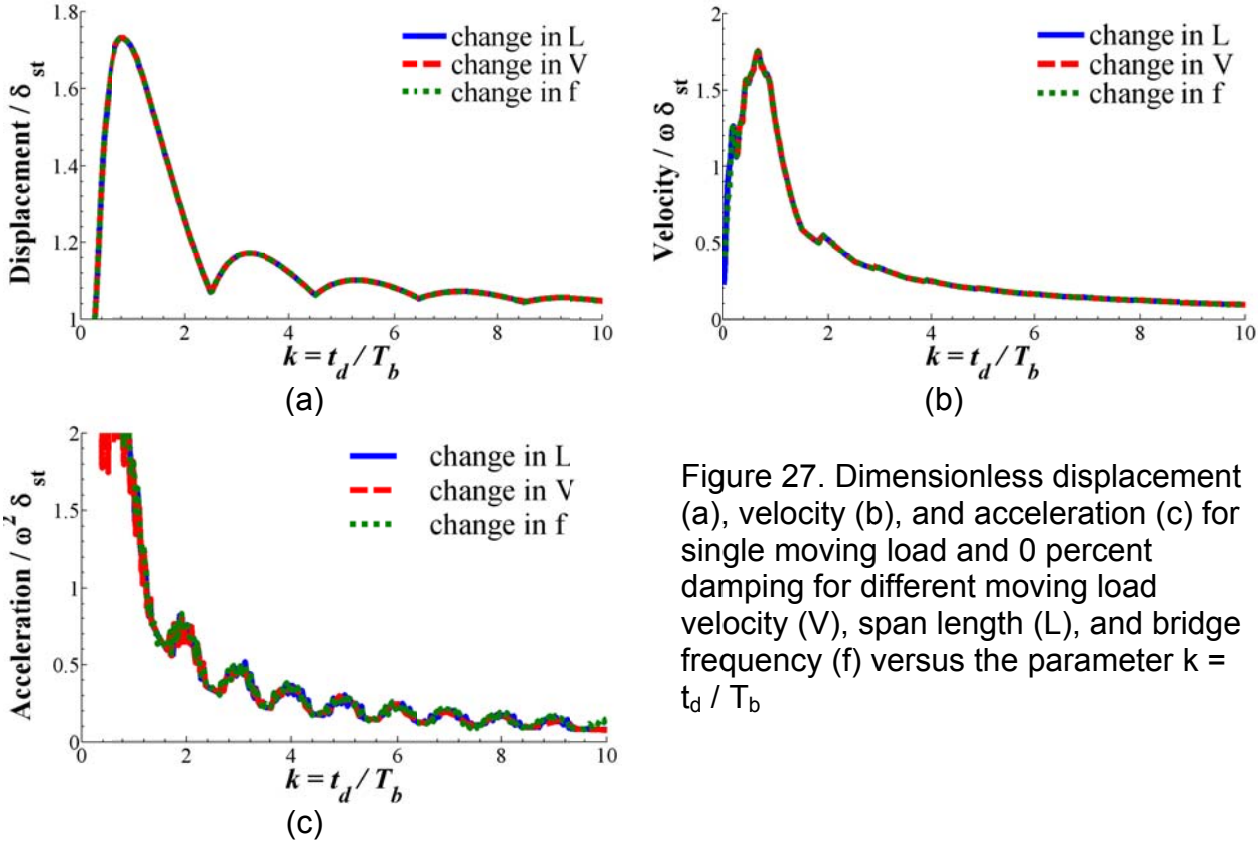

Figure 27. Dimensionless displacement (a), velocity (b), and acceleration (c) for single moving load and 0 percent damping for different moving load velocity (V), span length (L), and bridge frequency (f) versus the parameter k = t_d / T_b

Figure 28 shows the displacement, velocity, and acceleration time histories for simply supported beams subjected to a single moving load. The peaks and valleys in displacement response occur when the displacement time history is symmetric with respect to mid-span. The symmetric response occurs when ***k*** is equal to an integer number plus half ***(i+0.5)***. However, for odd numbers plus half (1.5, 3.5, 5.5), the maximum displacement response occurs and for even numbers plus half (2.5, 4.5, 6.5) the minimum response occurs. As it can be seen the transient part of the vibration is equal to zero when ***k*** is equal to ***i+0.5***, regardless of whether i is even or odd. This will be further explained in the following sections.

Acceleration is in its peak value when the duration (***t_d***) of the load is equal to an integer (***n***) order of the bridge natural period (***t_d = n .T_b***); and it is minimum when ***t_d = (n ± 0.5) .T_b***.

$$t_d = \frac{L}{V} = k.T_b = k.\frac{1}{f} \quad \Rightarrow \quad \frac{1}{k} = \frac{V}{Lf} \quad \Rightarrow \quad \alpha = \frac{V}{2Lf} = \frac{1}{2k}$$

Equation 15

The values of α and k in which the peaks and valleys of acceleration occur are shown in Table 9. In a study by Manning (1981), it was concluded that the maximum dynamic response occurs when the time to travel the span (***t_d***) is equal to the fundamental period (***T_b***) of the bridge. In such a situation, ***k*** is equal to 1 and the speed parameter, ***α***, is equal to 0.5 which supports the results of this study (Table 9). The maximum bridge

acceleration occurs when the load enters or leaves the bridge. If the time for the moving load to traverse the bridge is an integer factor of the bridge period then accelerations will be further amplified.

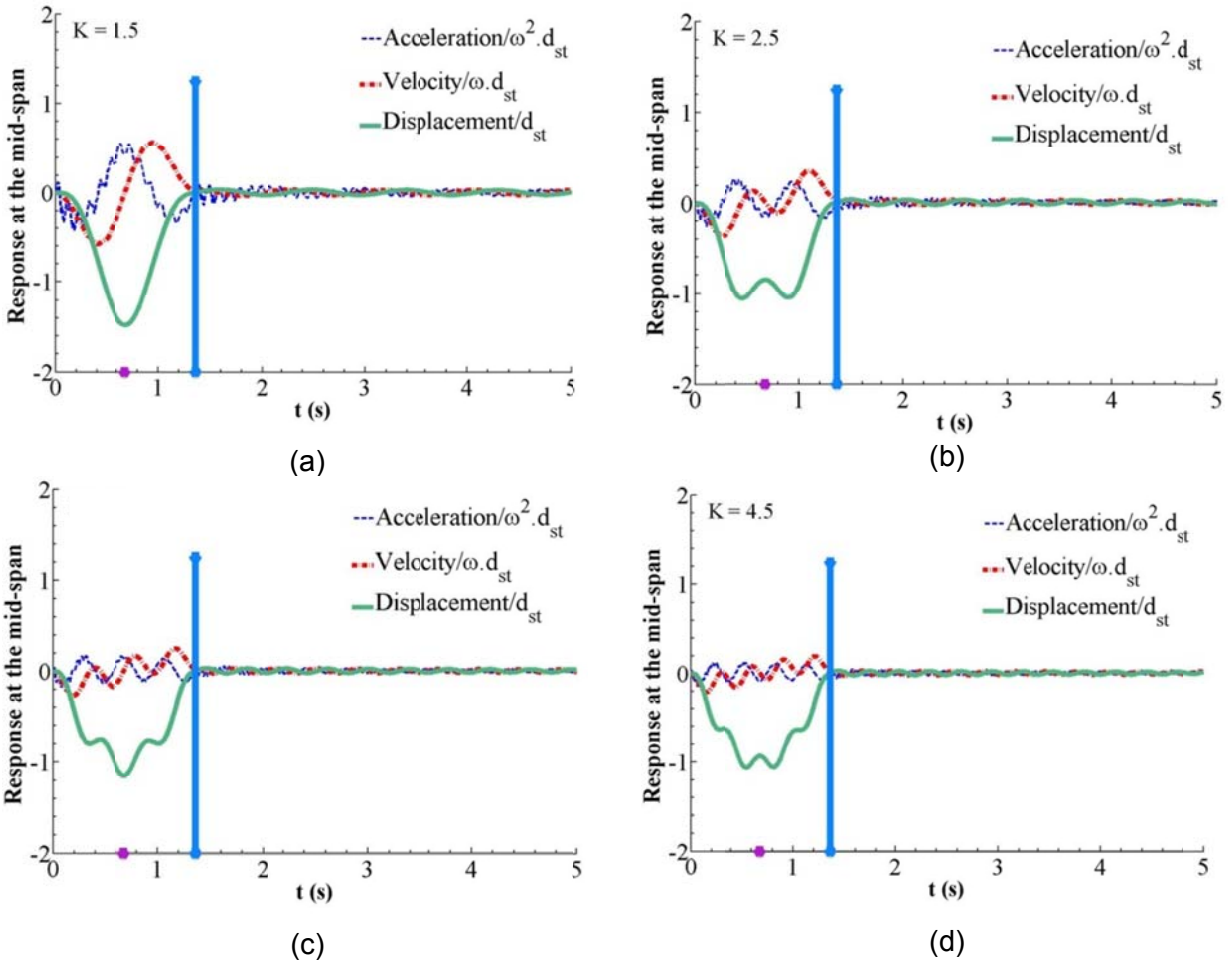

Figure 28. Displacement, velocity, and acceleration time history for simply supported beams and 1 axle moving load. n±0.25 = 0.75 (a), 1.25 (b), 1.75 (c), 2.25 (d).

Table 9 - Maximum and minimum of accelerations.

Acceleration	max	min	max	min	max	min	max	min	max	min	max	min	max
k	1	1.5	2	2.5	3	3.5	4	4.5	5	5.5	6	6.5	7
α	0.5	0.33	0.2	0.2	0.16	0.14	0.12	0.11	0.10	0.09	0.08	0.07	0.07

To investigate the common range for k-parameter among existing bridges, the results of a survey (Saadeghvaziri and Hadidi 2002) were used to calculate the practical range of k-parameter. k-parameter is from 2 to 5 for most bridges (Table 10).

Table 10 - calculated k-parameters for some bridges in New Jersey.

Bridge ID	span length (in)	frequency	k-parameter
0206-165	1082	3.32	2.5
1013-151	1498	2.81	2.9
1103-158	1143	3.57	2.9
1149-176	1575	2.63	2.9
1149-176	1488	2.95	3.1
1312-154	1361	3.55	3.3
1143-168	1320	3.75	3.6
1143-170	966	5.4	3.8
1143-166	1103	5.34	4.2

It is determined that the natural frequency of highway bridges is between 2 and 7 Hz. The effect of HPS on k-parameter was also investigated and it was determined that the use of HPS results in only marginal decrease in k-parameter. For example for a bridge designed with both 50W and 70W steel the frequency was decreased by 0.09 Hz resulting in a 0.1 decrease in k-parameter - from 2.84 to 2.72. Therefore, k-parameter is investigated within the range of 1 to 10. The range of α consistent with the range considered for k-parameter is 0.05 to 0.5.

Damping Ratio

The effect of damping ratio on dynamic response of the bridge was investigated with respect to both speed parameter and k-parameter. Figure 29 shows the results for 0 to 5 percent damping ratio for displacement, velocity and acceleration.

Every 1 percent damping ratio influences on displacement and acceleration by approximately 1.2 percent and 15 percent , respectively. Velocity is not much influenced by damping ratio. In this study the minimum damping ratio of 1 percent has been used for simulations so that the maximum possible dynamic response will be obtained.

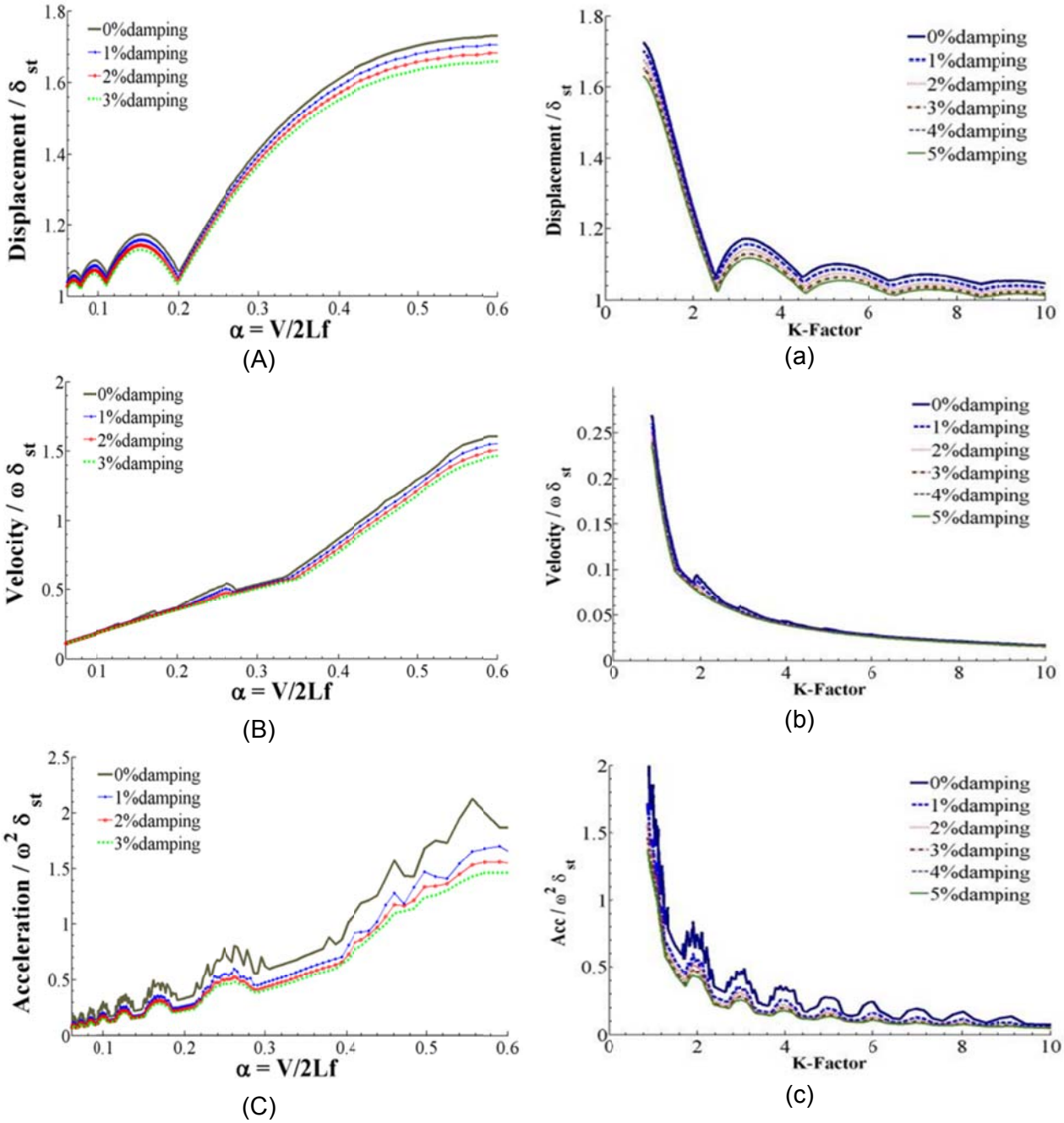

Figure 29. The effect of damping ratio on bridge dynamic response.

Load Sequence

The results shown in the previous sections are for a condition in which the bridge is at rest before the excitation begins. The pre-existing vibration can be investigated in two different conditions. First condition is when just one load is on the bridge at any time and the second load enters the bridge when the first load exits the bridge completely. At this condition, static deflection can always be determined by simple equations such as $PL^3/48EI$ for single span bridge.

Second is the condition in which two or more single-axle loads move over the bridge at the same time and the arrival time of each load varies relative to the previous one. To calculate the static deflection when more than one axle is over the bridge, all loads contributing in the response should be located over the bridge such that the maximum static deflection can be obtained.

Due to the large variety of trucks in terms of axle weight, axle distances and number of axles, only one and two-axle trucks with identical axle weights are considered in this study and the conclusion is based on these two load conditions.

Cosecutive One-axle loads

This type of loading is shown in Figures 30a and 30b. In both cases, at the time, there is just one load over the bridge and the time that the second load enters the bridge varies. The second load may enter the bridge exactly when the first load exists the bridge or a few seconds after that. This arrival time can be investigated relative to the bridge natural frequency/period. The ratio of arrival time to natural period of the bridge is considered as 0, 0.25, 0.5, 0.75, and 1 and the maximum bridge response for each arrival time has been graphed.

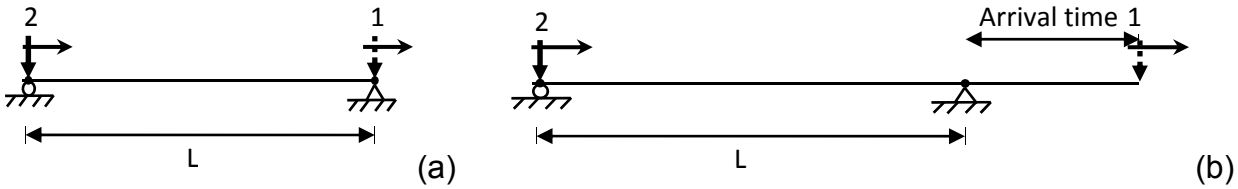

Figure 30. The schematic of one axle load over the bridge at the time with (a) zero arrival time and (b) with non-zero arrival time.

Figure 31 shows the results for k-parameter equal to 2, 2.5 and 3. Steady state part of vibration refers to bridge dynamic response while the load is over the bridge, and transient part of vibration refers to bridge dynamic response while the load has cleared the bridge.

As it can be seen, when arrival time is equal to 0 or T, the maximum response occurs and the minimum response occurs in the vicinity of 0.5T. For k-parameter equal to 2.5 the response is nearly constant and it is not influenced by different arrival time. As it was mentioned before, the transient vibration is nearly equal to zero when k-parameter is equal to an integer number plus 0.5 (i+0.5). Bridges with k-parameter equal to i+0.5 has this advantage that they do not vibrate noticeably.

It was found that when two axle loads pass through a bridge with arrival time equal to zero or T (natural period of the bridge), the maximum response occurs. Now if three single loads pass through a bridge with constant arrival time, the response increases

furthermore. Figure 32 shows the results of 2-axle and 3-axle loads (one axle over the bridge at the time) for displacement, velocity and acceleration responses.

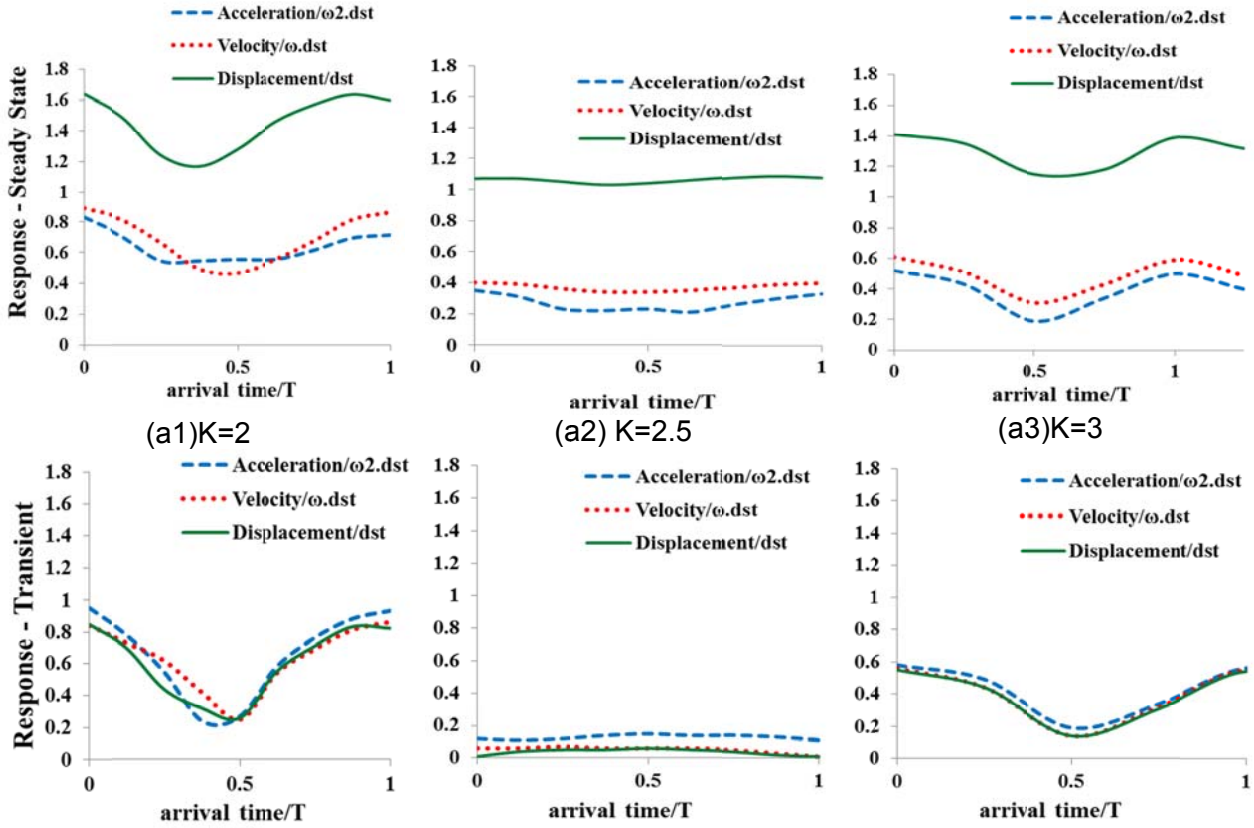

Figure 31. The maximum (a) steady state and (b) transient part of the bridge dynamic response under one-axle load at the time for (1) k = 2, (2) k = 2.5, and (3) k = 3.

The result of one axle loading with respect to k-parameter is shown for comparison. As it can be seen, bridge dynamic response is increased by higher number of axles.

As it was mentioned there is only one load over the bridge at the time and when it exits, the next load enters the bridge. However, the response is increased nearly 1.3 times when the consecutive loads enter the bridge with that time difference (zero or bridge period). Noting that for k-parameters equal to i+0.5, unlike integer k-parameters, the response is not increased noticeably by consecutive loads.

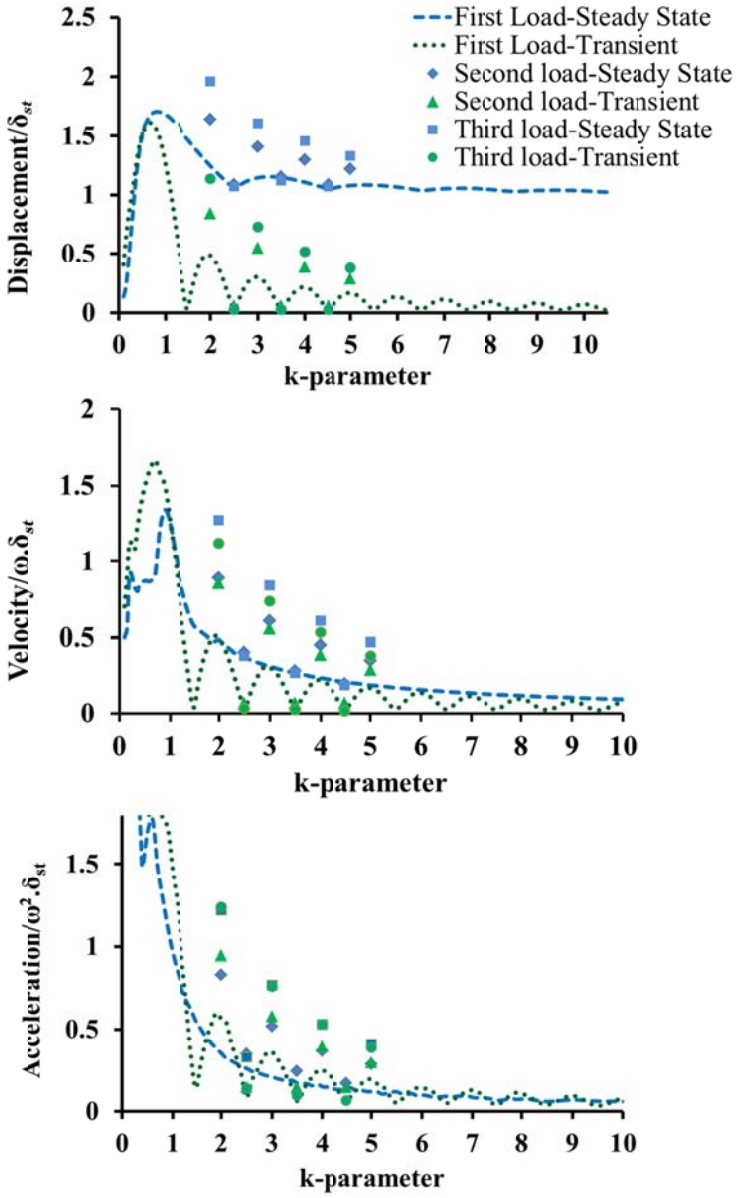

Figure 32. Vibration due to two and three consecutive loads, one axle over the bridge at the time

Two-Axle Loads

Under the condition that there is more than one axle over a bridge, simultaneously, investigating the bridge dynamic response becomes very complicated. Because not only the number of axle is a parameter that has to be considered but also axles arrangements, distances, and weights have to be considered. Moreover, static deflection varies from case to case depending on the distance between axles. In this chapter, bridge dynamic response is investigated for a two-axle load (Figure 33).

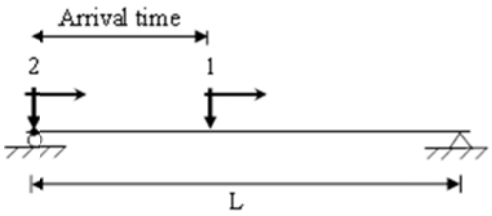

Figure 33. Tow axle load over a bridge at the time.

The value of "arrival time/T" is equal to axle distance, vehicle length (L_v) times bridge frequency (f) divided by vehicle speed (V). This value which has the same formula as k-parameter but with vehicle length instead of span length, can be called as vehicle k-parameter (k_v). The k-parameter referring to the whole bridge k-parameter can be called bridge k-parameter (k_b). Arrival time = t =L_v/V , where V is equal to truck speed.

$$k_v = \frac{t}{T} = \frac{L_v}{V} f \qquad \text{Equation 16}$$

$$k_b = \frac{L_b}{V} f \qquad \text{Equation 17}$$

For simplicity, static deflection is considered as the value resulted from one axle load and the results are shown in Figure 34 for k-parameter equal to 2, 2.5, and 3.

As it can be seen, when the arrival time to bridge period ratio is equal to 0.5, 1.5, and 2.5, the minimum dynamic response occurs; and when it is equal to an integer number, 0 or 1 or 2, the maximum response occurs. For k_b equal to 2.5, the transient part of the vibration is nearly equal to zero. The steady state part of the vibration is at its maximum value when the arrival time to bridge period ratio (k_v) is equal to zero or 1.

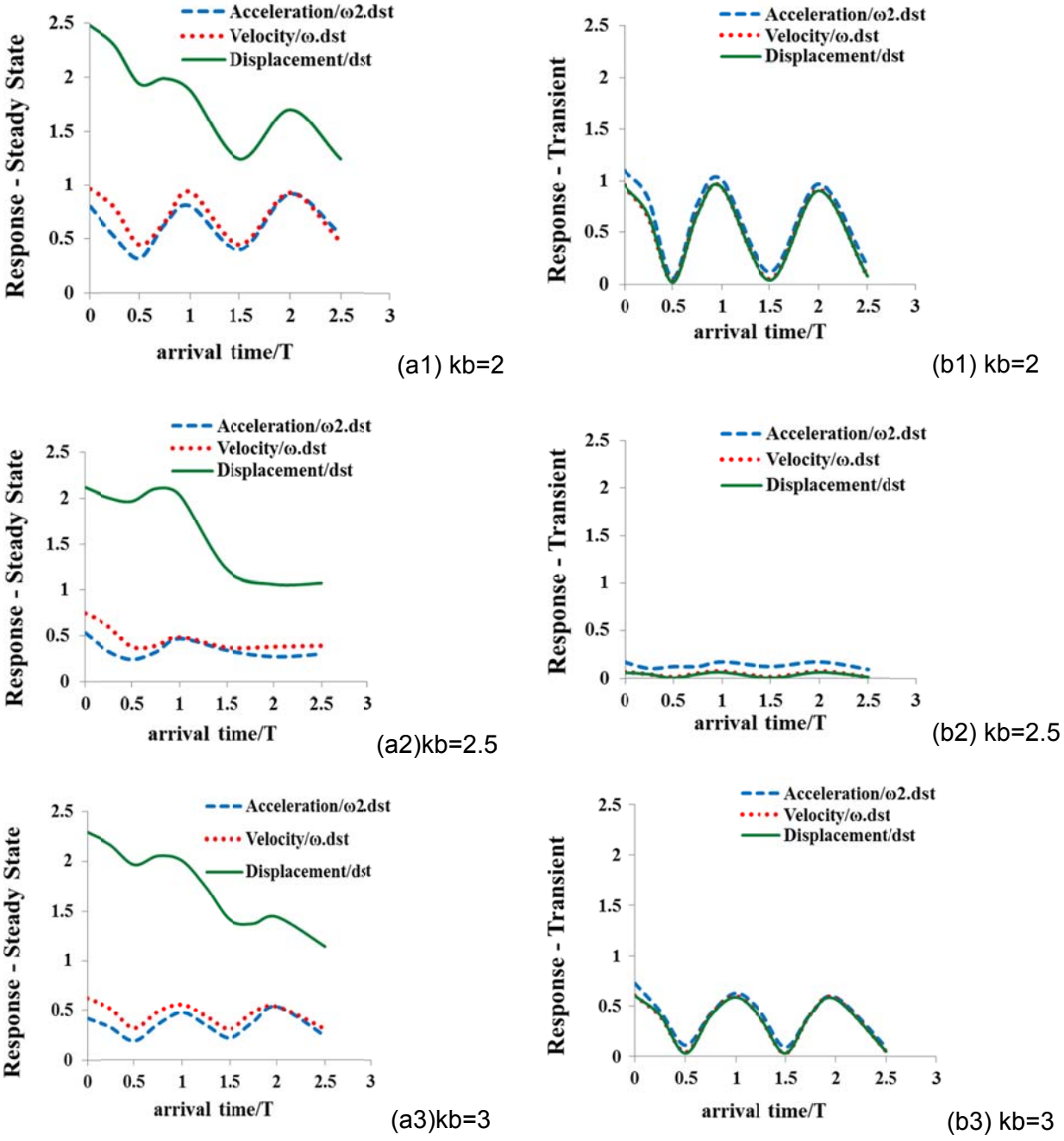

Figure 34. The maximum (a) steady state and (b) transient part of a bridge dynamic response under one-axle load at the time and different arrival time.

Number of Spans

Considering load sequence itself requires a large number of variations in different truck variables. In order to investigate one variable each time, one-axle loading has to be considered in this section. Bridge dynamic response has been investigated under a

one-axle moving load and k-parameter equal to 2.75 for 2, 3, 4, 5, and 6-span bridges with identical spans length.

The results are shown in Figures 35 to 39. As it can be seen, the maximum dynamic response in transient part has the same value as simply supported bridge. However, the vibration severity in transient part depends on the number of spans and the span under consideration. It appears that vibration waves move back and forth from one span to the others until it is damped out. This is more apparent in higher number of spans such as five and six span bridges.

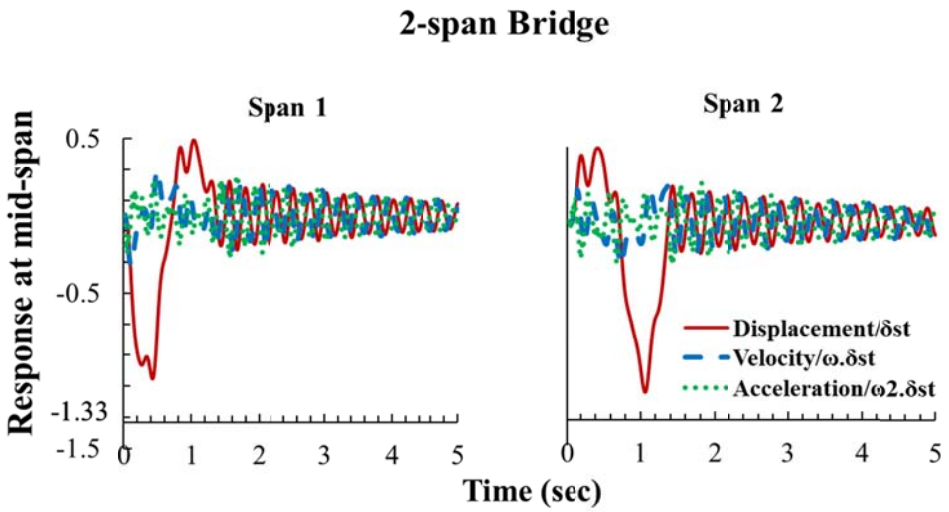

Figure 35. Dynamic response of a two-span bridge under one axle moving load.

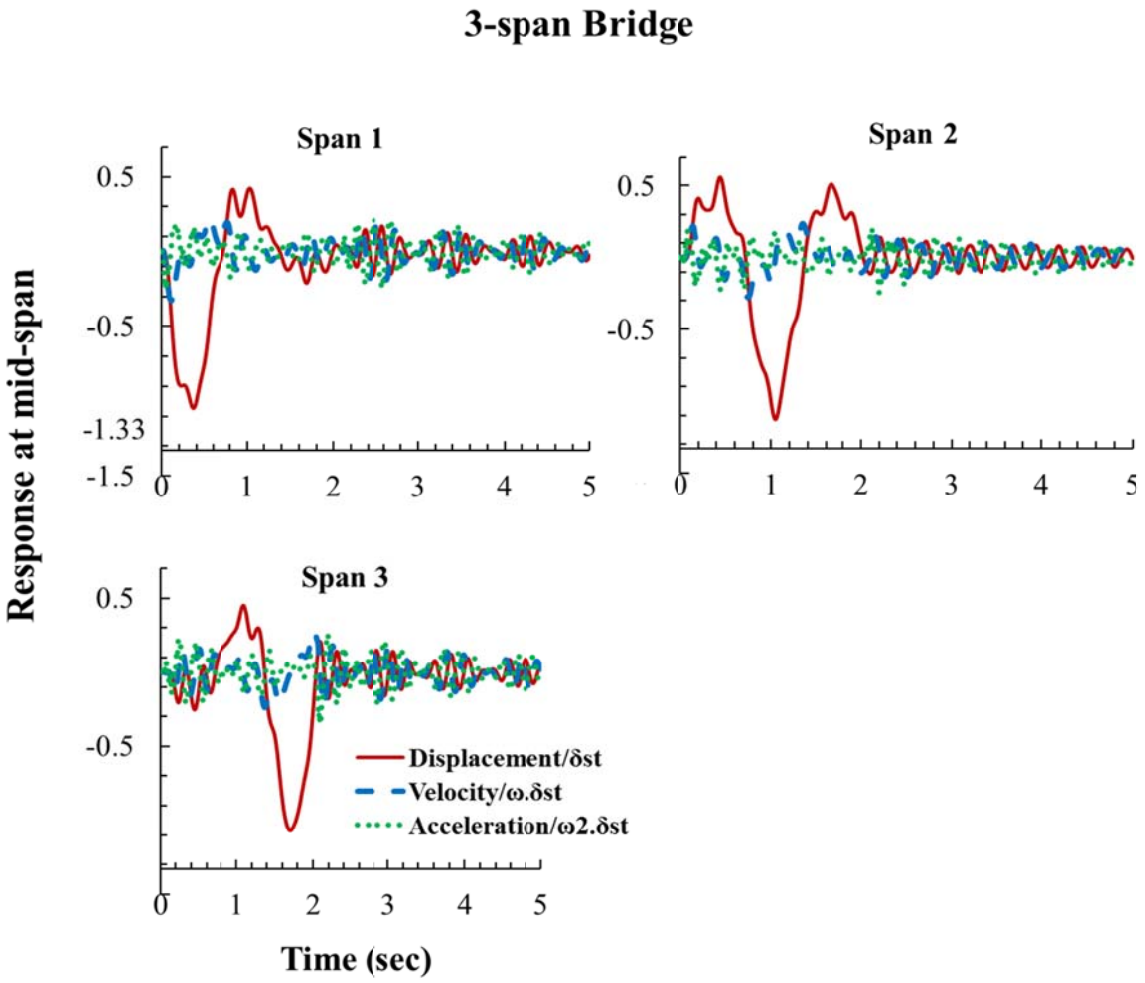

Figure 36. Dynamic response of a three-span bridge under one axle moving load.

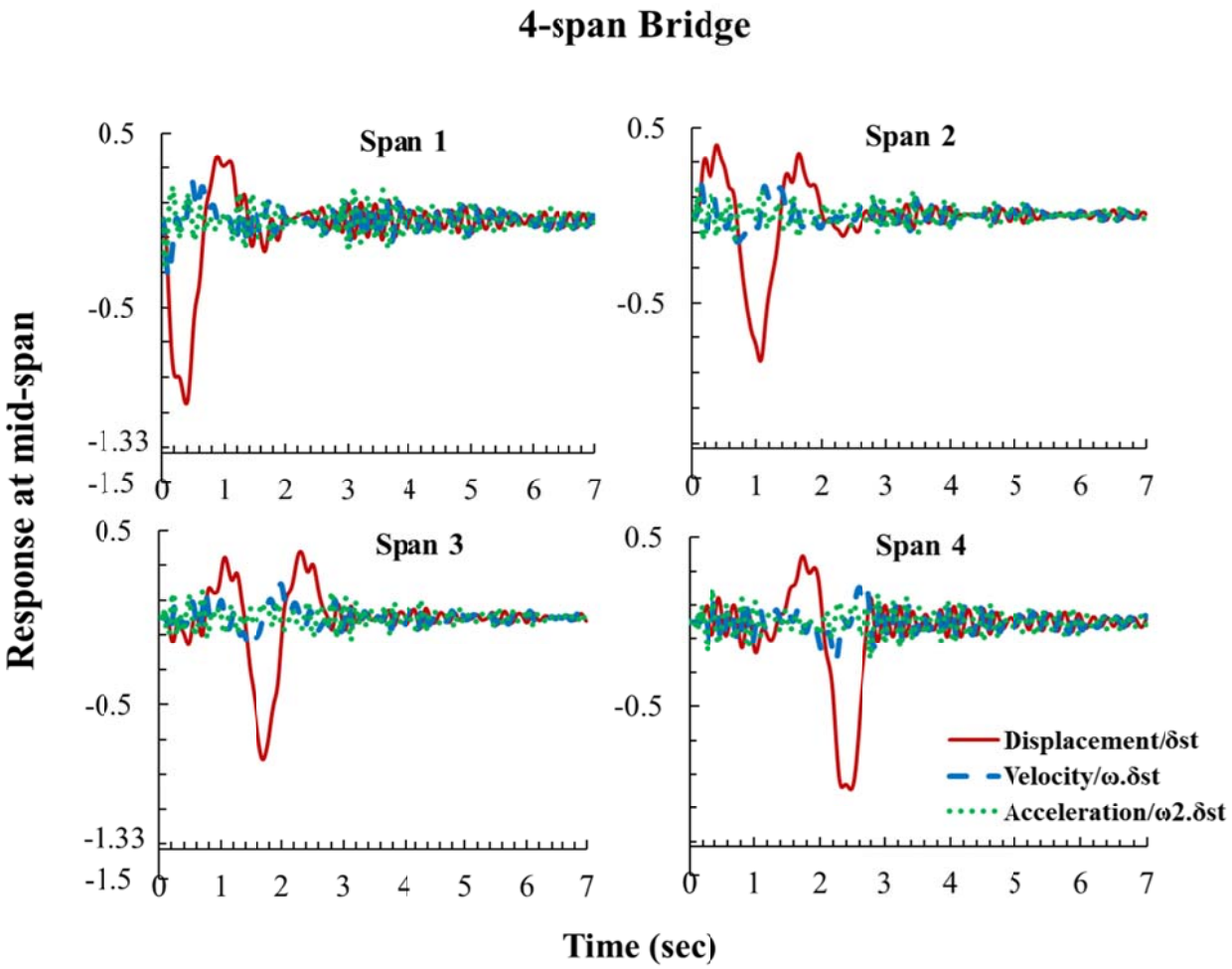

Figure 37. Dynamic response of a four-span bridge under one axle moving load.

Moreover, the response in transient part for multi-span bridges is lower than a simply supported bridge. The transient dynamic response decreases when the number of spans increases.

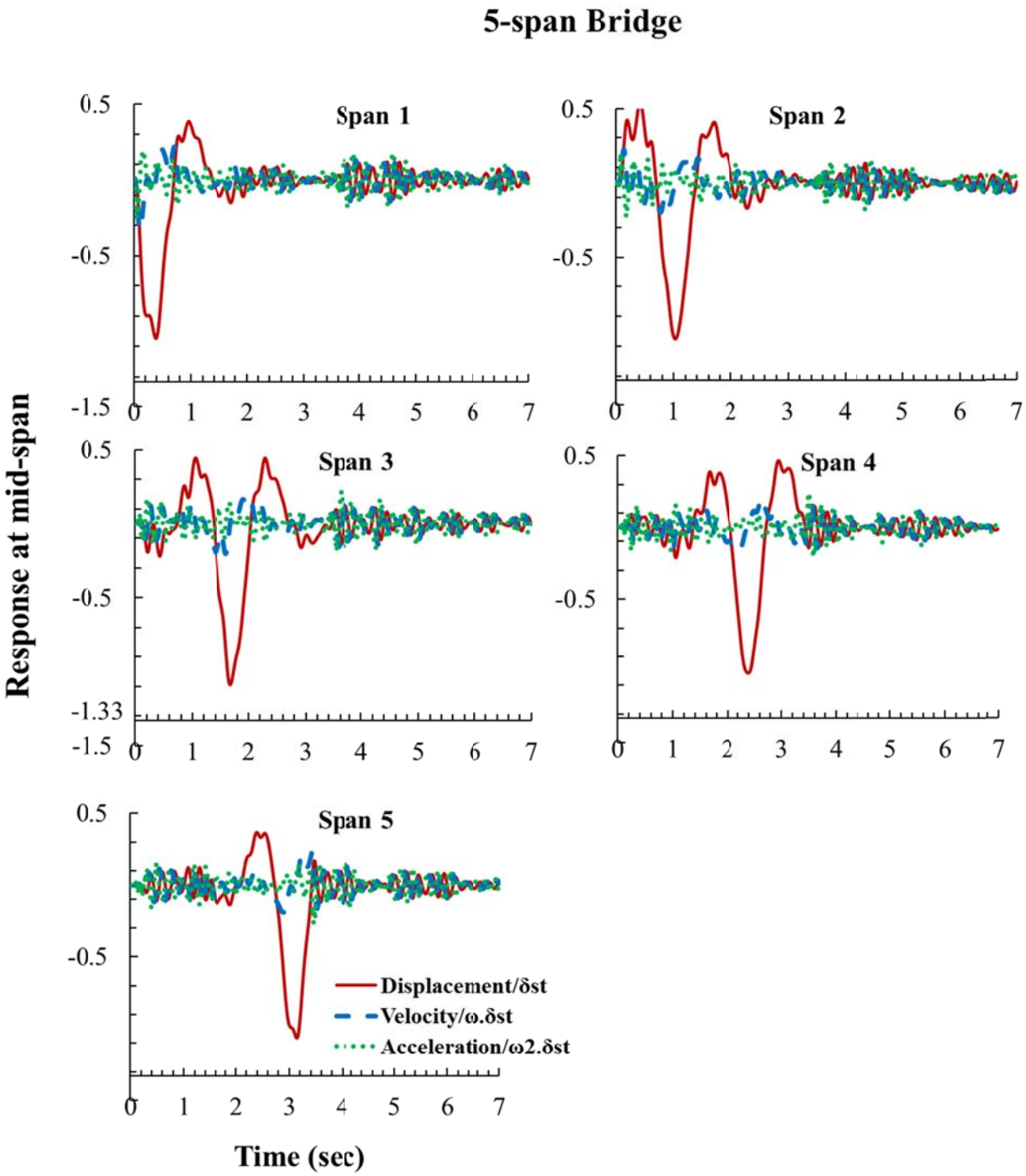

Figure 38. Dynamic response of a five-span bridge under one axle moving load.

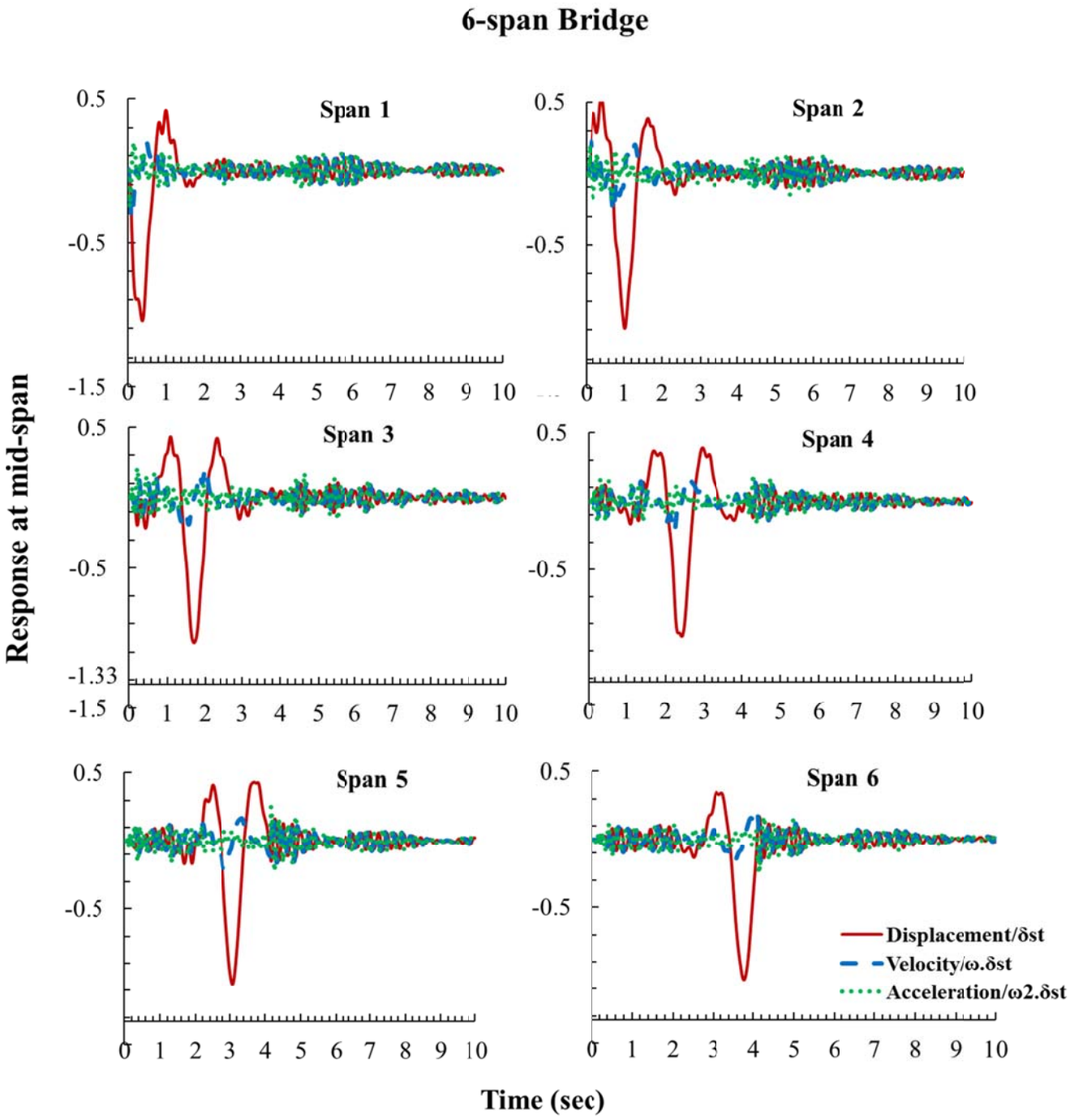

Figure 39. Dynamic response of a six-span bridge under one axle moving load.

Boundary Conditions

Boundary conditions can be investigated considering two aspects of the supports. One is investigating the effect of supports' properties such as supports stiffness and damping properties on bridge dynamic response. The other is to investigate the dynamic response for a continuous span with various lengths ratio (Figure 40). In this study, only

the latter aspect has been investigated. If the span length for the entire bridge is equal, the natural frequency of a bridge is calculated by using the formula for simply supported bridge. Bridge response for equal span lengths is the same as single span bridge. Once the ratio between the spans' length is not equal to one, dynamic response of a multi span bridge differs.

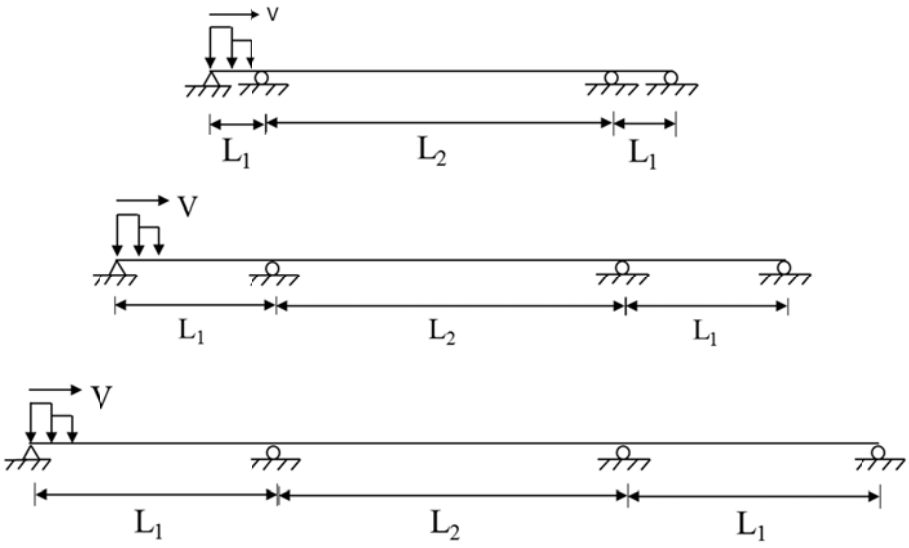

Figure 40. Different length ratio in multi-span bridges.

Analytical studies show that when the spans lengths are identical in a multi-span bridge, the frequency can be calculated using Eq. 18.

$$f_b = \frac{\pi}{2L^2}\sqrt{\frac{E_b I_b g}{w}}$$

Equation 18

However, when spans lengths are not identical in a bridge ($L_1 \neq L_2$ in Figure 41), frequency cannot be calculated by using Eq. 18.

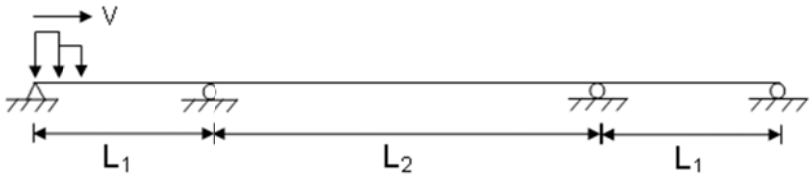

Figure 41. Continuous span with the span ratio of L1/L2 subjected to a moving truck

Dynamic response for a set of three-span bridges has been evaluated in this study and the effect of different span length ratio (L_1/L_2) has been investigated on bridge dynamic

response. Noting that in all these bridges natural frequency was kept constant. For a continuous span bridge, analytical studies show the identical response for displacement and velocity but not the acceleration (Figure 42).

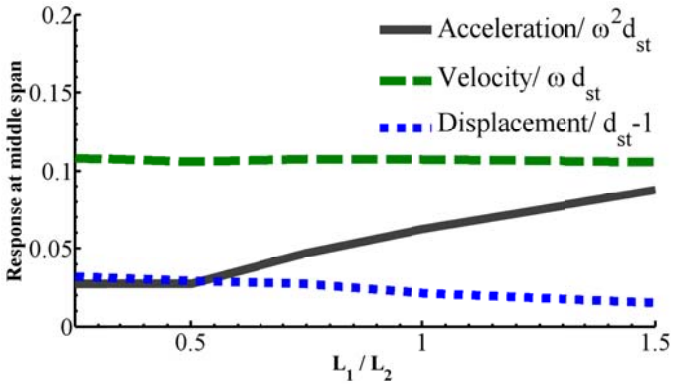

Figure 42. Responses for 3-span bridges with different span ratios (L_1/L_2) under a moving truck.

As it can be seen, the values of displacement and velocity do not vary by increasing L_1/L_2 ratio. However, the acceleration is significantly affected by this ration and it increases as L_1/L_2 ratio increases. This is due to the contribution of higher modes in acceleration response. Although in this investigation the first natural period/frequency is kept constant, the second mode period/frequency of the bridges differs for various span length ratios. Since the higher modes contribute to bridge acceleration, the acceleration response increases with higher period (lower frequency). The first and second mode periods of all cases investigated in this study are shown in Table 11. As it can be seen, the first mode period (T) is constant for all cases while the second mode period varies.

Table 11 - First and second periods of the 3-span bridges with different span length ratios.

L1/L2	0	0.25	0.5	0.75	1	1.5
1st mode T	0.51	0.51	0.51	0.51	0.51	0.51
2nd mode T	0.13	0.18	0.20	0.31	0.40	0.45

2D vs. 3D and Bracing Effect

Two dimensional (2-D) analyses were compared to three dimensional (3-D) analyses in CsiBridge software programs. Mesh size, number of modes, time step, and time function have been selected so that accuracy of dynamic response is insured. Both 2-D and 3-D models are subjected to the same truck loads and the results were normalized to dimensionless values using the model static deflection and frequency. Figure 43 shows the 2-D and 3-D models used in this study. In the 3-D models shell elements were used to represent the concrete deck and beam elements for stringers/girders. In 2-D models only beam elements were used and the beam parameters such as moment of inertia, cross section area and weight were computed by considering one stringer with its proportional deck.

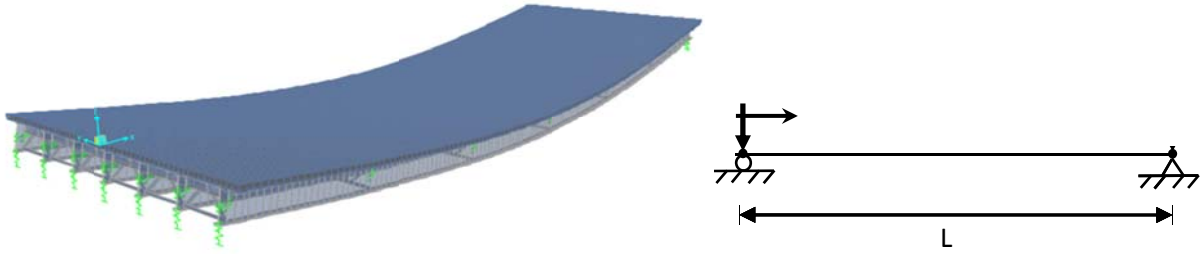

Figure 43. Two and three dimensional models for a sample bridge.

The results are shown in Figures 44 and 45 for single axle load and HL93 truck with identical axle distance, respectively. As it can be seen, two dimensional analyses provide enough accuracy for a bridge model if the loading conditions are identical. Therefore, 3-D analysis can be only used for cases that cannot be done in 2-D, such as the effect of bracing and torsional modes in transverse direction.

A sample bridge (Magnolia Bridge over Rt. 1 & 9) has been simulated using 3-D models with bracing and without bracing. The number of stringers and stringer distances are varied from 4 to 7, and 6.5 ft to 12 ft, respectively. The bracing dimensions and distances are shown in the drawings corresponding to this bridge and are provided in Appendices. The bridge was subjected to HL93 truck load on one lane and modal dynamic analysis was performed. Table 12 shows the results for this investigation. As it can be seen, dynamic responses are identical for all cases with or without bracing, regardless of the distance between stringers.

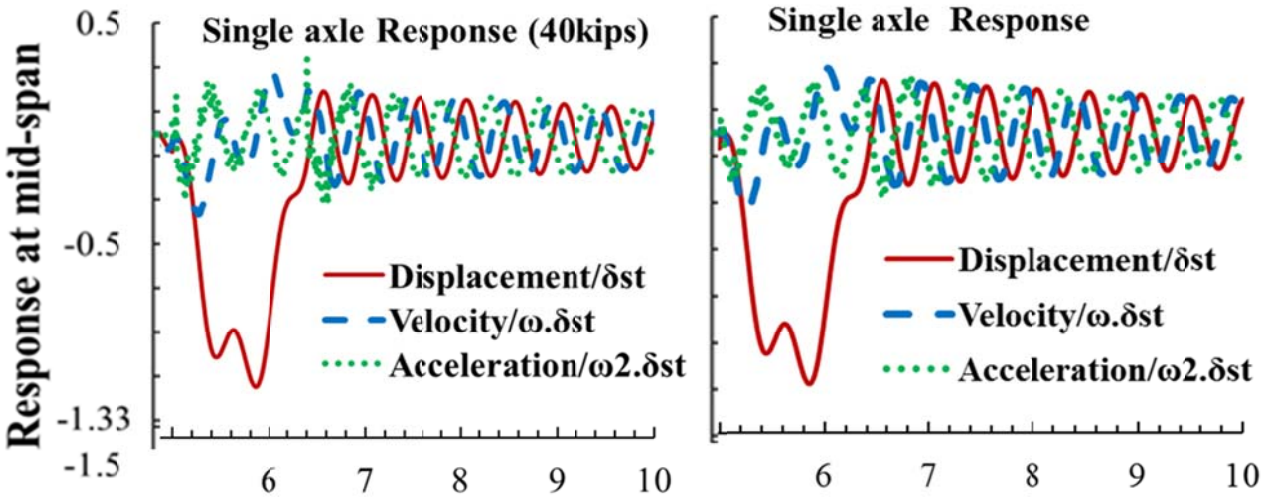

(a) 3D (b)2D

Figure 44. Dynamic response of a simply supported bridge in (a) 3D and (b) 2D for single axle load.

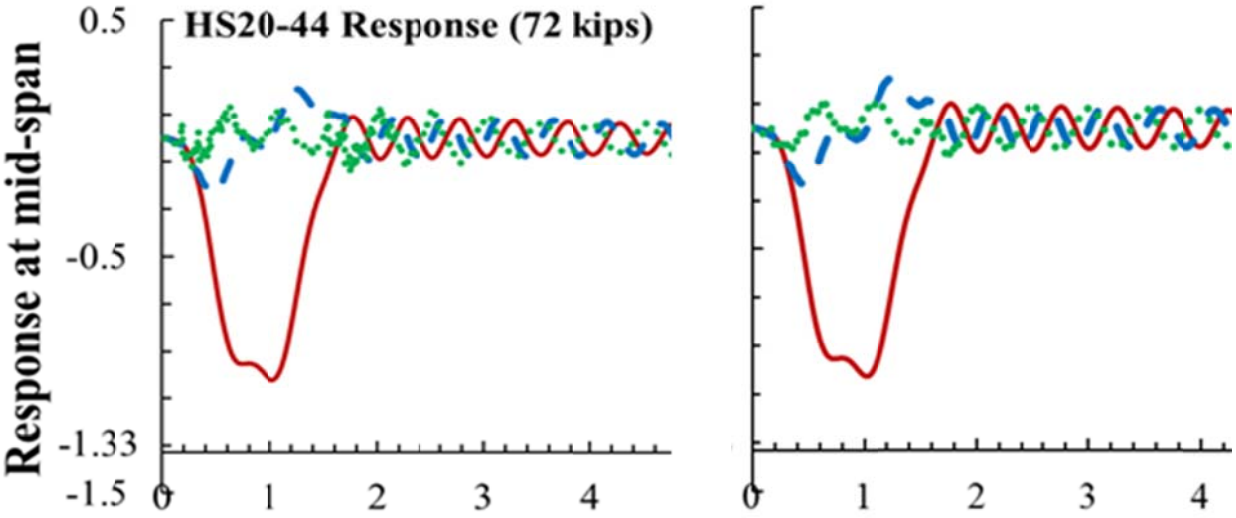

(a) 3D (b)2D

Figure 45. Dynamic response of a simply supported bridge in (a) 3D and (b) 2D for AASHTO truck.

Table 12 - The effect of bracings on bridge dynamic response.

Magnolia bridge							
stringer distance	number of stringers	Cross frames	k	f (Hz)	displacement (in)	Velocity (in/sec)	Acceleration (in/sec^2)
6.5 ft	7	with bracing	2.72	1.996	0.855	2.14	20.45
		No bracing	2.73	2.004	0.893	2.24	20.174
7.8 ft	6	with bracing	2.62	1.928	0.901	2.32	14
		No bracing	2.63	1.936	0.935	2.41	15.79
9.75 ft	5	with bracing	2.51	1.842	0.946	2.57	18.83
		No bracing	2.52	1.849	0.972	2.63	19.285
12 ft	4	with bracing	2.36	1.731	0.989	2.93	22.3
		No bracing	2.36	1.737	0.999	2.95	24.27

VIBRATION AND DURABILITY

Fatigue Problem due to Vibration

Fatigue is the active structural damage that occurs when a material is subjected to repeated loading and unloading. The stresses due to cyclic loading are less than the ultimate stress limit and may be below the yield point of the material. When the stresses are above a certain threshold, microscopic cracks may appear locally where the stress concentration exists. By the continuity of loading and unloading, the cracks sizes will increase and eventually the structure will collapse. The higher the stress ranges due to cyclic loadings, the lower the fatigue life.

Sharp corners, the edges that separate different cross sections throughout a member, notches, welded areas, and material rough surfaces lead to stress concentration which causes fatigue damage. Some manufacturing processes involving heat or deformation such as casting may produce shrinkage voids which initiate fatigue cracks inside the material. Cutting and welding can also produce a high level of residual tensile stresses that decrease fatigue life.

Structures with high cycles of vibration are more sensitive to fatigue failure. Those bridges with high-cycle vibration require a more accurate knowledge on the bridge vibration behavior due to moving trucks. The fatigue criterion in AASHTO Specifications is based on experimental data and it is about four decades old. Since bridge vibration is significantly affected by other parameters such as k-parameter[1] (k = Lf/V) and damping ratio (ζ), these parameters have to be taken into account for fatigue calculations. In this chapter, it will be shown that bridges with specific k-parameters and damping ratio risk the possibility of fatigue failure after 10 years while they are designed for a 75 years fatigue life by AASHTO.

Fatigue Loads

The worst case of fatigue loading is the case known as fully reversing load in which a tensile stress of some value is applied to an unloaded part and then released; then a compressive stress of the same value is applied and released; and this process continues until the failure occurs. Since the bridge self-weight causes a constant deflection, fatigue loads on bridges cannot be of this kind.

Other types of fatigue loads are less severe but not negligible; especially when the transient part of the vibration is considerably high in amplitude, fatigue due to vibration should be taken into account. Figure 46 shows different types of fatigue loading. The loading shown at the left side of the graph is more similar to the one that occurs due to bridge vibration.

---

[1] k- parameter is a parameter defined as Lf/V, span length (L) times bridge frequency (f) divided by vehicle velocity (V), and it is equal to the inverse of speed parameter divided by two, $k = \frac{1}{2\alpha}$.

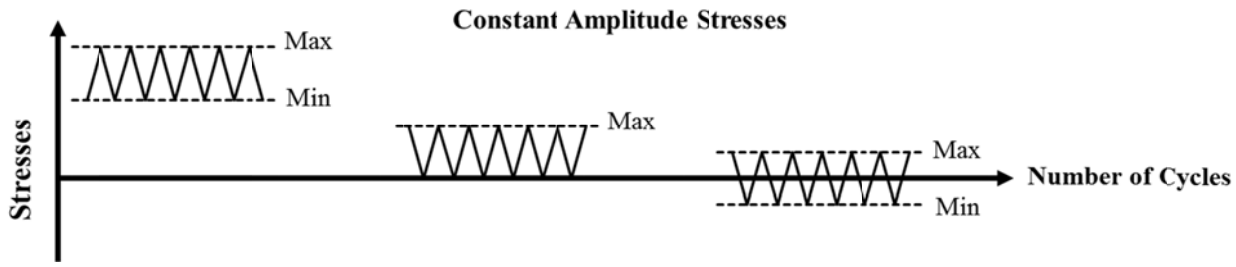

Figure 46. Types of fatigue loads

Bridges fatigue stresses cannot be simplified as a single stress range as shown in Figure 46. The stresses vary depending on the axle weights, number of axles, the axle distances, k-parameter, live load to dead load deflection ratio, and the truck location along the span length. Figure 47 shows how stresses may vary when a truck is passing over a short span bridge. The stresses increase when the first axle enters the bridge, and they decrease when the first axle exits the bridge. Consequently, when the second axle enters the bridge, the stresses increase and then decrease until the second axle exits the bridge.

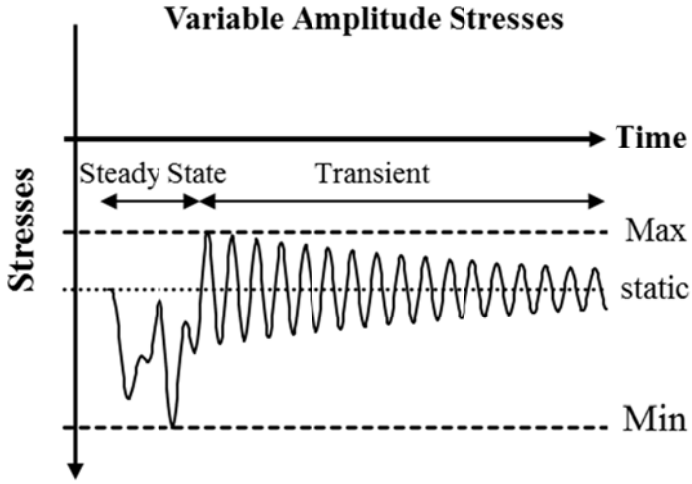

Figure 47. variable stress range in bridge vibration

As it can be seen in Figure 47, the stresses in the steady state part of the vibration do not fluctuate as much as they do in the transient part of the vibration. Since the fatigue life depends on the number of cycles and the range of stresses, neglecting the transient part of the vibration leads to underestimating fatigue life.

AASHTO LRFD Specifications for Fatigue

The first fatigue criterion was introduced in the 1965 specifications. Revisions were made in 1971 and 1974 based on experimental data. In LRFD Specifications, fatigue limit state is used to calculate fatigue stresses and only one truck is considered in the calculation. The design is based on 75 years life and one to two cycles of vibration per truck is considered in calculations. Nominal fatigue resistance is taken as:

$$(\Delta F)_n = (\frac{A}{N})^{\frac{1}{3}} \geq \frac{1}{2}(\Delta F)_{TH}$$ Equation 19

Where:

$(\Delta F)_n$ = Allowable fatigue stress.

N = Number of cycles the structure is subjected to the truck load for a 75 year design life. N can be calculated as:

$$N = (365)\ (75)\ n\ (ADTT)_{SL}$$ Equation 20

Where:

$(ADTT)_{SL}$ = Single-lane Average Daily Truck Traffic.

A= Detail category constant in ksi (Table 13)

$(DF)_{TH}$ = Constant amplitude fatigue thresholds in ksi (Table 13).

n = Number of cycles per truck passage (for span length shorter than 40 ft, n=2. For span length larger than 40 ft and near interior continuous supports, n=1.5, otherwise, n = 1).

Table 13 - Fatigue constant A and threshold amplitude based on detail category.

Detail Category	Detail Category Constant A (* 10^8 ksi^3)	Constant-Amplitude Fatigue Thresholds (ksi)
A (Rolled beams and base metal)	250.0	24.0
B (Welded girders)	120.0	16.0
B’	61.0	12.0
C (stiffeners and short 51 mm attachments)	44.0	10.0
C’	44.0	12.0
D (102 mm attachments)	22.0	7.0
E (cover plated beams)	11.0	4.5
E’	3.9	2.6
A325 Bolts	17.1	31.0
A 490 Bolts	31.5	38.0

Noting that, rolled beams and base metal are in Category A, welded girders are in Category B and B’, stiffeners and short 2 inches attachments are in Category C, 4 inches attachments are in Category D, and cover plated beams are in Category E and E’. In fatigue design calculations, AASHTO design truck (Figure 3) with a constant spacing of 30.0 ft between the rear axles is considered. The design truck is considered on one interior stringer and distribution factor is applied. Live load factor for the design truck is less than 1, because the fatigue damage due to a small number of heavy trucks is relatively less than the fatigue damage due to a large number of lighter trucks.

Therefore, the live load factor in AASHTO Specifications is equal to 0.75 of the design truck (low stress and high cycles loading). Live load impact factor is equal to IM = 0.15 in AASHTO specifications.

Analytical Studies on Fatigue

As it was shown in previous sections, the transient part of the vibration is a variable of k-parameter. Figure 48 shows the stress range for different k-parameters for both steady state part and transient part of the vibration.

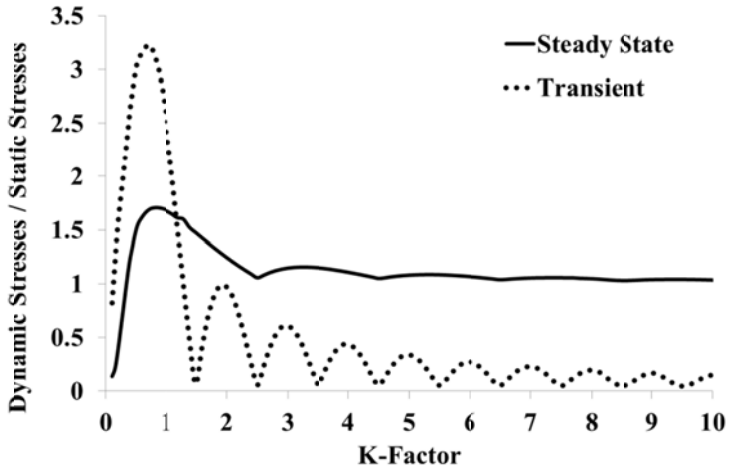

Figure 48. Dynamic stresses for transient and steady state parts of the vibration

As it was shown in Figure 47, the stresses in steady state part of the vibration do not fluctuate around the static equilibrium position. However, in the transient part of the vibration, the fluctuation is around the static equilibrium position. Therefore, the stress "range" in steady state part of the vibration is equal to the maximum value of the stresses within this time period, while the stress "range" in transient part of the vibration is twice as much as the maximum stresses in transient part (considering both under and above the static equilibrium position).

Since the number of cycles per truck, considered by AASHTO, is 1 for long span bridges and 2 for short span bridges (Table 14), the effect of transient part of the vibration to calculate allowable fatigue stresses is not considered.

Table 14 - Number of cycles per truck by AASHTO

Span Length	Simple span	Continuous span	
		not near interior support	near interior support
span > 40 ft	1	1	1.5
span < 40 ft	2	2	2

When span length is less than 40 ft, the axle length of the design truck exceeds the span length (30+14>40). At the time that the last axle enters the bridge the first axle has already left the bridge and the second axle is also about to exit. Therefore, one truck has the effect of two trucks over a short span bridge and it causes 2 cycles of vibration within the steady state part of the vibration. As it can be seen in Figure 47, the fluctuation during the steady state part of the vibration contains two cycles. However, the stress fluctuation is much more in the transient part of the vibration and can significantly affect fatigue life.

The number of vibration cycles that should be taken into account for each truck depends on both steady state and transient parts of the bridge vibration. Thus, all the stress ranges, whether in steady state or transient part, should be taken into account. For this, the complex stress range shown in Figure 47 should be reduced to a series of simple cyclic stresses. Then a histogram of cyclic stresses should be created to form a fatigue damage spectrum. For each stress level, the degree of cumulative damage incurred from the S-N curve (Figure 49) should be calculated. Finally, Miner's rule can be used to combine the individual contributions of each stress level.

The Miner's rule states that where there are k different stress magnitudes in a spectrum, S_i ($1 \le i \le k$), each contributing n_i cycles, then if N_i is the number of cycles to failure (Figure 49), failure occurs when:

$$\sum_{i=1}^{k} \frac{n_i}{N_i} = C$$

Equation 21

C is experimentally found to be between 0.7 and 2.2. Usually for design purposes, C is assumed to be 1.

Figure 49. stress range spectrum and S-N curve to find out the cumulative damage due to each stress range.

The numerical studies show that for some bridges with k-parameter equal to 2, damping ration 1 percent , and subjected to 1-axle loading the transient part of the vibration solely can increase the cumulative damage up to 530 percent . This is true theoretically when the endurance limit or fatigue threshold in S-N curve is not considered in fatigue design. In reality where the number of axles is higher than one, except for short span

bridges subjected to long trucks, and fatigue threshold should be considered for fatigue design, the 530 percent increase is not the case.

Assuming that the maximum static stress in the bridge due to the truck average weight is equal to f_{st} (or σ_{st}) , the cumulative damage due to the transient part of the vibration is as shown in Table 15. The ratio of $\sigma_{transient} / \sigma_{st}$ is obtained from Figure 49 (dotted line) for each k-parameter. The values of cumulative damage due to transient part of the vibration (TCD, transient cumulative damage) are shown as a percentage of the amount of damage caused by static loading. As it can be seen, the transient part of the vibration significantly affects fatigue life for k-parameters less than 6 and smaller damping ratio.

To explain the values stated in Table 15, the case of k = 3 and 3 percent damping is investigated in detail. Noting that the cumulative damage due to the transient part of the vibration for this case is equal to 52 percent . This percentage shows that the transient part of the vibration may increase the damage up to 52 percent of the static loading.

When the cumulative damage is increased to 1.52 times of the original amount of the damage due to static loading, the fatigue life is decreased by 1/1.52 = 0.66 = 66 percent .

$$\left(\sum \frac{n_i}{N_i}\right)_1 = C \quad \text{.....Equation 22}$$

$$\left(\sum \frac{n_i}{N_i}\right)_2 = 1.52\,C \;\rightarrow\; \left(\sum \frac{n_i}{N_i}\right)_2 . \frac{1}{1.52} = C \quad \text{.....Equation 23}$$

Table 15 - Cumulative Damage due to Transient part of the vibration (TCD)

k	$\sigma_{transient} / \sigma_{st}$	Damage due to the transient part of the vibration with respect to the damage due to static stresses -TCD (%)				
		ζ=1%	2%	3%	4%	5%
2	0.97	532	292	212	173	150
2.5	0.06	0	0	0	0	0
3	0.61	129	71	52	42	37
3.5	0.06	0	0	0	0	0
4	0.44	48	26	19	16	14
4.5	0.05	0	0	0	0	0
5	0.34	22	12	9	7	6
5.5	0.05	0	0	0	0	0
6	0.27	12	6	5	4	3
6.5	0.05	0	0	0	0	0
7	0.23	7	4	3	2	2
7.5	0.05	0	0	0	0	0
8	0.19	4	2	2	1	1

To calculate the amount of damage caused by all stress ranges in transient part of the vibration, the stress value in each cycle should be calculated. The decrease of stresses

per cycle can be calculated using equation 24, where j is the number of cycles, ζ is damping ratio, u_i is the stress amplitude at the beginning, and u_{i+j} is the stress amplitude after j cycles.

$$j = \frac{1}{2\pi\zeta} \ln \frac{u_i}{u_{i+j}} \qquad \text{Equation 24}$$

For one cycle, j =1, the stress is damped out to 82.82 percent of the initial value.

$$\ln \frac{u_i}{u_{i+j}} = 2\pi.\zeta.j \rightarrow \frac{u_i}{u_{i+j}} = e^{2\pi.\zeta.j} = e^{2\pi*0.03*1} \rightarrow u_{i+j} = 0.8282\, u_i \qquad \text{.Equation 25}$$

Assuming that the static stress due to live load is equal to f_{st} ,for k-parameter equal to 3, the stress at the first cycle of the transient part of the vibration is equal to 0.61 f_{st} (Figure 49). if N_1 cycles are required to result in failure for the stress range equal to f_{st}, the number of cycles which results in failure for a stress range equal to 0.61 f_{st} can be obtained using the following equation:

$$Stress = \left(\frac{A\ constant\ based\ on\ design\ details}{Number\ of\ Cycles}\right)^{\frac{1}{3}} \qquad \text{or} \qquad Number\ of\ Cycles \sim \frac{1}{Stress^3}$$

Therfore, it takes ($1/0.6^3$) N_1 cycles for the bridge to exhibit fatigue failure under a stress range equal to 0.6 f_{st}. the stress in the second cycle of transient vibration is 82% of the stress in the first cycle of the transient vibration and is equal to 0.6 * 82 percent f_{st}. Since the number of cycles which result in failure is inversely proportional to the cube of stress range, the number of cycles required to result in fatigue failure for a stress range equal to 0.82 * 0.6 * f_{st} , is equal to $\left(\frac{1}{0.8282^3} * \frac{1}{0.6^3} N_1\right)$. The number of cycles to failure for each stress range in transient part of the vibration is calculated and shown in Table 16.

Thus, the total cumulative damage due to transient part of the vibration is equal to half (50 percent) of the cumulative damage due to static stress.

$$\sum \frac{n_i}{N_i} = \left(\frac{n_1}{\frac{1}{0.6^3}N1} + \frac{n_1}{\frac{1}{0.8282^3}*\frac{1}{0.6^3}N1} + \frac{n_1}{\frac{1}{0.8282^{3*2}}*\frac{1}{0.6^3}N1} + \cdots + \frac{n_1}{\frac{1}{0.8282^{3*(n-1)}}*\frac{1}{0.6^3}N1}\right) \qquad \text{Equation 26}$$

$$\sum \frac{n_i}{N_i} = \frac{n_i}{N1}\left(0.6^3 + 0.8282^3 * 0.6^3 + 0.8282^{2*3} * 0.6^3 + \cdots + 0.8282^{(n-1)*3} * 0.6^3\right) = 0.6^3 * \frac{1-(0.8282^3)^{n-1}}{1-(0.8282^3)} = 2.32\frac{n_1}{N1}\,(0.6^3) = 0.5\,\frac{n_1}{N1} \text{.....} \qquad \text{.....Equation 27}$$

As it can be seen in Table 16, the cumulative damage due to transient part of the vibration varies from 0 percent to 532 percent . Therefore, for the bridges with higher transient vibration (k-parameter less than 6), the effect of transient part and damping ratio should be taken into account for fatigue calculations.

k-parameter for many bridges in New Jersey is about 2.0 to 5 (Table 10).

The fatigue life decreases as the result of cumulative damage due to the transient part of the vibration. The values of fatigue life decrease can be obtained using equation 28.

Decrease in fatigue life = $\frac{1}{1+\frac{TCD}{100}}$ Equation 28

Where TCD is equal to the Transient Comulative Damage in percentage, which is shown in Table 15 for some k-parameters.

Table 16 - The number of cycles to fatigue failure for each individual stress range in transient part of the vibration

Cycle in Transient Part	Stress	Number of cycles required to cause failure
Static loading	f_{st}	N_1
1st	$f_{1\ (transient)} = 0.6\ f_{st}$	$\frac{1}{0.6^3} N_1$
2nd	$f_{2(transient)} = 0.8282 * 0.6\ f_{st}$	$\frac{1}{0.8282^3} * \frac{1}{0.6^3} N_1$
3rd	$f_{3(transient)} = 0.8282^2 * 0.6\ f_{st}$	$\frac{1}{0.8282^{3*2}} * \frac{1}{0.6^3} N_1$
….	…….	……..
nth	$f_{n(transient)} = 0.8282^{n-1} * 0.6\ f_{st}$	$\frac{1}{0.8282^{3*(n-1)}} * \frac{1}{0.6^3} N_1$

Figure 50 shows the effective life of the structure due to fatigue failure for the bridges designed by AASHTO criteria. The structure life time in AASHTO is assumed to be 75 years while ,as it can be seen, only for few cases the structure life reaches to 75 years. In some cases the structure life would be even less than 20 years. Therefore, considering k-parameter and damping ratio is important to calculate the fatigue life.

As it was mentioned, k-parameter (Lf/V) depends on vehicle velocity (V), span length (L), and bridge frequency(f). The calculated k-parameters for Magnolia Bridge and Interstate I-80 over I-287 for the vehicle velocity of 65 mi/h, are equal to 2.5 and 4.1, respectively. Therefore the effective fatigue life, using the graph shown in Figure 50 would be equal to 75 years for Magnolia Bridge while it will be equal to 50 years for I-80 over I-287 assuming 1 percent damping ratio for both bridges. Since k-parameter has not been considered in bridge design, it is very likely that a bridge with k-parameter equal to 3 or 2 exist. Then the fatigue life for such bridges would be 30 or 10 years, respectively for 1 percent damping ratio.

As it can be seen, k-parameter significantly affect fatigue life and for those bridges with specific k-parameters, fatigue life could be as low as 10 years. Therefor, k-parameter

and damping ratio should be taken into account to calculate allowable fatigue stresses. Especially, since connections and joints are more sensitive to fatigue problem, they should be designed with respect to all parameters affecting fatigue such as k-parameter and damping ratio.

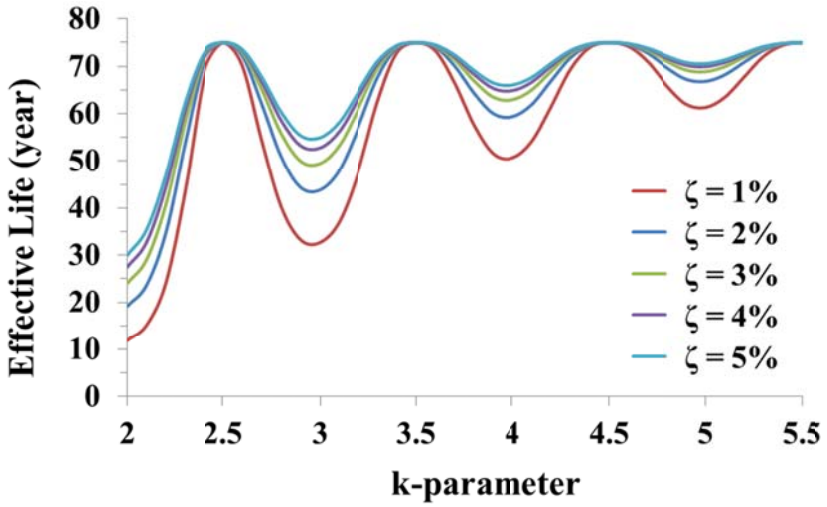

Figure 50. Effective fatigue life due to both steady state and transient parts of the vibration.

Fatigue Modification

To conclude the results of this chapter, it is suggested to calculate the fatigue stresses based on the procedure proposed below.

- Find σ_{st} (maximum static stress) and apply live load and impact factor, as suggested by AASHTO.
- Find k-parameter which is equal to Lf/V, span length by bridge frequency over vehicle velocity (65 mi/h = 1144 in/sec).
- Using k-parameter and the graph shown in Figure 48, find the ratio of the maximum transient stress range over static stress ($\lambda = \sigma_t / \sigma_{st}$).
- Find $\sigma_t = \lambda * \sigma_{st}$
- Assume damping ratio (ζ).
- Find σ_{TH} from Table 13 for a specific detail category which is being designed.
- Find j using equation 29. j is the number of cycles in which the stresses are higher than σ_{TH}.

$$j = \frac{1}{2\pi\zeta} Ln \frac{\sigma_t}{\sigma_{TH}}$$ Equation 29

- TCD, transient comulative damage, can be calculated using equation 30.

$$TCD = \lambda^3 . \frac{1-(e^{-6\pi\zeta})^{j-1}}{1-e^{-6\pi\zeta}}$$ Equation 30

- Modify N, number of cycles that the structure is subjected to the truck load for a 75 year design life, by using equation 31.

$$N = (365)\ (75)\ (n + TCD)\ (ADTT)_{SL}$$ Equation 31

Although the proposed procedure result in a better estimation of fatigue life, especially for the design of connections and sensetive parts of the bridge, more investigation is required in this aspect. Practical concepts and more field test results are required to verify the results obtained in this study.

Fatigue Remedy

Fatigue cracks that have begun to propagate can sometimes be stopped by drilling holes, called drill stops, in the path of the fatigue crack. This is not recommended as a general practice because the hole represents a stress concentration factor which depends on the size of the hole and geometry, though the hole is typically less of a stress concentration than the removed tip of the crack. The possibility remains of a new crack starting in the side of the hole. It is always far better to replace the cracked part entirely.

Changes in the materials used in parts can also improve fatigue life. For example, parts can be made from better fatigue rated metals. Complete replacement and redesign of parts can also reduce if not eliminate fatigue problems. Thus conventional steel can be replaced by composite HPS. They are not only lighter, but also much more resistant to fatigue. They are more expensive but the extra cost is amply repaid by their greater integrity.

EVALUATION OF L/D RATIO

Although the L/D limit is not required under NJDOT design manual, an objective of this study is the evaluation of L/D limits to, as stated in the RFP, “verify the applicability of the listed span-to-depth rations and establish ratio limitations that address the use of structural steel Grades 50 and 70.”

L/D limits are supposedly established to indirectly control the maximum live load deflection. As states before, the origin is traced to more than a century ago when AREA specifications were developed in 1905. While these limits have been employed for so many years, there have been significant changes in the definition of span length, L, and cross-section depth, D, over time. Span definitions of center-to-center bearing distance or the distance between points of contraflexure have been commonly used by engineers. Steel section depth (d) and total composite depth (D) are depth definitions that have regularly been used. These differences, while may appear small, have significant impact on cross-section geometry and application of the deflection and L/D limits.

As it was mentioned, deflection and L/D limits originated more than a century ago where bridges were simple and employed basic materials. Sophistications in today’s bridge designs combined with advances in development of high performance materials of various grades demands equally advanced and sophisticated approach to considering serviceability and durability requirements such that it will not negate the economical benefits of advances made in material development.

A simple example is provided in this chapter to show that the ratio of span-to-depth is not independent of span-to-deflection ratio. For a simply-supported beam loaded with a concentrated load at the center (Figure 51), the maximum moment, M_{max}, which is equal to PL/4, is used to size the member cross-section.

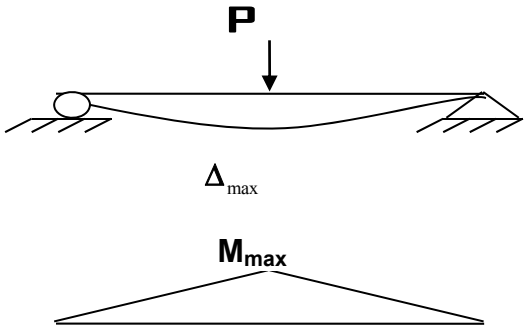

Figure 51. Simply Supported Beam under Concentrated Mid-span Load

Using the normal stress equation caused by bending moment, eq. 32, and simply supported beam deflection equation, eq. 33, the relation between yield strength and deflection can be obtained, eq. 34. Noting that in these equations, M, c, I, L, and E are bending moment, distance from the neutral axis to the top or bottom of the cross section, moment of inertia, span length, and modules of elasticity, respectively.

$$\sigma = \frac{Mc}{I} = \frac{\frac{PL}{4}c}{I} = \frac{PLc}{4I}$$ Equation 32

$$\Delta_{max} = \frac{PL^3}{48EI}$$ Equation 33

$$\Delta_{lim} = \frac{1}{12E}\frac{L^2}{c}\sigma_Y$$ Equation 34

Equation 34 shows that the higher strength materials require the higher deflection limit. This is a flaw in existing design specifications that rather penalizes the use of high strength material. Rational design methods will ensure that higher performance materials are used while structural serviceability and durability are achieved. It should be noted that similar equation is obtained for other loading (such as distributed load) and boundary condition. The same is true for multi-span beams.

Equation 34 can be re-written in the form of equation 35 substituting d/2 for c.

$$\frac{\Delta}{L} = \frac{1}{24E}\frac{L}{d}\sigma$$ Equation 35

As it can be seen, L/d ratio and deflection limits are correlated. In this study a bridge with 160 ft span length has been designed with A36, A709 grade 50, hybrid 70 and 50W, HPS70W, and HPS 100W. The weight saving, L/d, L/D, deflection, and AASHTO limits are provided in Tables 17 and 18. All L/d and L/D ratios exceed AAHTO limits except for ASTM A36. However, deflection meets AASHTO L/800 and L/1000 limits except for 100W.

Considering Table 17, L/D ratio based on AASHTO is larger than the design value by 20 percent for normal strength steel (ASTM A 36). For HPS 70W the AASHTO value is smaller than the design value by 26 percent . It must be noted that NJDOT does not require satisfying the L/D criterion, and it appears that it has been retained in the design manual simply to facilitate initial design trials. The provided L/D ratio appears to overestimate or underestimate the normal strength/high strength material within the same margins; therefore, it is recommended that these ratios be used for both normal and high strength steel. However, to prevent any confusion in part of designers - as it appears to be the case now - it is recommended that this article be moved into appendices so that the designers do not construed it as a requirement to check.

Table 17 - Span to depth ratio for different material configurations.

Steel Grade	Span (ft.)	Beam Depth d (inch)	L/d Ratio	AASHTO L/d Ratio	Steel Weight/Girder (Lbs)	(Beam + Slab +Haunch) D (inch)	L/D Ratio	AASHTO L/D Ratio
ASTM A 36	160	82	23.4	30.3	61400 A36	92	20.9	25
A 709 Grade 50	160	63.5	**30.2**	**30.3**	48900 Gr. 50	73.5	26.1	25
HYBRID 70W-50W-70W	160	57	33.7	30.3	42700 Mixed	67	28.7	25
HPS 70W	160	51	37.6	30.3	39200 70W	61	31.5	25
HPS 100W	160	42	45.7	30.3	36800 100W	53	36.2	25

Table 18 - Deflection for different material configurations.

Steel Grade	Span (ft.)	HL-93 (inch)	ML-80 (inch)	Permit (inch)	HS-20/ Max. Lane Load (inch)	H-20/Max. Lane Load (inch)	Controlling AASHTO L/800 NJDOT L/1000 (inch)	Actual L/K for HL-93
ASTM A 36	160	0.5	0.53	1.34	0.58	0.58	**2.40 (1.92)**	L/3840
A 709 Grade 50	160	0.92	0.98	2.46	1.07	1.07	**2.40 (1.92)**	L/2268
HYBRID 70W-50W-70W	160	1.23	1.3	3.28	1.43	1.43	**2.40 (1.92)**	L/1560
HPS 70W	160	1.56	1.67	4.17	1.82	1.82	**2.40 (1.92)**	L/1230
HPS 100W	160	2.3	2.44	6.13	2.67	2.67	**2.40 (1.92)**	L/835

CASE STUDY

The use of HPS 70W steel has been increased during the last decade. It is expected that this trend will continue and majority of new and replacement bridges in New Jersey will be constructed in HPS 70W steel. Currently there are four bridges in New Jersey that use high performance steel with another 3-4 awarded/advertised, recently.

Magnolia Avenue over Route 1 & 9, Scotch Road over I-95 with integral abutments, and Route 130 over Route 73 are owned by NJDOT and have been constructed. Nottingham Way Bridge over Assunpink Creek is owned by Mercer County and it is still under construction. Out of these four bridges, two of them have been analyzed in CsiBridge software program and the results for 2D and 3D models have been provided in this chapter. Moreover, the bridges are investigated under common trucks in New Jersey and the responses due to AASHTO truck is compared to the responses due to New Jersey common trucks.

Magnolia Ave. Bridge

Magnolia Avenue Bridge is located over Route 1 & 9. It is a composite bridge with single effective span of 129' 6". The bridge has two 15 feet lanes with two sidewalks. NJDOT Bridge Manual required that the live load deflection under HL-93 Live Load be less than L/1000 (1.5 in). The bridge has 7 stringers with the depth of 42 in and 6.5 ft distance between stringers. Stringers flanges are made of 70W steel and stringers webs are in 50W. The computed moment of Inertia for one stringer with the proportional converted deck section is equal to 68,121 in^4. The frequency, speed parameter, and k-parameter for this bridge are equal to 2.0 Hz, 0.18, and 2.72, respectively. The deflection due to truck was computed using CsiBridge software and was equal to 2.76 in. impact factor (IM) or dynamic load allowance is only applied to the deflection resulted from truck load and it is equal to 1.33 according to AASHTO LRFD. Therefore, the deflection due to truck plus impact would be equal to 3.67 in. Deflection due to 0.64 kips/ft lane load is equal to 2.05 in using equation 36

$$\Delta_{lane} = \frac{5\omega L^4}{384EI} = \frac{5(\frac{0.64}{12})(1554)^4}{384(29000)(68121)} = 2.05 \text{ in} \qquad \text{Equation 36}$$

The deflection resulted from design truck itself (3.67 in) is higher than the deflection resulted from design lane plus 25 percent of design truck (2.97 in). Multiple presence factor for two lane bridge is equal to m = 1. Distribution factor is computed assuming all girders deflect equally as suggested in AASHTO LRFD (Article 2.5.2.6.2).

$$DF = \frac{\#\ of\ Lanes}{\#\ of\ Stringers} = \frac{2}{7} = 0.286 \qquad \text{Equation 37}$$

By applying DF and m factors to the maximum deflection resulted from HL 93 design truck plus impact, the final computed deflection would be equal to 1.05 in which is less than 1.55 in (L/1000 limit).

If an owner chooses to invoke controls on span-to-depth ratios, L/D and L/d ratios should be less than 25 (D>0.04L) and 30 (d>0.033L) in which D is the overall depth of composite I-beam and d is the depth of I-beam portion of composite I-beam. The overall depth of Magnolia bridge final design is equal to 52.5" as a result of 8.5" concrete deck, 42" stringer depth (d) and 2" haunch. Therefore, computed L/D and L/d for Magnolia bridge are equal to 29.6 and 37, respectively. Therefore, Magnolia bridge final design meets the deflection criteria while it does not meet either of L/D and L/d limits.

Magnolia bridge has been redesigned for two alternative materials of steel 50W and 100W and compared with final design, 70W. Figure 52 shows the stringers cross sections for final design with 70W steel and two alternative designs with 50W and 100W steel for flanges. The stringer depths are kept constant and all webs are made of 50W steel. Table 19 shows the final computed deflection, L/D and L/d for all the Magnolia bridge designs. As it can be seen, deflection is higher for HPS 100W.

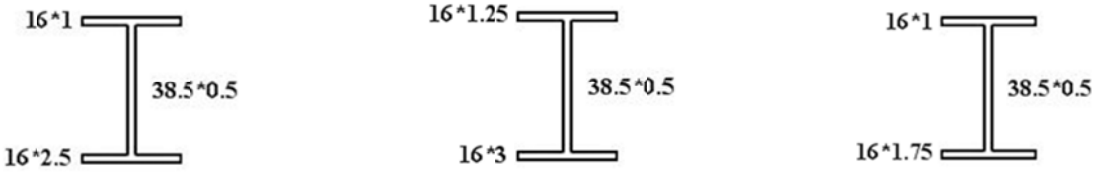

(a) Final (b) 50W (c) 100W

Figure 52. Magnolia bridge final design (a), 50W alternative design (b) and 100W alternative design (c)

Table 19 - Deflection and span-to-depth values for Magnolia bridge

Magnolia Bridge	Δ (in)	L/D	L/d
Alternative 50W	0.92	29.2	36.4
Final Design-70W	1.05	29.6	37.0
Alternative 100W	1.32	30.0	37.7

These three designs of Magnolia Bridge have been simulated using Finite Element software program, CsiBridge. The time history graphs for these cases are provided in Figure 53 for two alternatives. Bridges have been modeled in three dimensions (3D). The vehicles considered in 3D models are HL93 truck and NJ122 truck. NJ122 truck is the most common truck in New Jersey (44 percent of all truck in a random day in Rt. I-80 highway-refer to the field test chapter) and will be further discussed. The dynamic results from bridges designed with 50W and 100W were normalized and compared to each other in Figure 53. As it can be seen, the transient part of the vibration for 100W bridge is almost equal to zero while for 50W bridge, it is not. This is true for both vehicles crossing the bridge. The number of vibration cycles for 50W bridge is more than 100W bridge. Since the transient vibration of Magnolia Bridge designed with 100W steel is less than the transient vibration of the bridge designed with 50W steel, the bridge with 50W steel exhibit more vibration than the bridge constructed with 100W. This may affect both structural performance and human comfort.

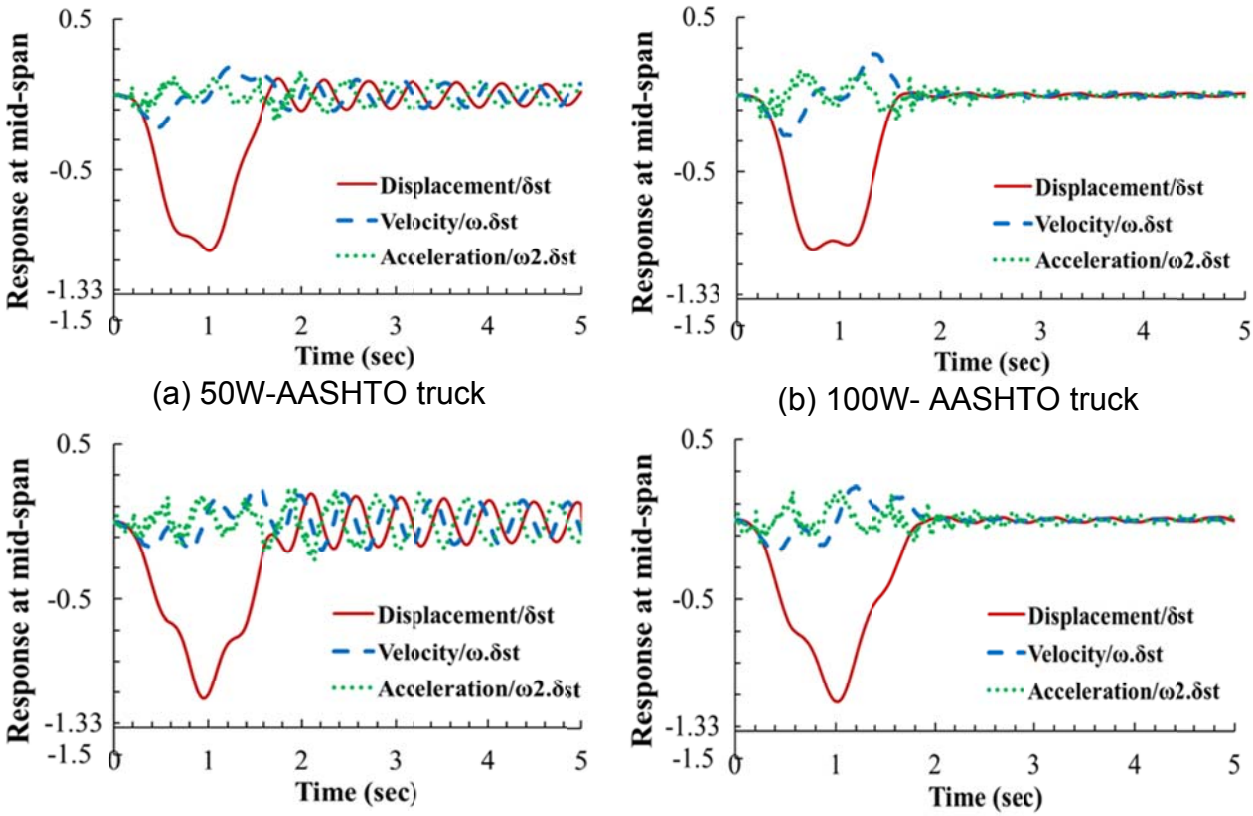

(a) 50W-AASHTO truck (b) 100W- AASHTO truck

(a) 50W- NJ 122 truck (b) 100W- NJ 122 truck

Figure 53. Magnolia bridge response time history for two alternatives of 50W (a) and 100W (b) for two types of truck, AASHTO design truck (1), and NJ 122 (2)

Figure 54 shows the midspan deflection time histories for all 50W, 70W, and 100W designs. Unlike steady state deflection, deformation in transient part of vibration is higher in 50W and 70W bridges than 100W bridge. Noting that, it is not the material that affects bridge vibration but rather it is k-parameter and load sequence which causes excessive vibration in some designed bridges. Therefore, applying a deflection limit cannot assure less vibration on a bridge.

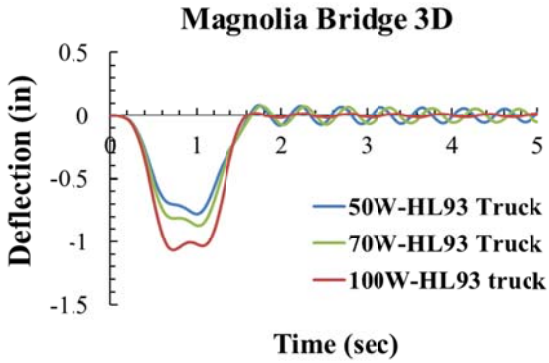

Figure 54. Midspan deflection time history of Magnolia bridge under HL93 truck.

Transient vibration for bridges with k-parameter equal to an integer number plus 0.5 (i+0.5) is nearly equal to zero and these types of bridges will exhibit the longest fatigue life regardless of how load sequence is. However, bridges with other k-parameters may or may not exhibit zero transient vibration depending on load sequence. k-parameter is a newly introduced parameter (introduced by the authors) and needs to be further investigated with respect to load sequence. Table 20 shows the numerical values of the dynamic response of three dimensional Magnolia bridge under HL93 truck in US units.

Table 20 - Magnolia bridge 3D dynamic results for HL93 truck load.

Material	δ_{static} (in)	f (Hz)	k parameter	$\delta_{Steady\ State}$ (in)	Velocity (in/sec)	Acceleration (in/sec^2)	IM (%)	$\delta_{Transient}$ (in)
50W-HL93 Truck	**0.75**	**2.09**	**2.84**	**0.78**	**2.15**	**21.50**	**4**	**0.08**
70W-HL93 Truck	**0.86**	**2.00**	**2.72**	**0.87**	**2.50**	**20.53**	**2**	**0.07**
100W-HL93 Truck	**1.06**	**1.83**	**2.49**	**1.07**	**3.23**	**22.67**	**1**	**0.02**

Rt 130 Over Rt. 73

Route 130 over route 73 is a simply supported single span bridge with 128.3 ft span length, six stringers, and three lanes. The slab thickness and width are 9 in and 46 ft, respectively. Haunch is equal to 1.5 inch. The bridge is designed with three material configurations including two alternatives, Grade A36 and 100W for all parts of the stringers, and the final design is with 70W for flanges and 50W for webs. The stringers dimensions, L/d ratio and deflections are provided in Figure 55 and Table 21. Deflection has been computed using the same procedure as used for Magnolia bridge for both lane and truck loads and the governing maximum deflection results are provided in Table 21.

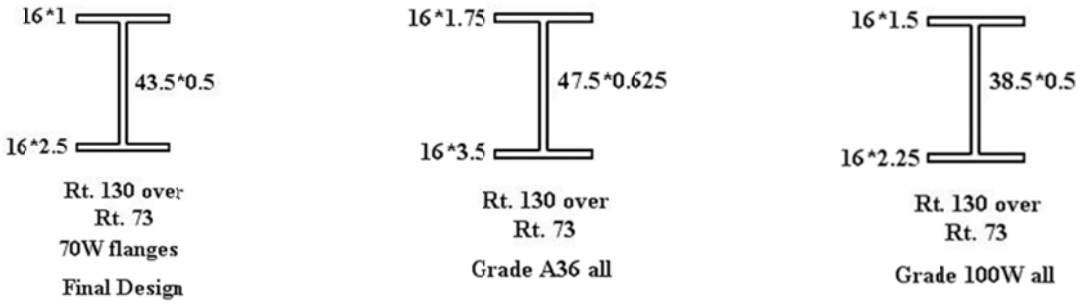

Figure 55. Rt. 130 over Rt. 73 (a) Final design and alternative designs with (b) grade A36 and (c) 100W.

As it can be seen, deflection, L/d, and L/D ratios increase by using higher strength materials in the design. The bridge has been simulated in three dimensional and loaded with HL93 truck.

Table 21 - Deflection and span-to-depth values for Rt 130 over Rt. 73 bridge

Rt. 130 over Rt. 73 Bridge	Δ (in)	L/D	L/d
Alternative Grade A36 flanges and webs	0.75	24.3	29.2
Final Design-70W flanges and 50W webs	1.19	26.8	32.8
Alternative 100W flanges and webs	1.49	29.2	36.5

Table 22 shows the dynamic response of the bridge in I-130 over I-73 under AASHTO design truck, HL93. Static deflection (δ_{static}) increases by using a higher strength steel, while the vibration is not truly correlated with δ_{static}. As it can be seen, for 100W steel, k-parameter is equal to 2.5 which result in smaller transient vibration and zero impact factor (IM). For 70W bridge, final design, with k-parameter equal to 3.82, transient vibration is 11 percent of its static deflection, 0.08/0.70. The case with A36 steel exhibit zero transient vibration and low impact factor. This is due to specific arrangement and arrival time of different axles which causes lower dynamic effect on this bridge. Simulations with other truck types do not result in low impact factor and zero transient vibration. Impact Factor (IM) increases from 5 percent to 16 percent when the bridge is designed for HPS 70W instead of A36, in Rt. 130 over Rt.73.

Table 22 - Three dimensional analysis results for Rt 130 over Rt. 73 bridge-3D.

Material	δ_{static} (in)	f (Hz)	k parameter	$\delta_{Steady\ State}$ (in)	Velocity (in/sec)	Acceleration (in/sec^2)	IM (%)	$\delta_{Transient}$ (in)
A36-HL93 Truck	**0.53**	**2.49**	**3.35**	**0.55**	**1.37**	**18.03**	**5**	**0.02**
70W-HL93 Truck	**0.70**	**2.11**	**2.85**	**0.81**	**2.20**	**26.31**	**16**	**0.08**
100W-HL93 Truck	**1.00**	**1.86**	**2.50**	**1.00**	**3.02**	**27.33**	**0**	**0.02**

Figure 56 shows the time history of all design configurations. As it can be seen in Figure 56d, although the steady state deflection is higher for higher strength materials, the transient vibration is only influenced by k-parameter and load sequence (truck types).

As it was mentioned, the deflection criteria cannot be a good scale to control bridge vibration. The deflection limits were introduced in 1936 based on experimental data for the bridges built during that era. Since then, bridge design, materials, connections, supports, and vehicles types, axle distances, axle weights, and tires flexibility have been changed.

As it was shown, impact factor, transient cumulative damage for fatigue design, and bridge acceleration are not dependent on bridge deflection, but k-parameter and load sequence. On the other hand, human is more susceptible to bridge acceleration than bridge velocity or displacement.

Therefore, more investigation on these two parameters is required in order to obtain a better understanding of bridge vibrational behavior under moving truck. The results of analytical studies then can be compared with experimental data which leads to a suitable conclusion to control bridge vibration.

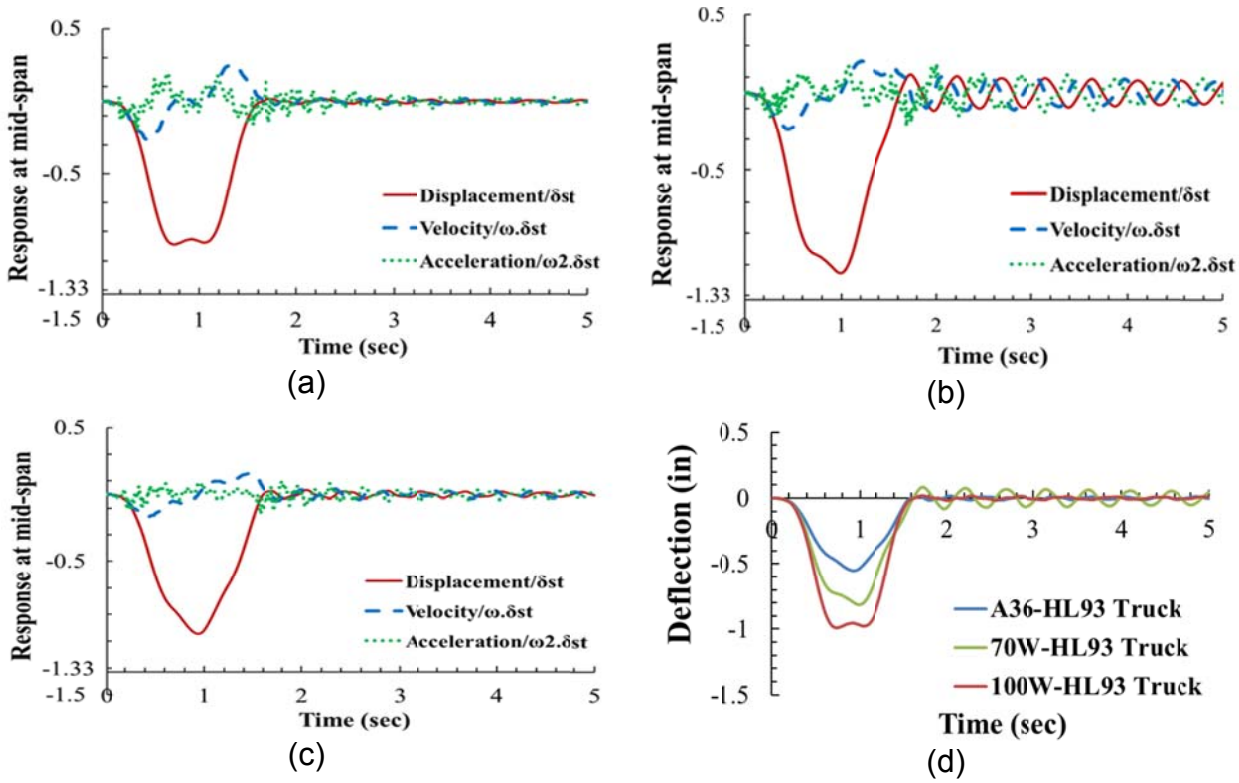

Figure 56. Dynamic response of Rt. 130 over Rt. 73 bridge under AASHTO HL93 (HS20) truck for three design configurations (a) 100W, (b) 70W Final design, and (c) A36; and (d) comparison.

FIELD MEASUREMENTS

The acceleration data from two bridges in New Jersey, one with concrete stringers and the other with steel stringers have been obtained. The steel-stringer bridge is located in Interstate I-80E over Interstate I-287N and the concrete-stringer bridge is located in the same highway, Interstate I-80, but over Smith Road. Bridges are very close to each other and there is no exit or entrance ramp between them. The vibration in the steel-stringer bridge was more tangible than the concrete-girder bridge.

The accelerometers used for measurement were not the suitable accelerometers for measuring ground acceleration. They were industrial accelerometers with the amplitude range of ±500 g peak and the frequency response from 1Hz to 10 kHz. The large ranges of amplitude and frequency provided by the industrial accelerometers decrease the measurement accuracy within the bridges' amplitude and frequency ranges which are less than one g for amplitude and between 1-5 Hz for frequency. Other accelerometer parameters have been provided here and the accelerometer is shown in Figure 57.

Frequency Response: 1 Hz to 10 kHz (up to ±10% rated output shift)
Rated Output: 10 mV/g nominal @ 100 Hz
Frequency Range: 2 Hz to 10 kHz (up to ±5% rated output shift)
Amplitude Range: ±500 g peak
Amplitude Linearity: ±2% up to 500 g peak
Discharge Time Constant: 0.5 s min
Strain Sensitivity: 0.001 g per microstrain @ 25°/μσ
Maximum g Without Clipping: ±1000 g
Base Strain: 0.03 g/microstrain nominal
Noise Floor (Wideband): 0.007 g (rms)

Figure 57. Accelerometer used in the field test.

I-80 Over I-287

The bridge in I-80 over I-287 is a simply supported steel stringer bridge with 87.75 ft, 51 ft, and 8 inch, span length, slab width and slab thickness, respectively. The concrete

deck is supported by 7 steel stringers with grade 50 steel and distance of 7.75 ft. Haunch distance is equal to 1.5 in and the bridge has 4 traffic lanes. The moment of inertia for one stringer cross section with its proportional deck is equal to 72,488 in^4 considering the converted concrete deck to steel material. The steel bridge is without side walk and deflection limit based on AASHTO LRFD is equal to L/800 = 1.32 in. New Jersey deflection limit is more conservative than AASHTO LRFD and it is equal to L/1000 for all bridges, with or without sidewalk. Therefore, deflection limit based on NJ Design Manual is equal to 1.05 in.

Using acceleration data measured over this bridge on October 8th, 2010, at noon, bridge damping ration and frequency was computed using Equation 38 (Chopra 2001) and fast Fourier transform. Figures 58 and 59 show two sample free vibration time histories of the bridge. The results show that damping ratio for Rt. I-80 over Rt. I-287 steel bridge is equal to 1.22 percent,

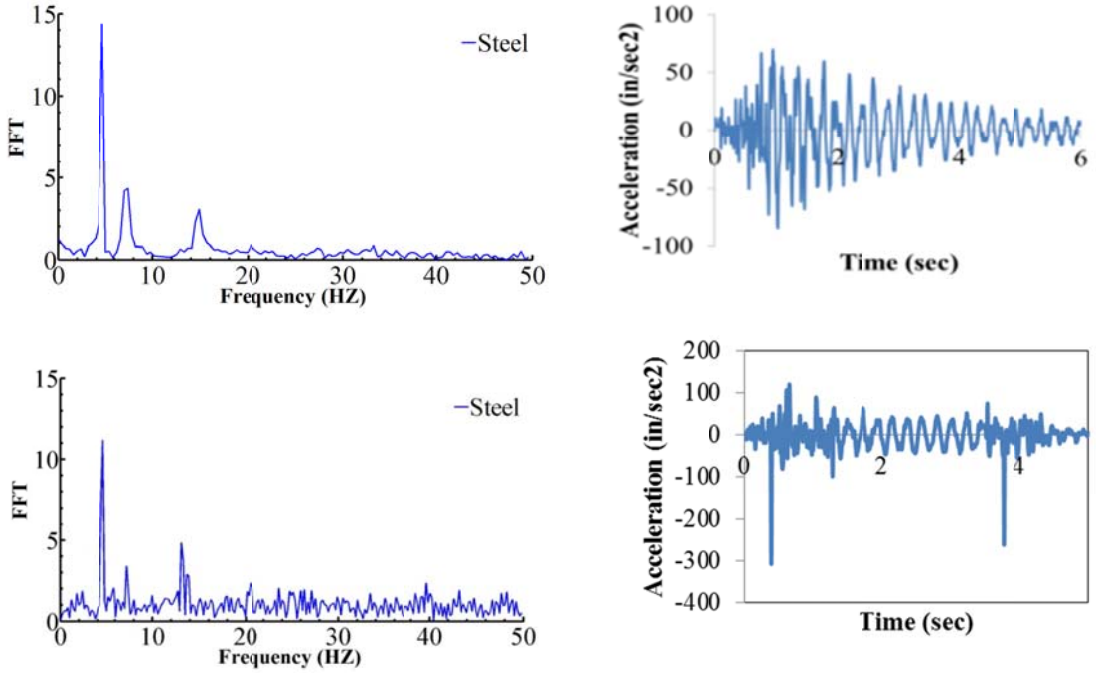

Figure 58. Fast Fourier transform for Rt. I-80 over Rt. I-287 steel bridge.

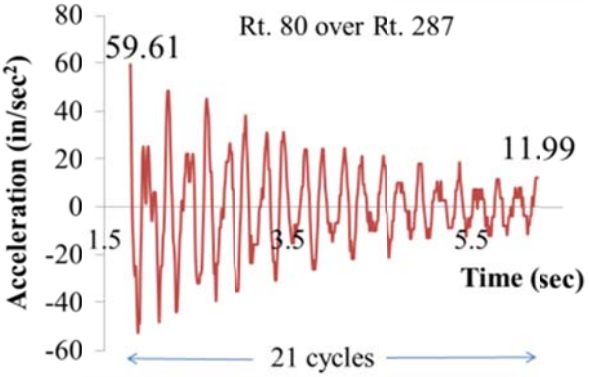

Figure 59. Time history free vibration for Rt. I-80 over Rt. I-287 steel bridge.

The static deflection for this bridge under HL93 truck and lane load is equal to 0.781 in and 0.406 in, respectively. Therefore, the maximum governing deflection is resulted from truck load alone and by applying m=0.65, DF=0.57 and IM=1.33 for multiple presence factor, distribution factor, and impact factor to the deflection resulted from design truck, the final computed deflection would be equal to 0.38 in. As it can be seen, the computed deflection is significantly less than the limit provided by NJ Design Manual. However, vibration on this bridge is strongly noticeable by human. The computed frequency, k-parameter, and speed parameter are equal to f = 4.6 Hz, k = 4.23, and α = 0.124, respectively.

Equation 39, and the bridge natural frequency is equal to 5 which corresponds the computed value.

$$\zeta = \frac{1}{2\pi j} \ln \frac{u_i}{u_{i+j}} = \frac{1}{2\pi j} \ln \frac{\ddot{u}_i}{\ddot{u}_{i+j}} \qquad \text{Equation 38}$$

$$\zeta = \frac{1}{2\pi(21)} \ln \frac{59.61}{11.99} = 0.0122 = 1.22\ \% \qquad \text{Equation 39}$$

I-80 Over Smith Rd.

The bridge in I-80 over Smith Road is a simply supported 80.8 ft long and 51 wide bridge over concrete stringers. This bridge is less than a mile away from Rt. I-80 over Rt. I-287 (east side) and has 4 lanes, 7 concrete stringers with the moment of inertia of 686,061 in^4 , frequency of 4.74 Hz, and k-parameter equal to 4.02. Deflection limit of L/800 is equal to 1.21 in and L/1000, stated by NJ manual, is equal to 0.97 in. Static deflection due to design truck is the governing deflection and it is equal to 0.514 in. Distribution factor, DF = 0.57, dynamic load allowance, IM = 1.33, and multiple presence factor, m = 0.65 should be applied to the deflection caused by truck load which result in 0.25 in deflection. This value is 26 percent of NJ limit and 20 percent of AASHTO limit.

Although the computed frequency for Rt. I-80 over Smith Rd. concrete bridge is equal to 4.9 Hz, the acceleration data measured by accelerometer and by using Fast Fourier transform show that the bridge actual frequency if equal to 10 Hz. In order to investigate the reason for this significant difference between computed frequency and measured frequency, more investigation and more detailed information on the constructed bridge is required. Figure 60 shows the acceleration time history for Rt. I-80 over Smith Rd. concrete bridge and the corresponding Fast Fourier Transform.

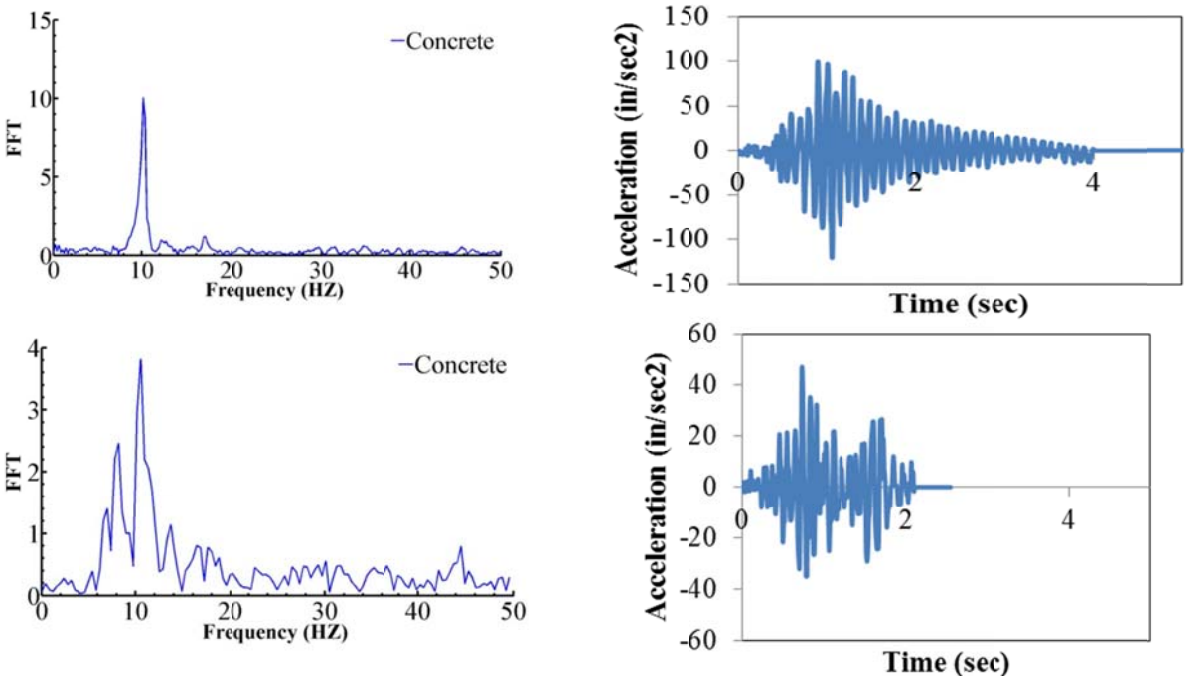

Figure 60. Fast Fourier Transform for Rt. I-80 over Smith Rd. concrete bridge.

Damping ratio has been computed for I- 80 over Smith rd. bridge and it is equal to 1.44 percent, Equation 40 and Figure 61.

$$\zeta = \frac{1}{2\pi(20)} \ln \frac{81.13}{13.35} = 0.0144 = 1.44\ \%$$ Equation 40

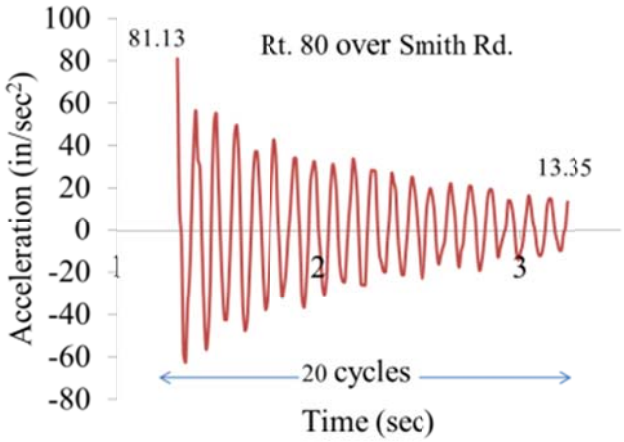

Figure 61. Time history free vibration for Rt. I-80 over Smith Rd. concrete bridge.

Comparison

The computed parameters for both Rt. I-80 concrete and steel bridges are nearly the same. However, the experimentally measured frequency for concrete bridge is twice as much as the computed frequency. More in-depth investigation and accurate measurements are required in order to clarify this difference in experimental frequency

and the computed one. Table 23 shows computed and measured frequency and k-parameter for both concrete and steel bridges. As it can be seen, actual k-parameter for concrete bridge is equal to 8.5 which is an integer number plus 0.5 (i+0.5). As it was mentioned earlier, bridges with such k-parameters do not exhibit any noticeable vibration for average truck speed of 65 mi/h.

Table 23 - computed and measured values for k and f for both bridges.

	concrete	steel
f (computed)	4.74 HZ	4.47 HZ
f (experimental)	10.00 HZ	4.50 HZ
k-parameter (computed)	4.02	4.23
k-parameter (experimental)	8.48	4.14

Figure 62 shows acceleration response for general bridges where these two bridges are located in the graph. Referring to this graph, it is expected that steel bridge with k-parameter equal to 4.14 exhibits higher dynamic response. Although both of these two bridges satisfy L/800 and L/1000 deflection limit criterion, the steel bridge exhibit much higher vibration than the concrete bridge. The results from field measurements indicate that the computed frequency for the concrete bridge is significantly less than the actual frequency obtained from test results. The less severe vibration observed in the concrete bridge is probably due to its higher frequency and lower vibration time duration compared to the steel bridge. Although vibration duration after a truck exits the bridge is an important factor for human response, it does not influence the bridge structure. Bridge structure is influenced by the number of vibration cycles regardless of the duration.

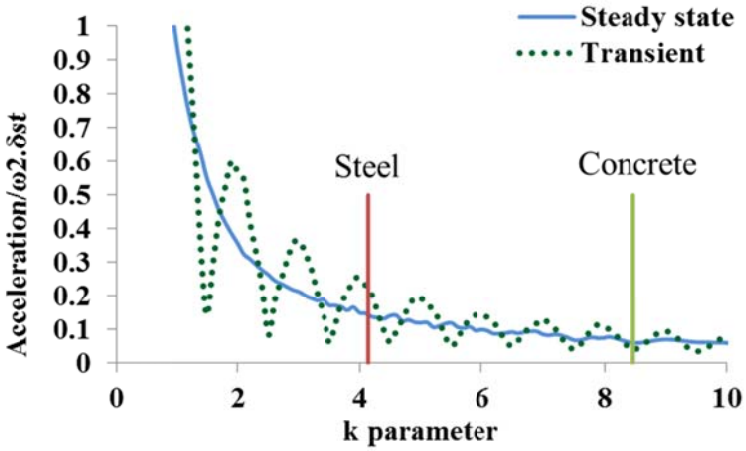

Figure 62. Comparison between concrete and steel bridges acceleration responses.

The damping ratio for both bridges is less than 1.5 percent which is less than the values suggested by British code, 4 percent steel composite bridges and 5 percent for concrete bridges (Brown, 1977).

Field measurements showed that vibration duration for concrete bridge does not exceed 2 seconds while the duration on steel bridge is more than 5 seconds. This is due to higher measured frequency for the concrete bridge than the steel bridge.

Vehicle Classifications

The very early truck types, H-20-35 and H-15-35, were introduced in AASHTO 1935, Figure 63. H series trucks are two-axle trucks. The number following the H designation is the gross weight of the trucks in US tons (1 US ton = 2000 lb). The number at the end of truck classification refers to the year of the specifications publication in which the truck is reported in. In 1944 specification, HS20-44 and HS15-44 were reported. The "HS" loading consists of tractor truck with semitrailer and they have three axles. As it can be seen in Figure 64, the rear axles' distance is equal to 14 ft for simply supported bridges while for continuous span bridges, this distance varies from 14 to 30 ft.

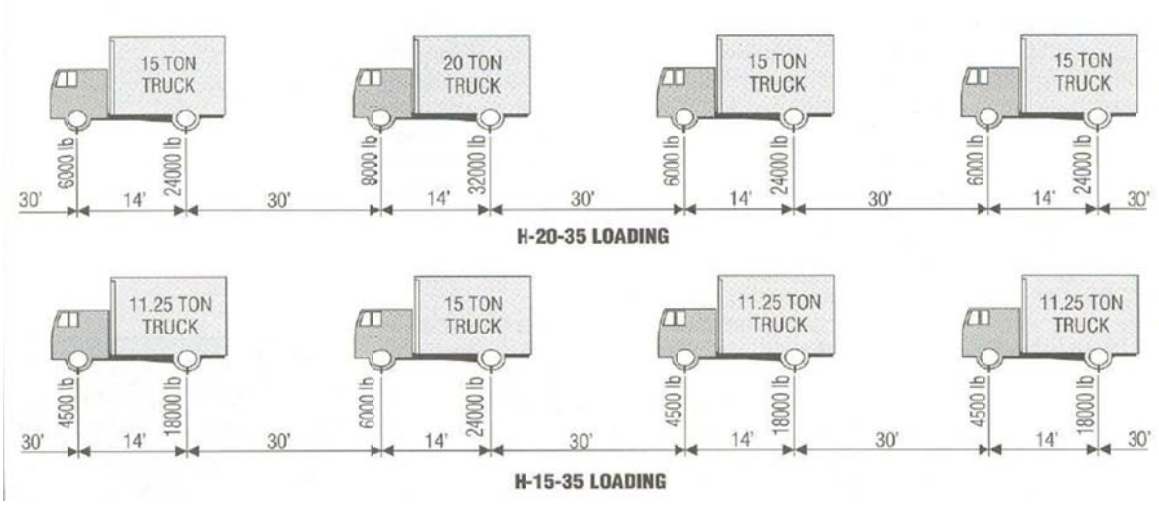

Figure 63. H series trucks as indicated in AASHTO 1935.

Figure 65 shows lane load and a concentrated load as indicated in AASHTO 1944. Design lane load has not been changed in AASHTO LRFD (2007). The design tandem shall consist of a pair of 25.0-kip axles spaced 4.0 ft. apart. The transverse spacing of wheels shall be taken as 6.0 ft. Design tandem load is identified in previous editions as Interstate load or alternative Military load which was a two-axle load, 24 kips each and 4 ft apart. This load represented heavy military loads. AASHTO LRFD has kept the axle distance and changed the axle weight to 25 kips.

During late 20th century, some engineers have required an HS25 truck load for underground precast structures. There was some concern that the HS20 truck load does not adequately reflect actual conditions. HS25 truck is 1.25 times larger than HS20 in axle weights. The increased load can in some cases create the need for additional reinforcing steel and sometimes a thicker top slab on underground structures installed in areas exposed to heavy truck loads.

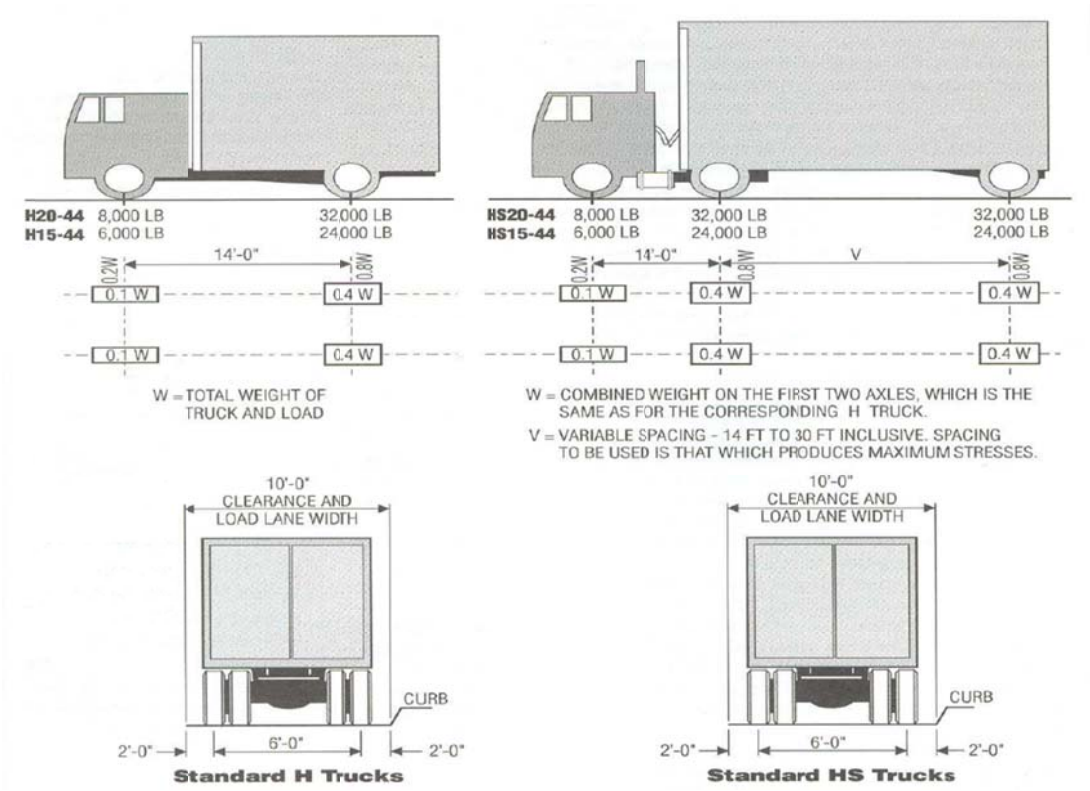

Figure 64. HS and H series truck as indicated in AASHTO 1944.

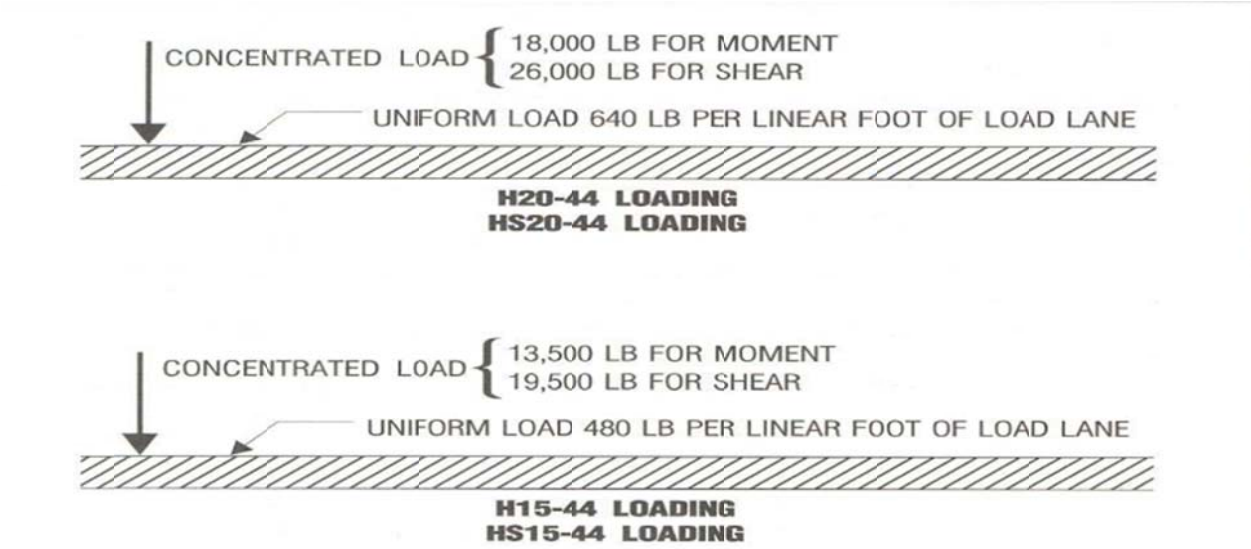

Figure 65. Lane load and concentrated load as indicated in AASHTO 1944.

The HL93 designation consists of a “design truck plus design lane load” or “design tandem plus design lane load,” whichever produces the worst case. A “design truck” is identical to the HS20-44 load configurations shown in Figure 64. The “design tandem” is a two-axle load of 25 kips and 4 feet apart.

A comparison of old AASHTO versus new one indicates that the difference is very small. The HL93 “design truck” wheel load is the same as the HS20 wheel load. The HL93 “design tandem” wheel load is only 0.5 kips more than the “Alternate Military Load”, 12.5 kips versus 12 kips. Noting that for deflection control only design lane and design truck is used and the design tandem is not used for deflection control.

From the 24-hour data provided by NJDOT for the field test done in this study on 10/08/2010 (Station ID: 00080C, FIPS State Code: 34, record type: W), class 9[2] was the most frequent (about 48 percent of the total truck transportation-classes) truck in Rt. I-80 at the nearest station to I- 287. The average axle weight and distance is shown in Figure 66. This truck has been called as NJ 122 and been used in simulations for comparison. NJ 122 contains 5 axles, one at the front, two in the middle, and two axles at the back of the truck.

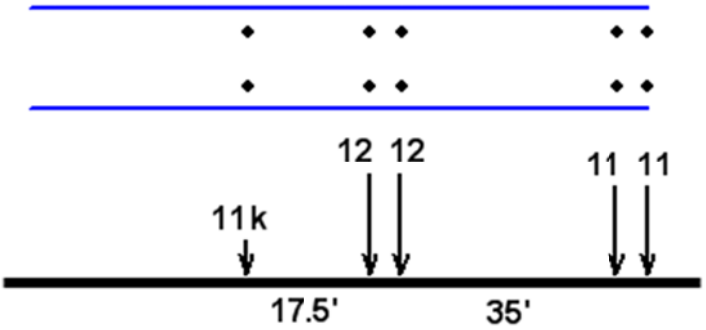

Figure 66. NJ122 truck, possibly the most common truck type in New Jersey.

[2] Class nine is for Five-Axle, Single-Trailer Trucks. All five-axle vehicles consisting of two units, one of which is a tractor or straight truck power unit.

SIMPLIFIED METHOD TO ESTIMATE DYNAMIC RESPONSE

As it was mentioned the existing deflection serviceability requirements are more than a century old and their origin is not known. Prior studies dispute their effectiveness in reducing dynamic effect and/or damage to bridges and they negate application of high performance materials. Thus, there is a need for a more rational serviceability requirement that accurately considers important dynamic parameters such as acceleration and velocity in addition to bridge deflection.

The research by Wright and Walker (1971) is the only work that proposed an equation to estimate bridge acceleration. However, it has not been implemented due to the lack of consensus as its application is limited. In this study a more general method is proposed to estimate the dynamic response of bridges subjected to moving load.

Figure 67a shows acceleration versus speed parameter for the most general case of a 3-axle truck load and 1 percent damping along with Wright and Walker equation. As it can be seen the Wright and Walker equation does not give accurate estimates for this general case. Similar results are shown for velocities in Figure 67b.

Based on these results, Equations 41 and 42 are proposed to estimate the bridge acceleration and velocity, respectively. The proposed equation for acceleration is an improved version of Wright and Walker that consider practical situations.

$$\begin{cases} \dfrac{A_{max}}{\omega^2 \delta_{st}} = 1.2\alpha & for \quad \alpha \le 0.35 \\ \dfrac{A_{max}}{\omega^2 \delta_{st}} = 4.5\alpha - 1.15 & for \quad \alpha > 0.35 \end{cases} \qquad \text{Equation 41}$$

$$\begin{cases} \dfrac{V_{max}}{\omega \delta_{st}} = 1.5\alpha & for \quad \alpha \le 0.35 \\ \dfrac{V_{max}}{\omega \delta_{st}} = 4\alpha - 0.9 & for \quad \alpha > 0.35 \end{cases} \qquad \text{Equation 42}$$

Where A_{max} is the maximum bridge acceleration; and α, ω, and δ_{st} are speed parameter, natural frequency, and static deflection, respectively. The equation(s) to estimate the maximum bridge velocity, V_{max}, has been added as literature review indicates that future development in serviceability limits most likely will require the use of velocities too.

The proposed equations are plotted in Figure 67 and as it can be seen they estimate bridge dynamic response with good accuracy. These equations can be used in development of a more rational serviceability requirement that will ensure human

comfort while better allowing for application of high performance materials in new designs.

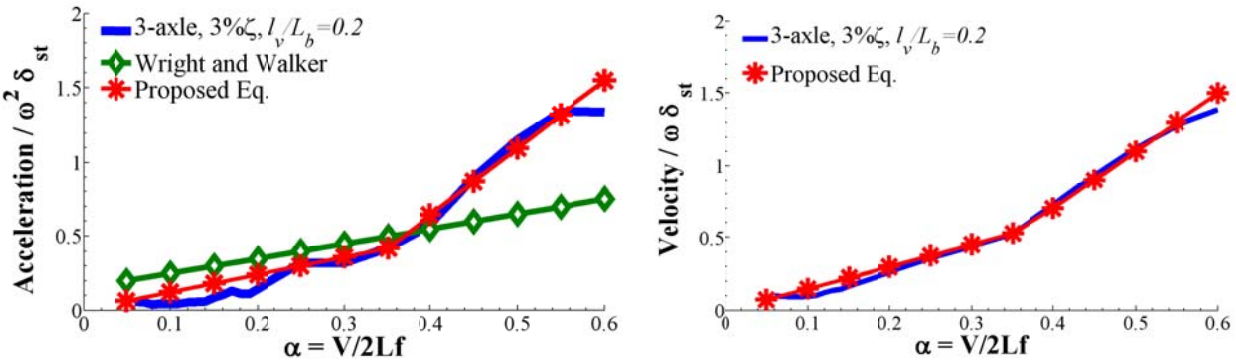

(a) (b)

Figure 67. Proposed formula for dynamic acceleration (a), and velocity (b) for the simply supported bridge.

Noting that speed parameter is equal to half of inverse k-parameter and ω is equal to 2πf.

It is proposed that Equation 43 is used for deflection limitation. The equation is obtained by applying the acceleration limit suggested by Wright and Walker to the proposed equation for computing acceleration, Equation 41.

$$\delta_{st} < \frac{L.}{270f} \qquad \text{Equation 43}$$

$$\delta_{st} < \frac{A_{limit\cdot}}{1.2\ \alpha\ \omega^2} = \frac{A_{limit\cdot}2Lf}{1.2\ V\ (2\pi f)^2} = \frac{100\left(\frac{in}{\sec^2}\right)*2*L}{1.2*1144\left(\frac{in}{\sec}\right)*4*\pi^2*f} = \frac{L}{270f} \qquad \text{Equation 44}$$

CONCLUSIONS AND RECOMMENDATIONS

With continued development of High Performance Steel (HPS), design for lighter and more economical bridges is unavoidable. HPS offers high yield strength, high fracture toughness, good weldability, and the ease of fabrication with the choice of weathering performance. In order to take advantage of these characteristics, some modifications are required in design codes so that they do not negate the use of such newly innovated materials. AASHTO LRFD optional deflection criterion, which is stated in the New Jersey Bridge Design Manual as a mandatory criterion, is based on experimental data which were obtained several decades ago. Nowadays, not only bridge's constructions, materials, and designs have been changed, but also vehicles types, weights, and flexibilities have been varied as well.

Literature review shows no correlation between bridge structural damages that can be attributed to excessive deflection. Damages are due to connection rotations and local deformations which could not be controlled by limiting the global deflection. It is now generally agreed by most researchers that deflection limits were based on the reactions of people to the bridge vertical acceleration rather than the structural effects.

Although human body is more sensitive to the derivatives of displacement rather than the displacement itself, it is believed that deflection limits have been established and used for decades, because computing deflection was much easier than computing acceleration of a bridge under moving truck. Although some researchers such as Wright and Walker suggested some simple methods to compute acceleration, these methods have not been adopted by AASHTO Specifications because of the lack of consensus.

A comprehensive analytical parameter study has been performed by this study to investigate bridge dynamic responses under moving truck. Existing finite element (FE) software programs provide an ideal platform for such a parameter study. However, one has to be careful in selecting the modeling parameters as the acceleration and velocity time histories are quite sensitive to specific assumptions such as time step, mesh quality, number of modes, and load representation. Therefore, to study acceleration and velocity responses, it is important to correctly select the finite element model parameters. In this study, first, the results of Finite Element models have been compared to exact solution for single axle loading. Once the confidence was established in the accuracy of the models, they were used for parameter study. The dynamic results are in dimensionless values for all acceleration, velocity and deflection responses for bridges at their midspan.

Parameters considered are vehicle velocity, span length, bridge natural frequency, speed parameter, damping ratio, number of spans, stringers distances, bracing effect, support conditions, and load sequence. Vehicle velocity (V), span length (L), and bridge frequency (f) have the most influence on bridge dynamic response.

The results indicate that k-parameter which is the bridge natural frequency multiplied by span length divided by vehicle velocity (k=Lf/V), has the most influence on dynamic response. This parameter is equal to half the inverse of speed parameter which was

reported by several other researchers prior to this study. It was noticed that the bridges with k-parameters equal to an integer number plus half, i + 0.5 exhibit lower amplitudes of vibration under any types of trucks traversing with the regular speed of 65 mi/h. The vibration in transient part was nearly equal to zero and impact in steady state part was at the minimum values.

For those bridges in which k-parameter is not equal to an integer number plus half, i+0.5, truck axle distances and its ratio to vehicle velocity and bridge frequency (L_v f /V) significantly affect bridge response in both transient and steady state parts of the vibration. Load sequence is a vast area for research with a large number of possibilities in vehicle types and bridge dynamic parameters and should be further investigated. In this study only one-axle and two-axle truck loads have been considered. One axle truck load refers to short span bridges which are subjected to truck axles with long axle distances so that only one axle is located over the bridge at the time. Bridge acceleration and velocity are the maximum or the minimum when the vehicle k-parameter ($k_v = \frac{L_v}{V}$ .f) is equal to an integer number or an integer number plus half, respectively. The maximum deflection decreases when the axles are further from each other. However, in the vicinity of an integer number for k_v, deflection is the maximum; and in the vicinity of an integer number plus 0.5 for k_v, deflection is the minimum.

Number of spans did not significantly affect dynamic response. However, dynamic response in transient part of the vibration decreased slightly as the number of spans increased. Boundary conditions only influence the bridge natural frequency and the frequency of higher modes in a bridge. Analytical studies show that by keeping the frequencies constant and varying boundary conditions, bridge response do not vary.

Damping ratio was another parameter considered in this study. It was shown that higher damping ratio not only decreases the dynamic response, but also it decreases vibration duration. If damping ratio increases by the order of n, number of vibration cycles decreases by the order of 1/n. For instance, if damping ratio increases from 1 percent to 2 percent , the number of vibration cycles decrease to half. This can reduce fatigue problem caused by high number of cycles.

Case study was also performed in this project. Two bridges, Magnolia Bridge over Rt. 1 & 9 and Route 130 Bridge over Route 73, were considered in the case study. Both bridges are located in New Jersey and constructed using hybrid girders of 70W for flanges and 50W for webs. For case study, these two bridges were redesigned for different material configurations. Magnolia bridge was redesigned for 50W and 100W for flanges. The stringers depths have been kept constant and all webs are made of 50W steel. The bridges were subjected to two truck types, AASHTO HL93 design truck and NJ 122. Mid-span deflection for the bridge designed with HPS 100W was more than 70W, and that for 70W was more than 50W and the deflection for all three designs was lower than L/1000. Both limits of L/d and L/D were not satisfied by any of these design configurations. However, the bridge designed with 100W exhibited the least vibration (in terms of number of cycles per truck passage) and impact factor for both truck types. k-parameter computed for this bridge was equal to 2.49 while k-parameters computed for

the bridges designed with 50W and 70W were equal to 2.84 and 2.72, respectively. As it was mentioned, dynamic response for those bridges with k-parameter equal to an integer number plus 0.5 is the minimum.

Rt. 130 over Rt. 73 was redesigned for two alternative material configurations. The final design of this bridge was constructed using HPS 70W for flanges and 50W for webs. The two alternatives are with Grade A36 and HPS 100W for all webs and flanges and web height was varied for all designs. Mid-span deflection values satisfied L/1000 New Jersey deflection limits for all design configurations. L/d and L/D ratios were only satisfied the limits for the bridge designed with grade A36. The bridge designed with 70W, the final design, exhibited the maximum vibration under HL93 truck with 14 feet axle distance. Number of vibration cycles and impact factor were both the least for 100W alternative bridge. Computed k-parameters for all design configurations show that k-parameter for the bridge designed with 100W was equal to 2.5; and again the results support the results obtained from the parameter study.

Despite not being a part of this project, acceleration response was measured on two bridges in Route 80, east side of Rt. I-80 over Rt. I-287 which is a steel girder bridge and Rt. I-80 over Smith Rd. which is a concrete girder bridge. These two bridges are less than one mile away from each other with the same frequency, number of girders, number of lanes, and span length. Vibration over the steel bridge was significantly more noticeable than vibration over the concrete bridge. Although both bridges satisfy the AASHTO and NJ Design Manual deflection limit criterion, the steel bridge exhibit much higher vibration under the same truck than concrete bridge. The computed frequency for steel bridge corresponded to the frequency determined by field test. However, surprisingly, the frequency determined by field test for concrete bridge was twice as much as the computed one. The reason could be attributed to support conditions or the fact that concrete deck is supported by end diaphragms thoroughly while concrete deck in steel girder bridge is only connected to end diaphragms through stringers. In either case, more investigation is required to obtain concrete conclusion on this matter.

Damping ratio for both bridges were less than 1.5 percent . Therefore, for those bridges that the value of damping ratio is not known, it is recommended that damping ratio be taken as 1 percent .

Based on the results of this project the following recommendations are provided:

Short Term (Incremental Changes)

- Use L/800 not L/1000 as the deflection limit
    - May want to even consider further increase to L/450
- Do not use L/D limit(s)
    - This is more a clarification notice to engineers as NJDOT design manual does not require its use. However, since it is listed the designers tend to

use it. This can be remedied by removing the article and providing the L/D ratios as an appendix to simply assist engineers during the initial design phase. The same can be used for HPS in estimating the initial depth.

- Do not use permit load for deflection criteria
    - This again might be an issue of clarity in language so that designers do not over conservatively interpret the manual as requiring the use of permit load.
- If permit load is used consider the following:
    - Impact factor is lower (essentially unity)
    - Not all lanes are loaded.
- Do not use moment distribution factor (DF) for deflection calculations. NJDOT manual correctly does not state its use. However, it does not clearly state that the deflection DF must be used. Therefore, designers tend to conservatively use the moment DF for deflection control.

- Do not use live load (LL) factor for deflection calculations. NJDOT design manual does not clearly state that Service I should be used for deflection control it just states the general load type of service limit state. It must be made more specific that Service I be used in checking serviceability criteria.

Long Term (Transformational Changes)

- Use acceleration in establishing the serviceability requirement as follow:

$$\delta_{st} < \frac{A_{limit}}{1.2\alpha\omega^2}$$

- Use 100 in/sec^2 as the acceleration limit
    - This is based on Wright and Walker and can benefit from additional work on human factor vs. bridge dynamic response
- Use the above equation for speed parameter (α) less than 0.35, which includes most typical highway bridges.
    - For other values use the modified equation as presented in the report (as simple)

- The following is a simple application using Wright and Walker acceleration limit and 65 mi/h truck speed (note that - V/2LF where V is truck speed, L is bridge length and f is bridge frequency):

$$\delta_{st} < \frac{A_{limit}\cdot}{1.2\ \alpha\ \omega^2} = \frac{A_{limit}\cdot 2Lf}{1.2\ V\ (2\pi f)^2} = \frac{100\ \left(\frac{in}{\sec^2}\right) * 2 * L}{1.2 * 1144\left(\frac{in}{\sec}\right) * 4 * \pi^2 * f} = \frac{L}{270f}$$

- Observations on proposed criterion (its improvement over existing approach):
  - It is more rational by relating the deflection limit to other important bridge dynamic factors and truck speed.
  - For acceleration limit of 100 and typical bridge frequency of 3 Hz it is consistent with existing requirement of L/1000
  - It does not penalize high performance steel as acceleration limit is rationally related to the bridge flexibility.
  - For bridges with higher frequencies, since the vibration duration is lower it is not significantly noticeable. Therefore, the limits may be neglected for bridges with higher frequencies (e.g. f > 5).

FUTURE WORK

Significant parameter study was performed in this study. As a result a new serviceability equation was proposed that can have national implications. Therefore, it is important to conduct further investigation on load sequence. Load sequence has been completed for one, two and three consecutive 1-axle loads. Moreover, the axle distance in a two-axle truck with identical axle weight was investigated. However, to enhance applicability of the proposed equation it is required to investigate three axle trucks with different axle distances too. Since axle weight is another parameter affecting bridge response, the effect of various axle weights should also be investigated.

The load sequence results from single-span bridges have to be expanded to multi-span bridges. The proposed method, which appears to be consistent with other national efforts, will require determination of bridge frequency. To facilitate day-to-day implementation by engineers there is a need for easy and practical calculation of bridge frequency. Bridge frequency can be computed for simply supported bridge using the available equation. However, there is no simple equation in order to estimate higher modes frequencies or the frequencies for multi-span bridges with various span lengths or single span with integral abutments.

There is also a need for more measurements of response of highway bridges to moving loads, especially the acceleration response as more rational serviceability requirements tend to consider this aspect of bridge response too. For the two bridges considered under this study since the computed bridge frequency for the concrete bridge was nearly twice as much as the measured frequency more investigation is required on this aspect to find the reasons for such a discrepancy. It should be noted that field tests where not within the scope of this project, thus, only limited measurements were made.

Additionally, the effect of bearing needs to be investigated. Besides literature review analytical model should be modified to accurately represent the bearing. For this purpose, the bearings can be modeled as spring dampers and the effect of different support stiffness and dampers can be investigated. This should be done for both single span and multi span bridges.

Furthermore, Vehicle characteristics and the initial oscillation of the vehicle suspension and road roughness should be investigated.

The results should also be expanded to include curved bridges. Similar to existing parameter study such investigation can include both 2-D and 3-D models with different boundary conditions, girder distances, and cross bracing spacing.

For durability evaluation the preliminary work conducted on fatigue under existing project should be broadened.

Finally determination of limiting acceleration considering human factor, bridge use, bridge-vehicle interaction for pedestrian and passengers in the cars should be further investigated too..

APPENDICES

Magnolia Bridge Drawings

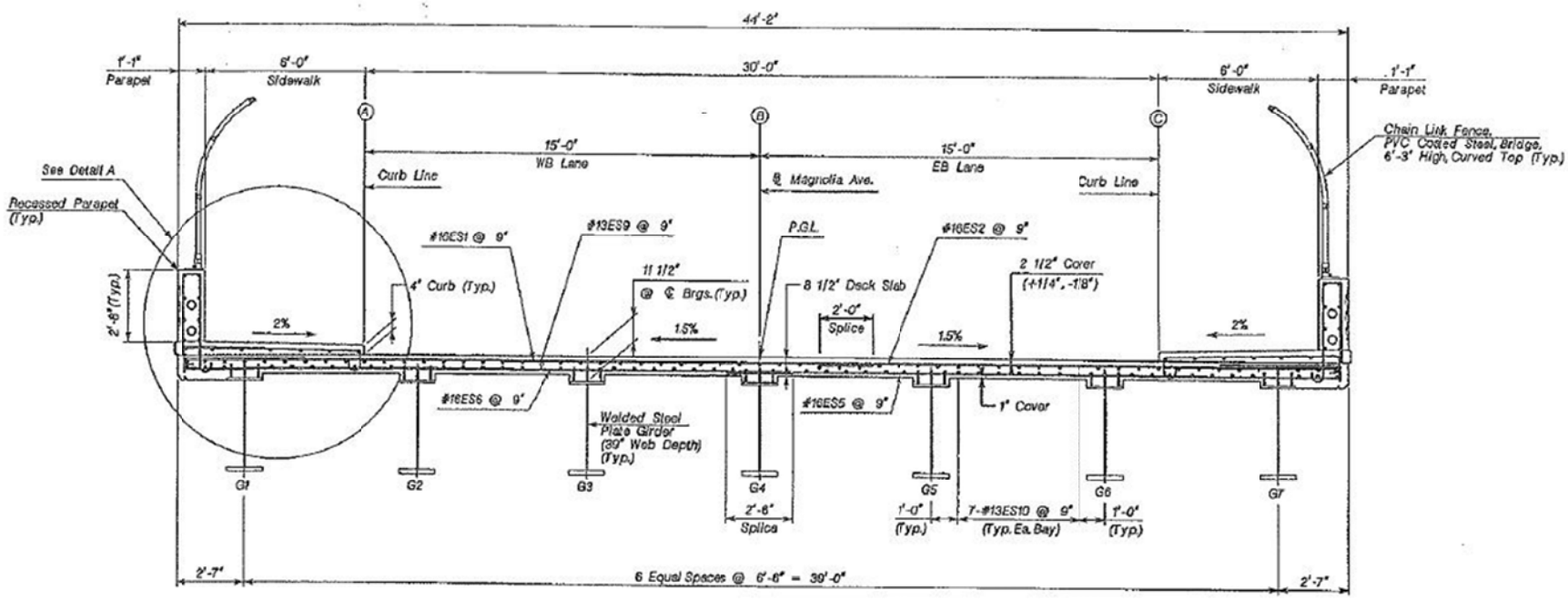

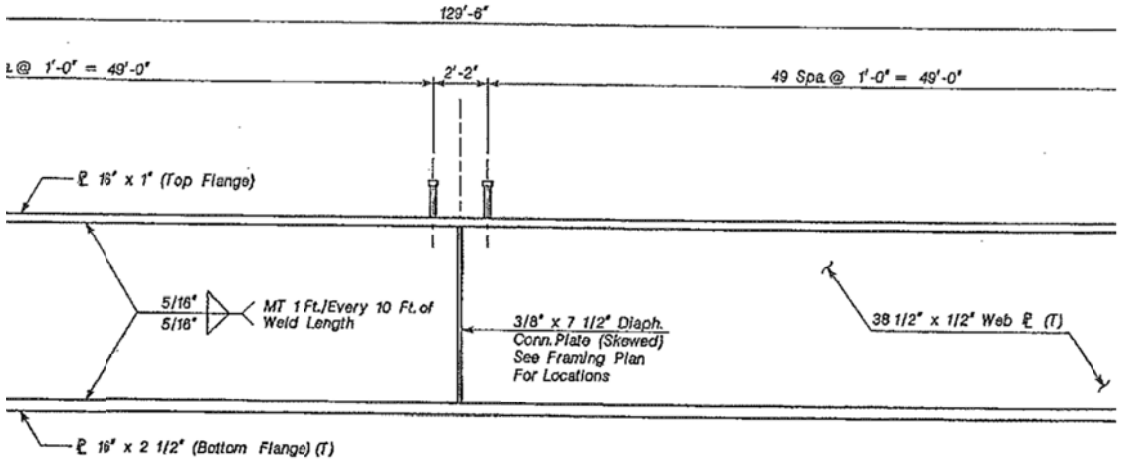

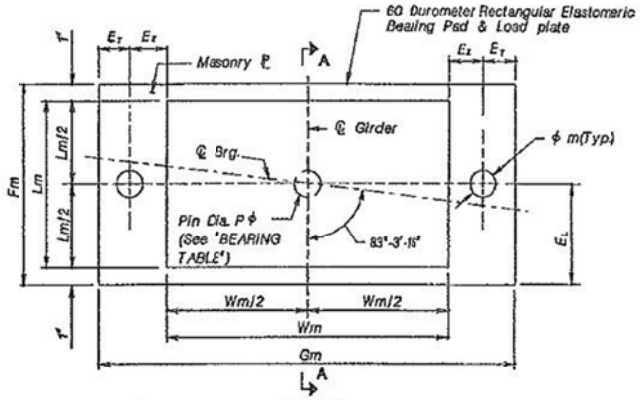

PLAN

FIXED BEARINGS

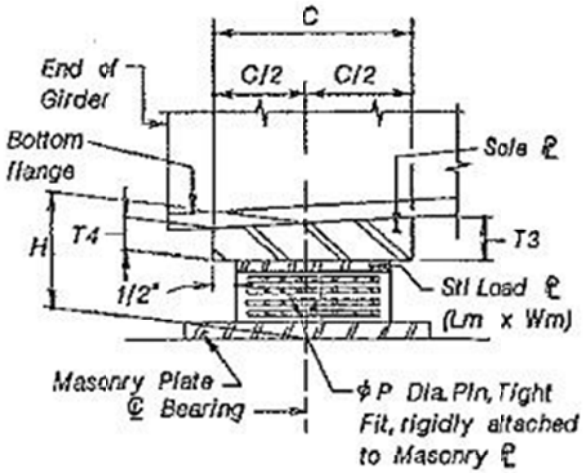

SECTION A-A

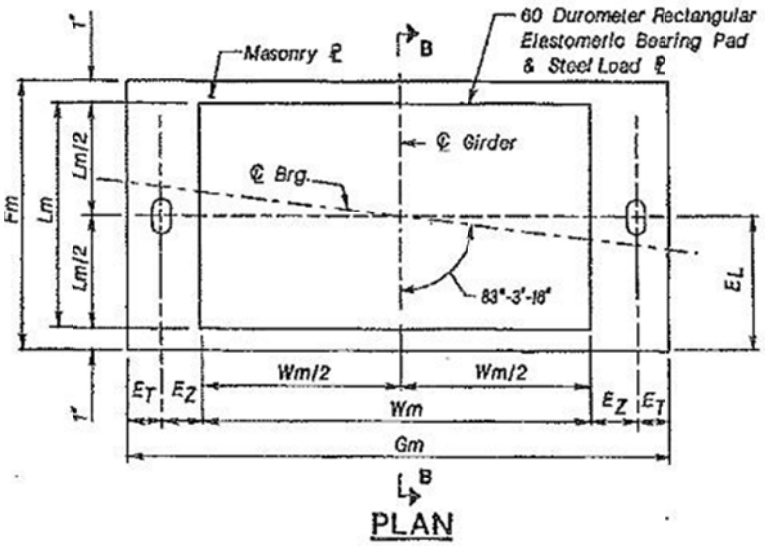

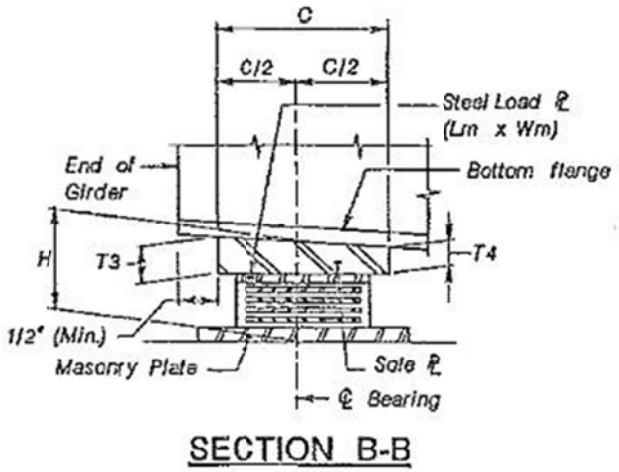

EXPANSION BEARINGS

Magnolia Bridge Drawing

Rt 130 over Rt.73 Drawings

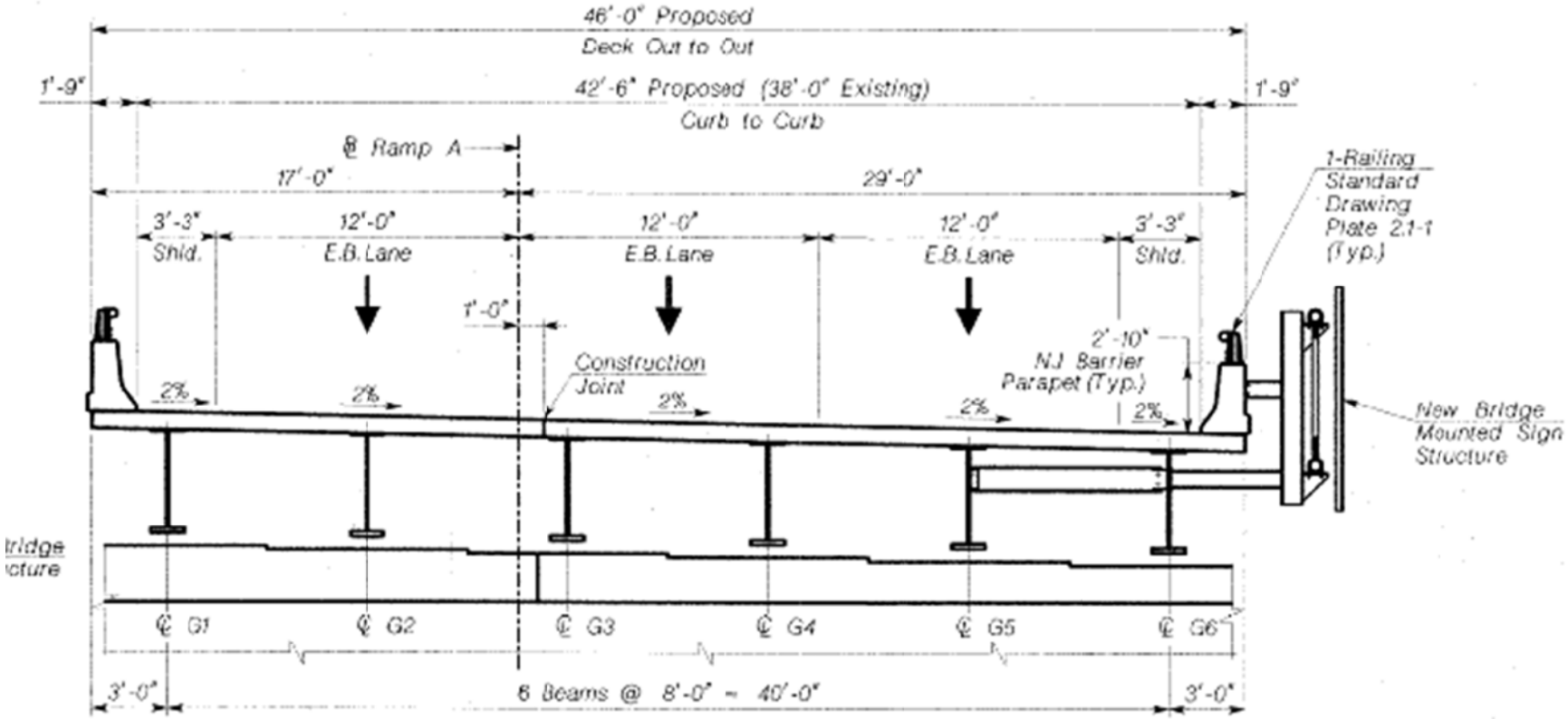

FINISHED BRIDGE
(LOOKING UPSTATION)
Scale: 1"=5'

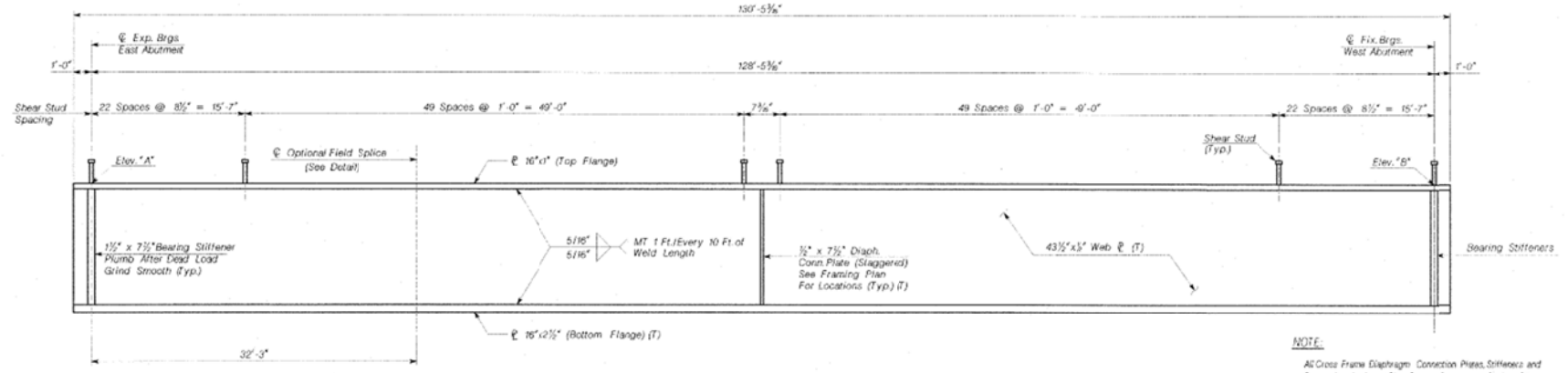

TYPICAL GIRDER ELEVATION
Not To Scale

NOTE:
All Cross Frame Diaphragm Connection Plates, Stiffeners and Connection Angles at Sign Support Structure at Girders G5 and G6 not shown for Clarity. See "Framing Plan" and "Sign Structure Details" sheets for Locations.

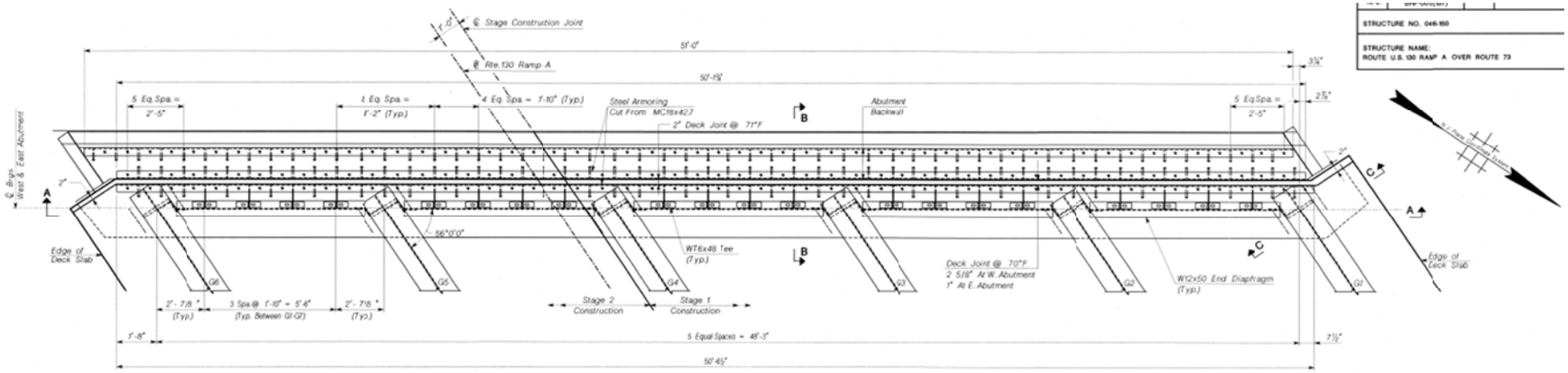

DECK JOINT PLAN
(WEST ABUTMENT SHOWN, EAST ABUTMENT SIMILAR)
Scale: ½" = 1'-0"

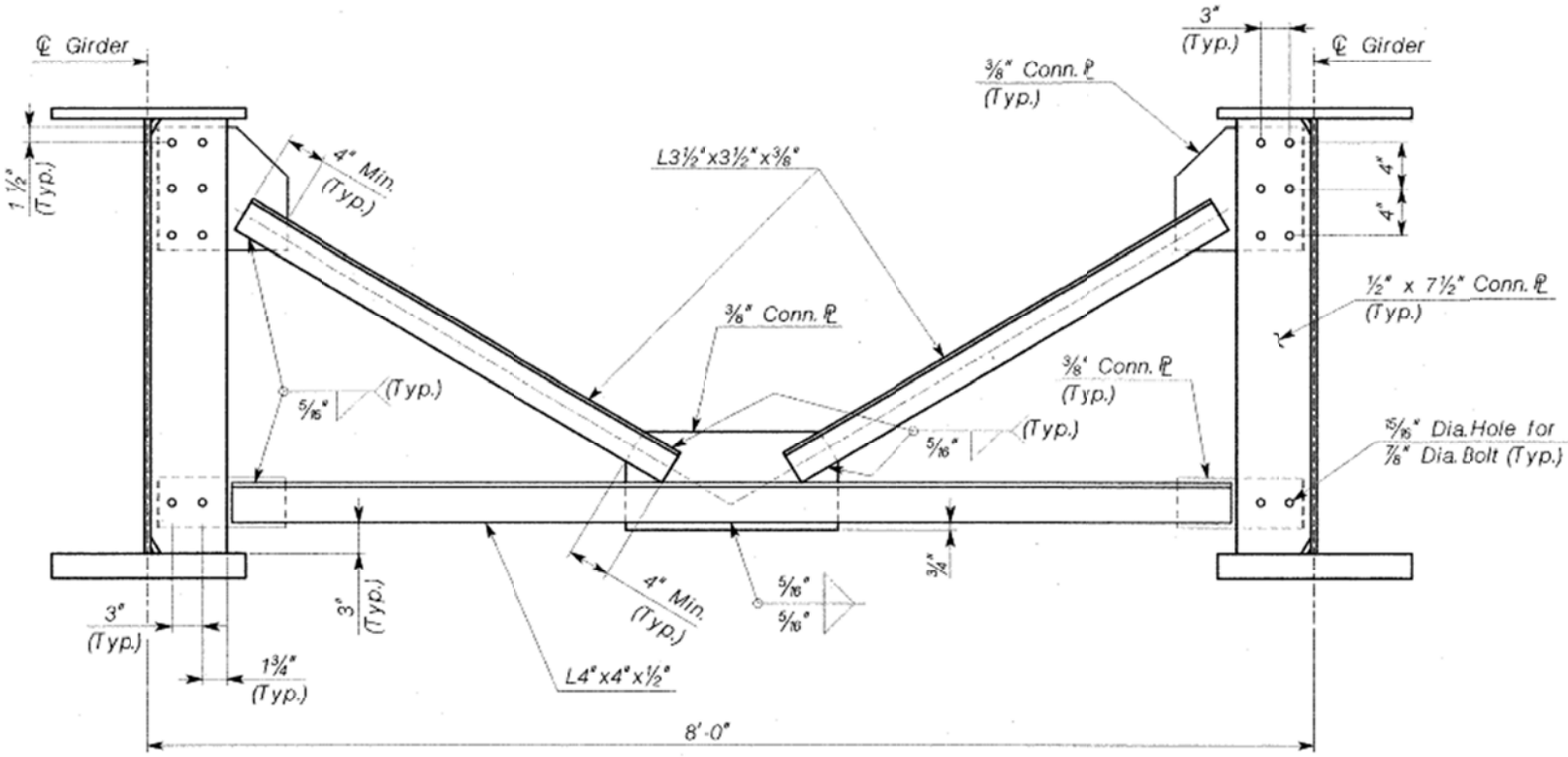

TYPICAL INTERMEDIATE DIAPHRAGM DETAIL

Not To Scale

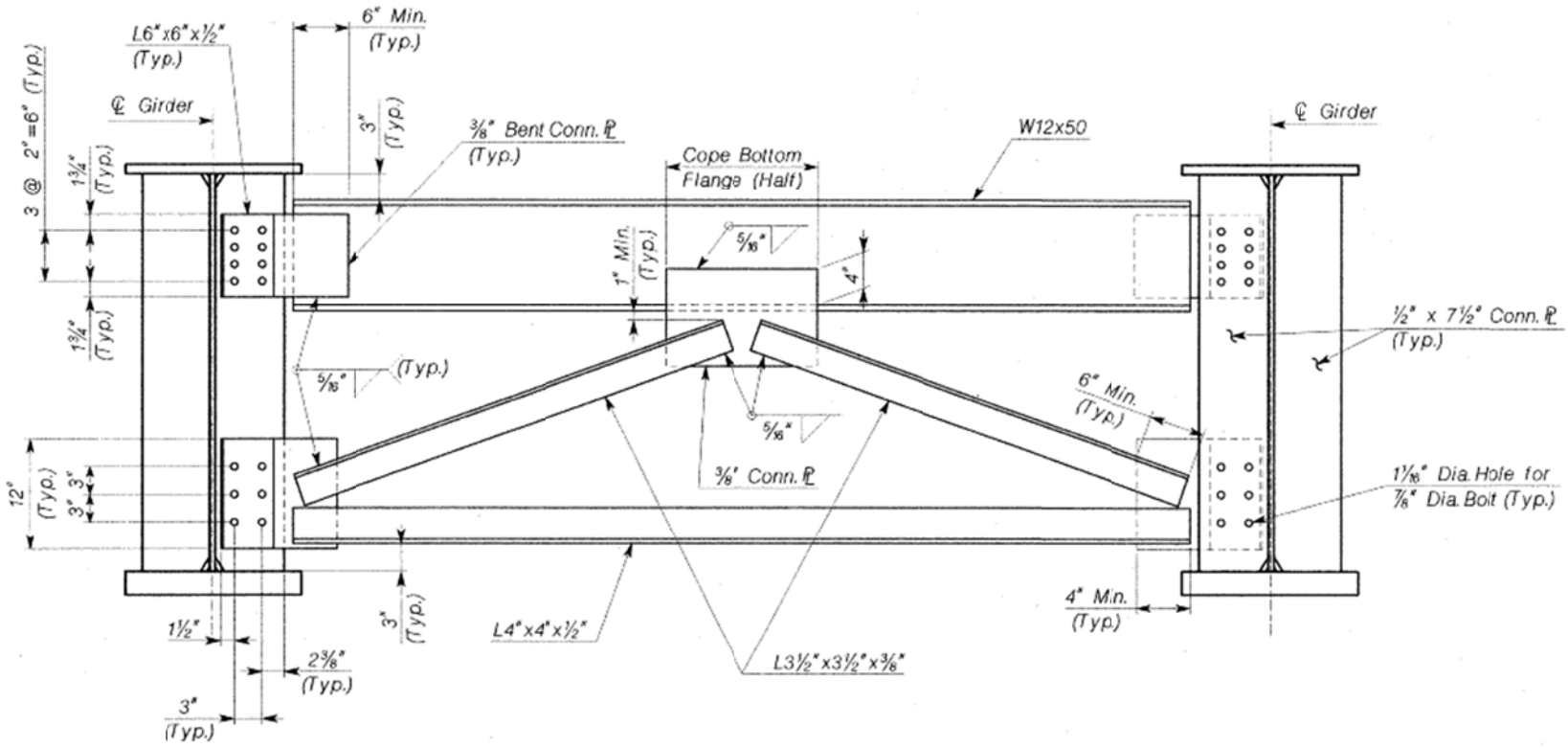

TYPICAL END DIAPHRAGM DETAIL

Not To Scale

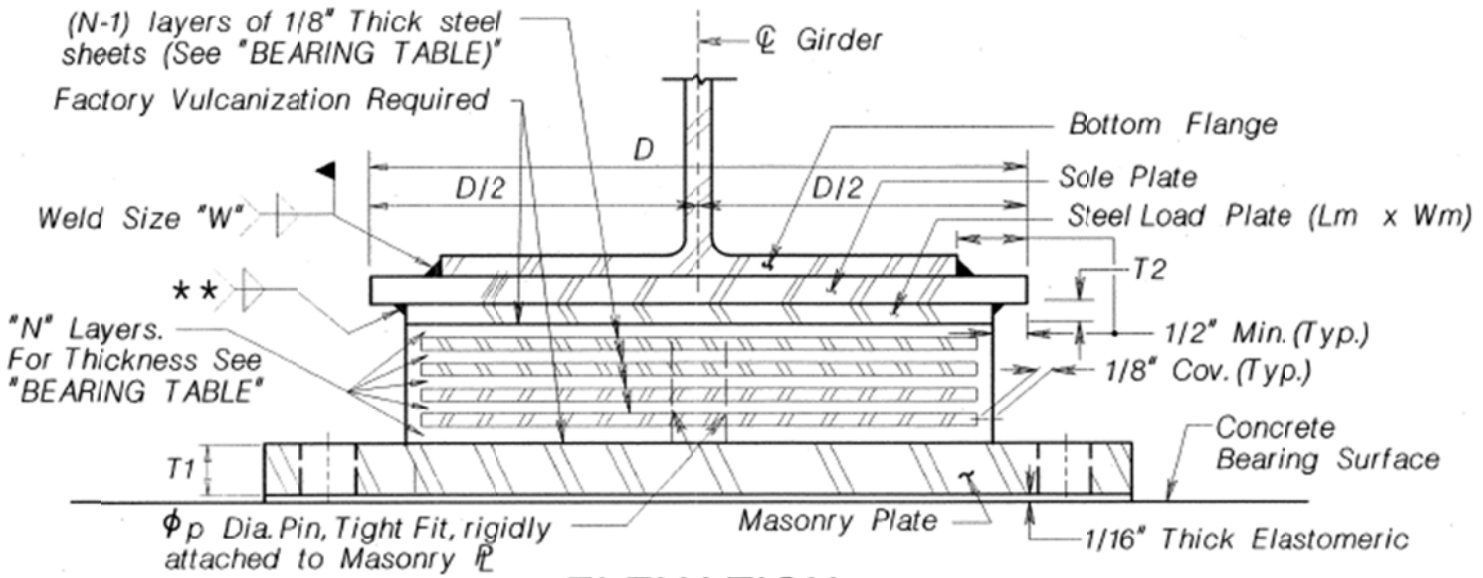

ELEVATION

Rt. I-80 over 287 Drawings

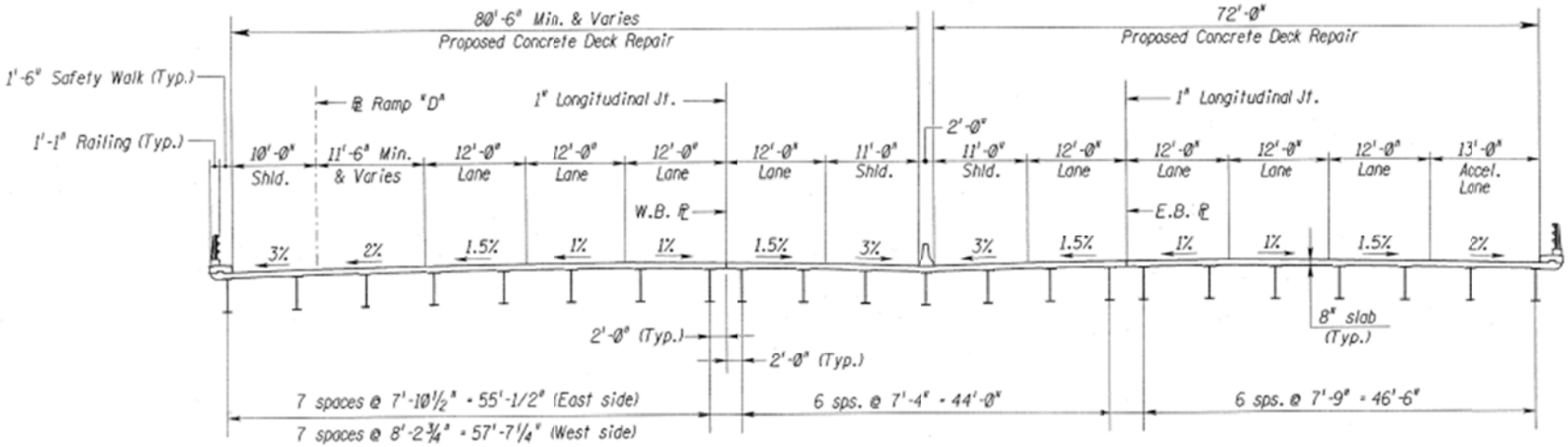

SECTION A-A
Scale: 3/32"=1'-Ø"

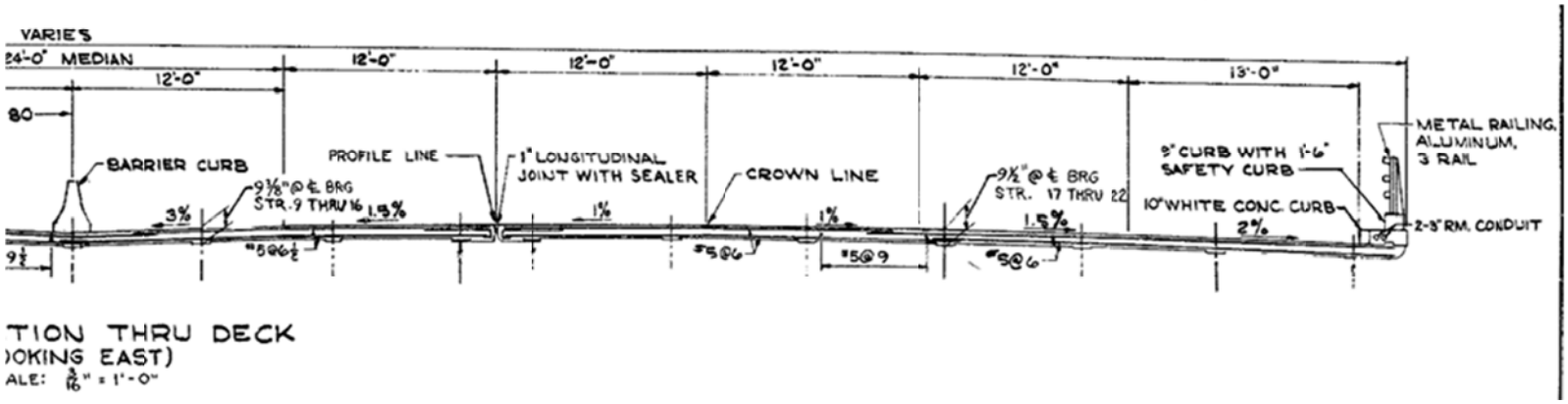

TION THRU DECK
)OKING EAST)
ALE: 3/16" = 1'-0"

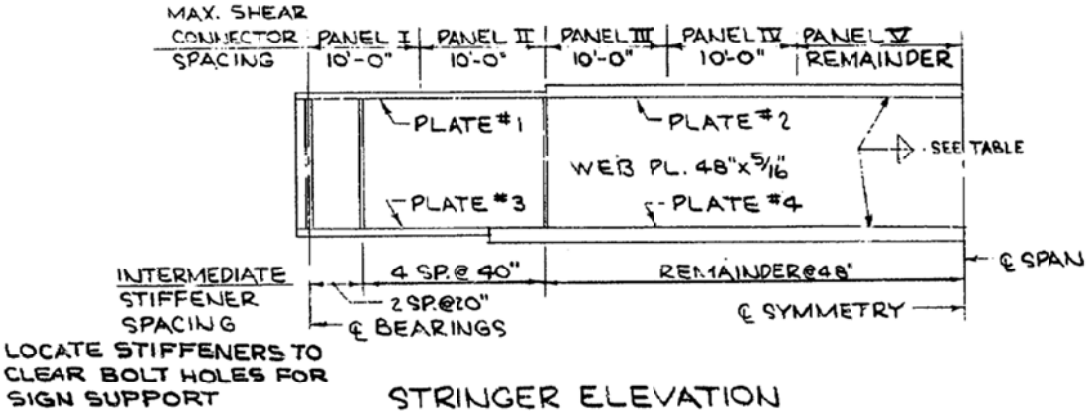

STRINGER ELEVATION

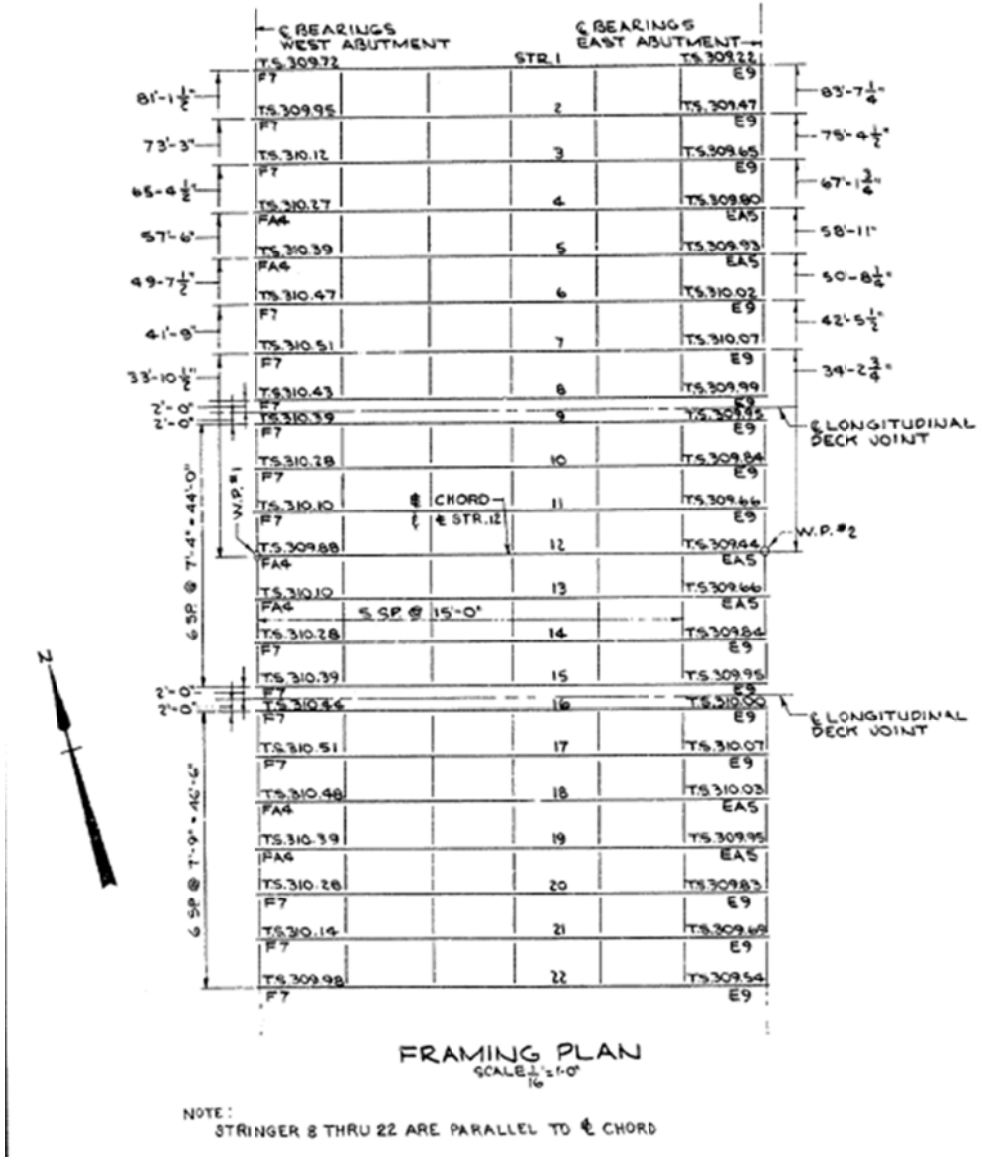

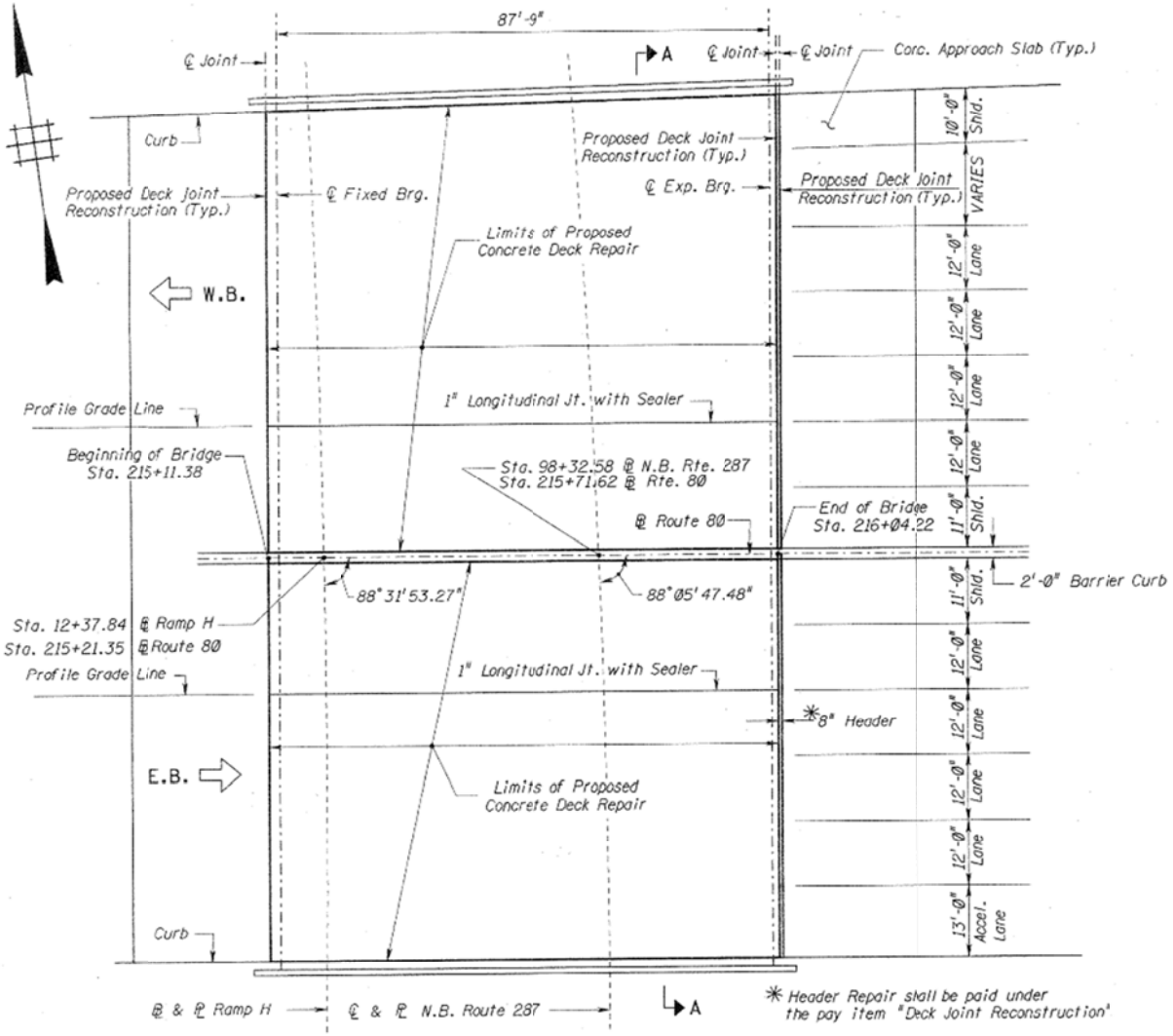

DECK REPAIR PLAN

WELDED STRINGER SCHEDULE

STRINGER NUMBER	LENGTH C. BRGS. TO C. BRGS.	FLANGE PLATES				MAXIMUM SHEAR CONNECTOR SPACING, 2 STUDS PER ROW					CAMBER D.L. DEFL.	
		PL. #1	PL. #2	PL. #3	PL. #4	PANEL I	PANEL II	PANEL III	PANEL IV	PANEL V	1/4 PT.	1/2 PT.
1	89'-0 7/16"	12"x1/2"	12"x1"x50'-0"	16"x7/8"	16"x1 5/8"x59'-0"	7 1/2"	8 1/2"	10 1/2"	13 1/2"	17 1/2"	1 5/8"	2 1/4"
2	89'-0 5/16"	12"x5/8"	12"x1 1/8"x48'-0"	16"x7/8"	16"x1 5/8"x59'-0"	7"	8 1/2"	10 1/2"	13 1/2"	16 1/2"	1 5/8"	2 1/4"
3	89'-0 7/16"	12"x5/8"	12"x1 1/8"x48'-0"	16"x7/8"	16"x1 5/8"x59'-0"	7"	8 1/2"	10 1/2"	13 1/2"	16 1/2"	1 5/8"	2 1/4"
4	89'-0 1/8"	12"x5/8"	12"x1 1/8"x48'-0"	16"x7/8"	16"x1 5/8"x59'-0"	7"	8 1/2"	10 1/2"	13 1/2"	16 1/2"	1 5/8"	2 1/4"
5 & 6	89'-0 1/16"	12"x5/8"	12"x1 1/8"x48'-0"	16"x7/8"	16"x1 5/8"x59'-0"	7"	8 1/2"	10 1/2"	13 1/2"	16 1/2"	1 5/8"	2 1/4"
7	89'-0"	12"x5/8"	12"x1 1/8"x48'-0"	16"x7/8"	16"x1 5/8"x59'-0"	7"	8 1/2"	10 1/2"	13 1/2"	16 1/2"	1 5/8"	2 1/4"
8	89'-0"	12"x1/2"	12"x1"x48'-0"	16"x7/8"	16"x1 5/8"x55'-0"	7 1/2"	8 1/2"	10 1/2"	13 1/2	17 1/2"	1 3/8"	2"
9 & 15	89'-0"	12"x1/2"	12"x7/8"x44'-0"	16"x7/8"	16"x1 1/2"x56'-0"	7"	8"	10"	13"	16 1/2"	1 1/2"	2"
10 TO 14	89'-0"	12"x1/2"	12"x7/8"x48'-0"	16"x7/8"	16"x1 1/2"x57'-0"	7"	8 1/2"	10 1/2"	13 1/2"	17 1/2"	1 5/8"	2 3/8"
16	89'-0"	12"x1/2"	12"x7/8"x48'-0"	16"x7/8"	16"x1 7/8"x57'-0"	7"	8"	10"	13"	16 1/2"	1 1/2"	2 3/8"
17 TO 22	89'-0"	12"x1/2"	12"x1"x50'-0"	16"x7/8"	16"x1 5/8"x59'-0"	7 1/2"	8 1/2"	10 1/2"	13 1/2"	17 1/2"	1 5/8	2 1/4

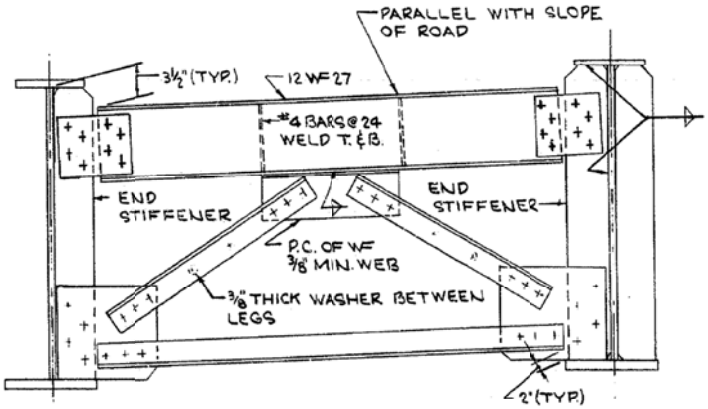

TYPICAL END DIAPHRAGM
SCALE 3/4"=1'-0"

NOTES: ALL ANGLES DOUBLE 4"x4"x5/16" ALL CONN. PLATES 3/8" THICK

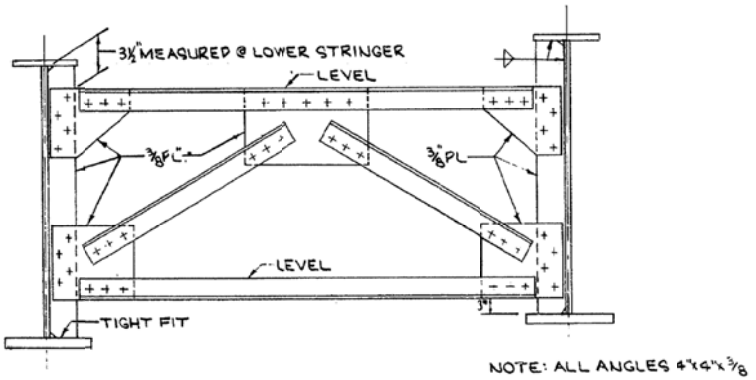

TYPICAL INTERMEDIATE DIAPHRAGM
SCALE 3/4"=1'-0"

NOTE: ALL ANGLES 4"x4"x3/8

Seismic Structure Report

04/23/01

Structure Identification

Route: 80 Structure Number: 1414-168 Milepoint: 043.620

Structure Name: I-80&RAMP D OVER I-287NB & RAMPS D&H

Seismic Deck Information

Deck Thickness:	08.000 in.
Abutment Joint Width:	01.000 in.
Pier Joint Width:	00.000 in.

Seismic Superstructure Information

# Beams Main Span:		22 Beams @ 08.052 ft
Structure Type:	302	STEEL STR/MB GR

Seismic Bearing Information

Bearing Height:	14.500 in.
Number of Anchor Bolts:	02
Anchor Bolt Dimensions:	12 in Length 01.250 in Dia.
Pin Diameter:	02.000 in.
Shoulder Dimensions:	02.500 in. Dia 00.500 in. Thick
Alignment Bearing:	Alignment Bearing Present
Transverse Restraint:	Restraint System Present

Seismic Substructure Information

Abutment Seat Width:		15.000 in.
Pier Seat Width:		
Column Reinforcement:		
Column Cross Section:		
Column Height:		
Column F'c:		
Longitudinal Reinforcement:		
Pile Embedment:		
Type of Pier:		NONE
Type of Abutment:	03	FULL HEIGHT

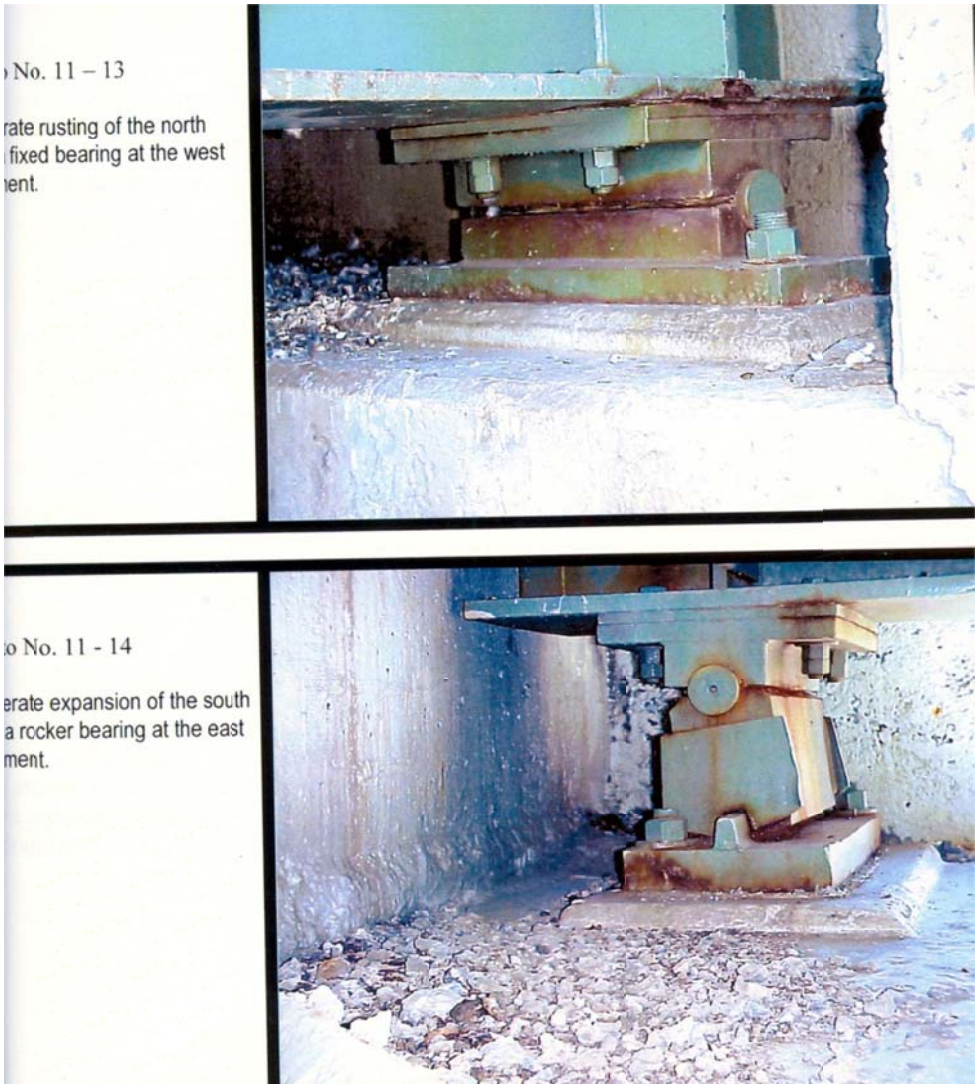

No. 11 – 13

rate rusting of the north
fixed bearing at the west
ent.

o No. 11 - 14

erate expansion of the south
a rocker bearing at the east
ment.

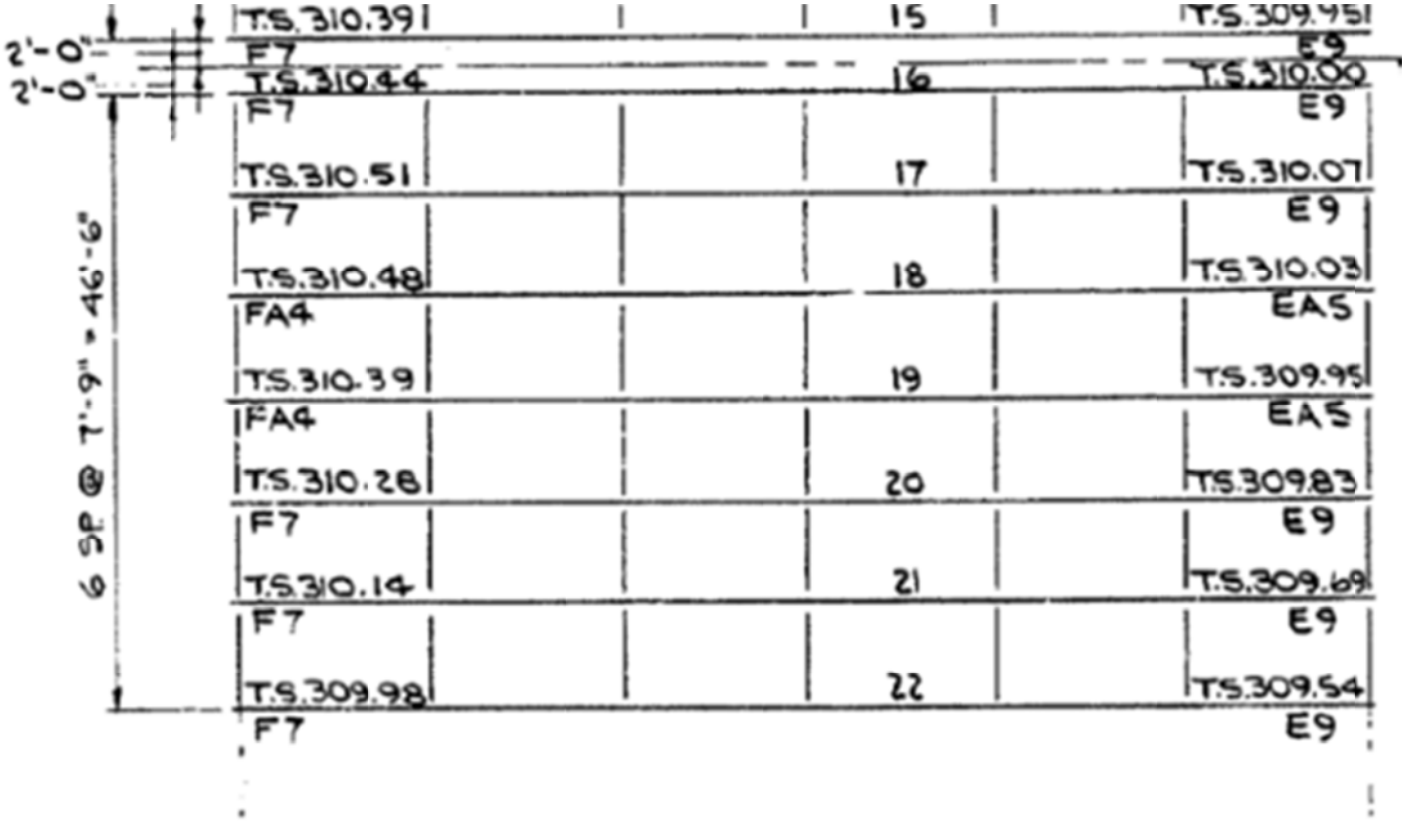

FRAMING PLAN
SCALE $\frac{1}{16}$" = 1'-0"

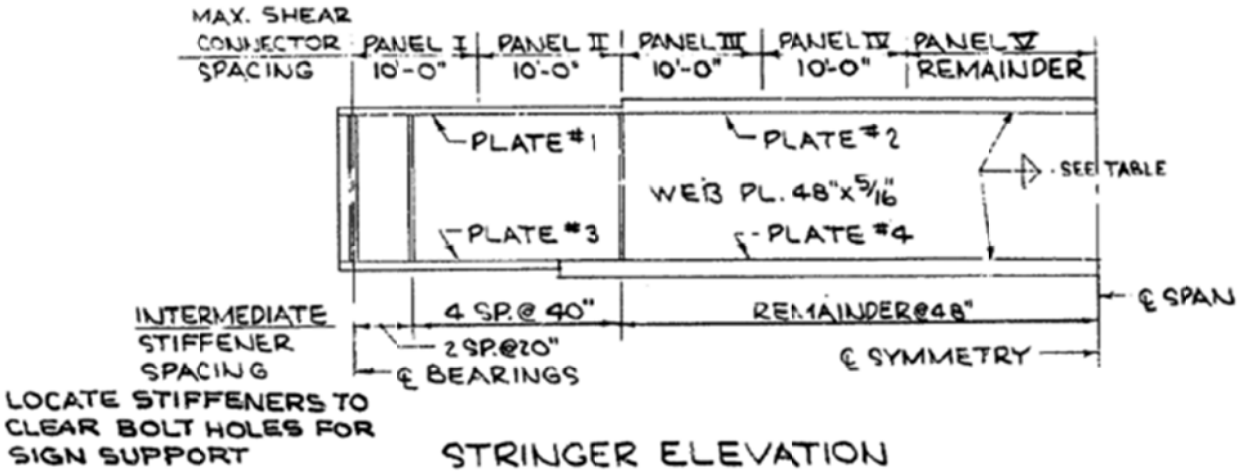

STRINGER ELEVATION

Rt. I-80 over Smith Rd Drawings

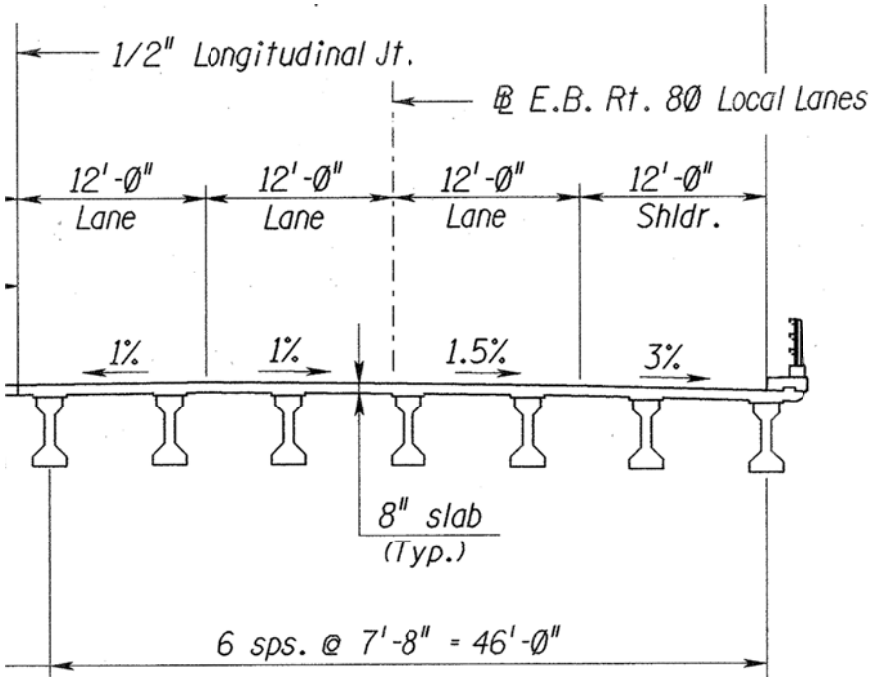

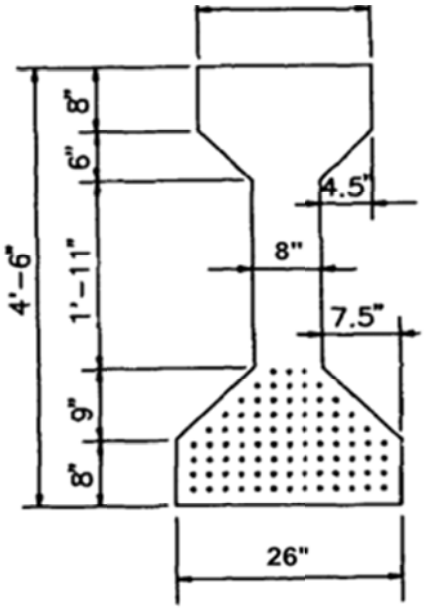

SECTION
TYPE IV BEAM
70 TO 100 FT. SPANS

FRAMING PLAN
SCALE: 1" = 10'-0"

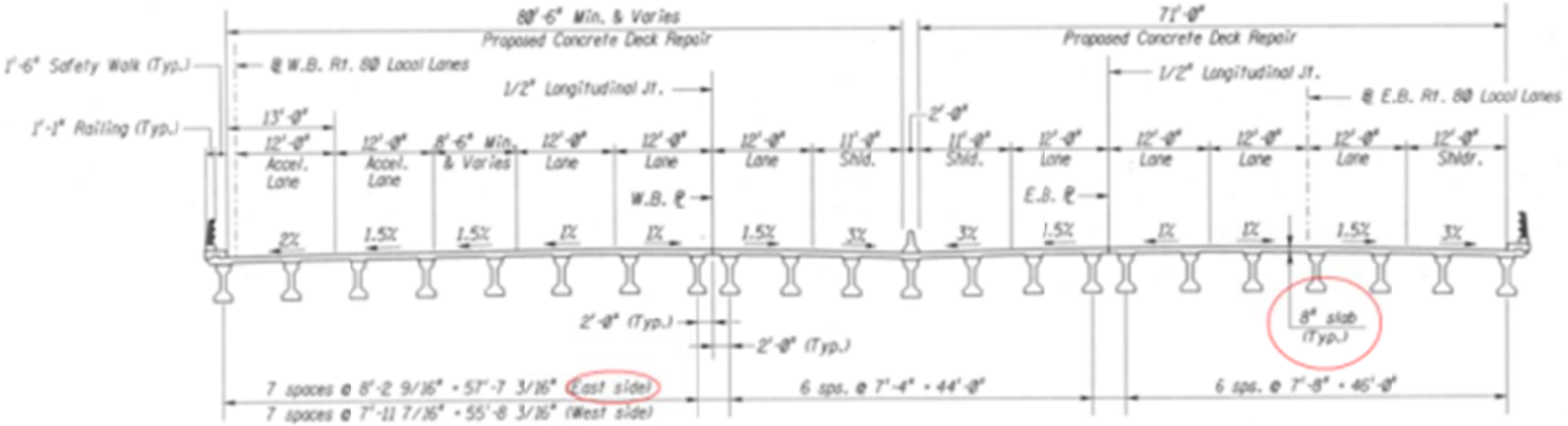

REFERNECES

1. AASHTO. *Load Factor Design: Bridge Design Specifications*, (16th edition). American Association of State Highway and Transportation Officials , Washington, D. C, 1996.
2. AASHTO, *Load Resistance and Factor Design: Bridge Design Specifications*, (first edition), American Association of State Highway and Transportation Officials, Washington D.C, 1998.
3. A. Alampalli. *Correlation between bridge vibration and bridge deck cracking: a qualitative study.* Special report 136, Transportation Research and Development Bureau, New York State Department of Transportation, 2001.
4. T. Amaraks. *Highway Bridge Vibration Studies,* Joint Highway Research Project, Indiana State Highway Commission, Purdue University, West Lafayette, IN, 1975.
5. ASCE. "Deflection limitation of bridges." *Journal of the structural division*, V 84:ST3, 1958.
6. A. Azizinamini, K. Barth, R. Dexter, and C. Rubeiz. "High Performance Steel: Research Front-Historical Account of Research Activities." *Journal of Bridge Engineering ASCE*, Vol. 9. Issue 3, 2004, pp. 212-217.
7. M. G. Barker, L Gandiaga, and J. Staebler. *Serviceability limits and economical steel bridge design*. University of Wyoming, in cooperation with U.S. Department of Transportation Federal Highway Administration, 2008.
8. M. J. Bartos (), "Ontario Write New Bridge Code", *Civil Engineering, ASCE*, Vol. 49, No 3, 1979, pp. 56-61.
9. BD 19/06. *Design Manual for Roads and Bridges*. Vol. 2, Section 2, part 8. Highway Agency, London, August 2006.
10. J. R. Billing, and R. Green. "**Design Provisions for Dynamic Loading of Highway Bridges**", *Second Bridge Engineering Conference, Transportation Research Record 950*, National Research Council, Washington D. C., Sept.24-26, 1984, pp. 94-103.
11. J. Blanchard, B. L. Davies and J. W. Smith. "Design Criteria and Analysis for Dynamic Loading of Footbridges", *Transport and Road Research Laboratory Supplementary Report 275*, Symposium on Dynamic Behavior of Bridges, Crowthorne, England, 1977, pp. 90-106.
12. C. W. Brown. "An Engineer's Approach to Dynamic Aspects of Bridge Design", *Transport and Road Research Laboratory Supplementary Report 275*, Symposium on Dynamic Behavior of Bridges, Crowthorne, England, 1977, pp. 107-113.
13. A. K. Chopra. *Dynamic of Structures: Theory and Applications to Earthquake Engineering.* 3rd Edition, Prentice Hall, New Jersey, 2007.
14. B. F. Clingenpeel. *The economical use of high perfoemance steel in slab-on-steel stringer bridge design*. Department of Civil and Environmental Engineering, College of Engineering and Mineral Resources at West Virginia University, Masters' Thesis, 2001.
15. CSA International. CAN/CSA–S6- 00. *Canadian Highway Bridge Design Code.* Canadian Standards Association, Toronto, Ontario, Canada, 2000.

16. CsiBridge. Computer and Structure. Inc structural and Earthquake Engineering Software. www.csiberkeley.com/csibridge
17. J. R. Demitz, D. R. Mertz, J. W. Gillespie."Deflection Requirements for Bridges Constructed with Advanced Composite Materials." *Journal of Bridge Engineering, ASCE,* Vol. 8, No. 2, 2003, pp. 73-83.
18. R. J. Dexter, W. J. Wright, and J.W. Fisher. "fatigue and fracture of steel girders". *Journal of Bridge Engineering ASCE,* Vol. 9, issue 3, 2004, pp. 278-286.
19. K. F. Dunker and B.G. Rabbat. "Performance of Highway Bridges", *Concrete International: Design and Construction*, Vol. 12, No. 8, 1990.
20. K.F Dunker and B.G. Rabbat. "Assessing Infrastructure Deficiencies: The Case of Highway Bridges", *ASCE, Journal of Infrastructure Systems,* Vol. 1, No. 2, 1995.
21. A. Ebrahimpour, R. L. Sack."A review of vibration serviceability criteria for floor structures", *Computers and Structures*, Vol. 83, 2005, pp. 2488-2494.
22. E. Esmailzadeh and N. Jalili. "Vehicle-passenger-structure interaction of uniform bridges traversed by moving vehicle." *Journal of Sound and Vibration*, Vol. 260, 2003, pp. 611-635.
23. J.W. Fisher*. Distortion-Induced Fatigue Cracking in Steel Bridges*, NCHRP Report 336, TRB, National Research Council, Washington, D.C, 1990.
24. J. W. Fisher and W. J. Wright. "High toughness of HPS: Can it help you in fatigue design" *Journal of Constructional Steel Research*, Vol. 63, 2007, pp. 922-940.
25. R.S. Fountain, and C.E. Thunman. "Deflection Criteria for Steel Highway Bridges." *Proceedings of the National Engineering Conference & Conference of Operating Personnel,* New Orleans, LA, 1987, pp.20.1-20.12.
26. L. Fryba*. Vibration of solids and structures under moving loads.* 3rd Edition, Publisher, Thomas Telford , Publish Date,1972-01-31.
27. L. Fushun, Huajun, L., Guangming, Y., Yantao, Z., Weiying, W., and Wanqing, S. (2007). "New Damage-locating Method for Bridges Subjected to a Moving Load." Journal of Ocean University of China, Vol.6, No.2, 2007.
28. J. T. Gaunt and C. D. Sutton. *Highway Bridge Vibration Studies.* Joint Highway Research Project, FHWA/IN/JHRP-81/11, Engineering Experiment Station, Purdue University, 1981.
29. A. N. Gergess and R. Sen."Cold bending HPS 385W steel bridge girders". *Journal of constructional steel research.* Vol. 65. 2009, pp. 1549-1557.
30. D.E. Goldman. "A Review of Subjective Responses to Vibratory Motion of the Human Body in the Frequency Range 1 to 70 Cycle per Second." *Naval Medical Research Institute*, National Naval Medical Center, Bethesda, MD, 1948.
31. D.W. Goodpasture and W.A. Goodwin, *Final Report on the Evaluation of Bridge Vibration as Related to Bridge Deck Performance*, The Tennessee Department of Transportation, The University of Tennessee, Knoxville, TN, 1971.
32. R. Hadidi and M. A. Saadeghvaziri. "Transverse Cracking of Concrete Bridge Decks: the State-of-the-Art," *Journal of Bridge Engineering, ASCE,* Vol. 10, No.5, 2005.
33. K. Homma and R. Sause. "Potential for high performance steel in plate-girder bridges". *Proceeding of the 13th structures concress, Boston*, MA, April 3rd-5th, Structures Congress- Proceedings Vol. 1, 1995, pp. 177-192.

34. k. Homma, M. Tanaka, K. Matsuoka, T. Kasuya and H. Kawasaki. *Development of application technologies for bridge high-performance steel, BHS.* Nippon steel technical report No. 97, 2008.
35. ISO, International Standards Organization. *Evaluation of human exposure to whole-body vibration _ part 2: Continuous and shock-induced vibration in buildings (1_80 Hz)*. International standard ISO- 2631/2- Geneva, Switzerland, 1989.
36. A.W. Irwin. "Human Response to Dynamic Motion of Structure." *Structural Engineer*, Vol. 56A, No. 9, 1978, pp. 237-244.
37. R.N. Janeway."Vehicle Vibration Limits for Passenger Comfort. From Ride and Vibration Data." *Special Publications Department (SP-6)*, Society of Automotive Engineers, Inc., 1950, p. 23.
38. P. D. Krauss and E. A. Rogalla. **Transverse Cracking in Newly Constructed Bridge Decks,** Transportation Research Board. National Research Council *, (National Cooperative Highway Research Program Report No. 380)*. Washington, DC, 1996.
39. M. A. Machado. "Alternative Acceleration-Based Serviceability Criterion for Fiber Reinforced Polymer Deck-on-Steel girder Bridges", PhD thesis, August, Perdue University, West Lafayette, Indiana, 2006.
40. M. Majka and M. Hartnett (). "Effects of speed, load and damping on the dynamic response of railway bridges and vehicles." *Journal of Computers and Structures* Vol. 86, 2007, pp. 556-572.
41. D. G. Manning. **Effects of Traffic-Induced Vibrations on Bridge-Deck Repairs**, *National Cooperative Highway Research Program Synthesis of Highway Practice, Report No. 86, Transportation Research Board*, National Research Council, Washington, D. C., 1981.
42. MATLAB, http://www.mathworks.com/, Last visited July 30, 2010.
43. Ministry of Transportation, Quality and Standards Division. *Ontario Highway Bridge Design Code/Commentary*, (3rd edition). Toronto, Ontario, Canada, 1991.
44. H. Moghimi and H. R. Ronagh. "Development of a numerical model for bridge_vehicle interaction and human response to traffic-induced vibration". *Journal of Engineering Structures*. Vol.30, 2008, pp. 3808-3819.
45. G. I. Nagy. *Development of an optimized short-span steel bridge design package*. Department of Civil and Environmental Engineering, College of Engineering and Mineral Resources at West Virginia University, Masters' Thesis, 2008.
46. K. Nishikawa, J. Murakoshi, and T. Matsuki."Study on the fatigue of steel highway bridges in Japan". *Construction and Building Materials*, Vol. 12, No 2-3, 1998, pp. 133-141.
47. J.B. Nevels and D.C. Hixon. *A Study to Determine the Causes of Bridge Deck Deterioration*, Final Report to the State of Oklahoma Department of Highways. Oklahoma City, OK, 1973.
48. A.S. Nowak, and H.N. Grouni. "Serviceability Considerations for Guide ways and Bridges." *Canadian Journal of Civil Engineering*, Vol.15, No.4, 1988, pp.534-537.
49. L.T. Oehler. *Vibration Susceptibilities of Various Highway Bridge Types.* Michigan State Highway Department, Project 55 F-40, No. 272, 1957.

50. L.T. Oehler. *Bridge Vibration – Summary of Questionnaire to State Highway Department.* Michigan State Highway Department, Project 55 F-40 No. 272, 1970.
51. Ontario Highway Bridge Design Code, Second Edition, Ontario Ministry of Transportation and Communications Highway Engineering Division, Toronto, Ontario, 1983.
52. F. Postlethwaite. "Human Susceptibility to Vibration", *Engineering,* Vol. 157, 1944, PP. 61-63.
53. C. W. Roeder, K. Barth, and A. Bergman. **Improved Live Load Deflection Criteria for Steel Bridges.** *National Cooperative Highway Research Program Transportation Research Board of the National Academies*, 2002.
54. H. Reiher and F.J. Meister. "The Effect of Vibration on People. (in German: Forschung auf dem Gebeite des Ingenieurwesens)."*Headquarters Air Material Command,* Vol. 2, No. 2, pp381. Translation: Report No. F-TS-616-RE, Wright Field, Ohio, 193.
55. A. Saadeghvaziri and R. Hadidi. *Cause and Control of Transverse Cracking in Concrete Bridge Decks.* FHWA-NJ-2002-19, Final report,Federa l Highway Administrat ion U.S. Department of Transportation Washington, D.C, 2002.
56. M. A. Saadeghvaziri. "Finite Element Analysis of Highway Bridges Subjected to Moving Loads," *Journal of Computers and Structures*, Vol. 49, No. 5, 1993, pp 837-842.
57. J.W. Smith. "Vibration of structures, application in civil engineering design." Chapman and Hall, London, 1988.
58. G. P. Tilly, D. W. Cullington, and R. Eyre. "Dynamic Behavior of Footbridges", *IABSE Surveys, IABSE*, Vol. 26, No.84, May 1984, pp.13-23.
59. J. Wei and B. Chen. "Estimation of dynamic response for highway CFST arch bridges" *5th International conference on arch bridges*, Madeira, Portugal, September 12-14, 2007.
60. J. F. Wiss and R. A. Parmelee. "Human perception of Transient Vibrations", *Journal of the Structure Division*, ASCE, Vol. 100:ST4, April 1974, PP. 773-787.
61. D.T. Wright, and R. Green. *Human Sensitive to Vibration*. Report No.7, Ontario Department of Highway and Queen's University, Kingston, Ontario, 1959.
62. D. T. Wright and R. Green. *Highway Bridge Vibration. Part II: Report No. 5 Ontario Test Program.* Ontario Department of Highways and Queen's University. Kingston, Ontario, 1964.
63. R. N. Wright and W. H. Walker. "Criteria for the deflection of steel bridges", *American Iron and Steel Institute*, Bulletin No. 19, November 1971.
64. H. Wu. "Influence of live load deflection on superstructure performance of slab on steel stringer bridges." College of Engineering and Mineral Resources at West Virginia University, PhD Dissertation, 2003.
65. S. Zhou, D. C. Rizos, and M. F. Petrou."Effects of superstructure flexibility on strength of reinforced concrete bridge decks." *Computers and Structures*, No. 82, 2004, pp 13-23.
66. S. Zivanovic, A. Pavic, and P. Reynolds. "Vibration Serviceability of Footbridges under Human-Induced Excitation: a Literature Review." *Journal of Sound and Vibration,* Vol. 279, No. 1-2, January 2005, pp. 1-74.